



CONTRACT NO. A133-053
FINAL REPORT
MARCH 1995

**Effect of Canopy Structure
and Open-Top Chamber Techniques
on Micrometeorological Parameters
and the Gradients and
Transport of Water Vapor, Carbon
Dioxide and Ozone in the Canopies
of Plum Trees (*Prunus salicina*)
in the San Joaquin Valley**

CALIFORNIA ENVIRONMENTAL PROTECTION AGENCY



**AIR RESOURCES BOARD
Research Division**

Effect of Canopy Structure and Open-Top Chamber Techniques
on Micrometeorological Parameters and the Gradients
and Transport of Water Vapor, Carbon Dioxide and Ozone
in the Canopies of Plum Trees (*Prunus salicina*) in the
San Joaquin Valley

Final Report
Contract No. A133-053

Prepared for:

California Air Resources Board
Research Division
2020 L Street
Sacramento, California 95814

Prepared by:

David A. Grantz, Principal Investigator
D.L. Vaughn, P.A. Metheny, P. Malkus, K. Wosnik, and X. Zhang

Department of Botany and Plant Sciences
and
Statewide Air Pollution Research Center
University of California, Riverside
Kearney Agricultural Center
Parlier, California 93648

March, 1995

DISCLAIMER

The statements and conclusions in this report are those of the contractor and not necessarily those of the California Air Resources Board. The mention of commercial products, their source or their use in connection with material reported herein is not to be construed as either actual or implied endorsement of such products.

ACKNOWLEDGMENTS

The authors acknowledge the helpful input of L.E. Williams, T.M. DeJong and W.A. Retzlaff, and their maintenance of the experimental trees and fumigation apparatus which made these experiments possible.

This report was submitted in fulfillment of ARB contract # A133-053, "Effect of Canopy Structure and Open-Top Chamber Techniques on Micrometeorological Parameters and the Gradients of Ozone, Carbon Dioxide, and Water Vapor in the Canopies of Plum Trees (*Prunus salicina*) in the San Joaquin Valley"; by the Department of Botany and Plant Sciences and the Statewide Air Pollution Research Center, University of California, Riverside, under the sponsorship of the California Air Resources Board. Work was completed as of 15 March 1995.

ABSTRACT

Trees of a commercial cultivar of plum were grown under commercial management protocol including annual pruning to the "open-vase" morphology, as part of a larger ozone exposure study using open-top-chambers (OTCs). Intensive microenvironmental and physiological measurements were made on the trees subjected to ambient (non-filtered and non-ozone enriched) air inside and outside of the OTC, i.e., the Ambient Control and Non-Chamber Control of the larger study. Concentrations of ozone, carbon dioxide, and water vapor were obtained within the canopy by sampling air from each of nine positions, comprising a matrix from interior to exterior and from top to bottom of the active canopy. Leaf and air temperature, photosynthetically active photon flux density, and wind speed were also obtained from this matrix.

Two upper interior canopy positions were averaged, and two upper exterior canopy positions were averaged, inside and outside the OTC to provide four well-characterized canopy zones. Gas exchange measurements were made in these interior and exterior zones of individual trees inside and outside of the chambers. Transpiration by each canopy zone was measured with heat balance sap flow gauges.

Objectives were to 1) map the distribution of microenvironmental parameters within canopies inside and outside the OTC to quantify canopy and OTC effects on exchange with the atmosphere and on cross-canopy gradients, 2) use redundant measurements of transpirational water flux (as vapor and liquid) to determine transport parameters for exchange of gases between the atmosphere and leaves in contrasting positions in the canopies, and 3) develop a protocol to calculate ozone flux (effective dose, uptake) by canopy region to rationalize future and past ozone yield response studies using diverse OTC and non-chamber exposure protocols on a common basis of whole-canopy ozone uptake.

Significant differences in bulk (measured above the canopy) gas concentrations and micrometeorological parameters were observed between inside and outside the OTC. Significant vertical and horizontal gradients in these parameters were observed within the canopies, despite the open canopy architecture of the pruned trees. The gradients were diminished and often inverted inside, relative to outside, the OTC, due to air distribution at the bottom of the OTC, as opposed to entry from the canopy top outside the OTC. More uniform exposure of leaves, fruiting sites and growing points throughout the canopy, to the ozone concentration entering the canopy, occurred inside the OTC than outside. Transpiration and

ozone uptake by interior leaves was greater inside than outside the OTC, though the largest values were observed in the exterior zone of the outside tree. Canopy-averaged stomatal conductance was greater inside than outside the OTC, and accounted for only 59% of the total transport resistance for gas exchange, compared to 79% outside, resulting in greater stomatal control of transpiration and ozone flux in the outside tree. Total ozone uptake by the canopy was greater outside the OTC than inside, due to dominance of the exterior of the outside tree and the reduction of ozone concentrations inside the chamber by distribution losses. Penetration of ambient ozone concentrations to the leaf surfaces would have reversed this pattern.

As suggested by others, expression of ozone exposure as a dose is physiologically more significant, and more process-based for modelling applications, than as an ambient ozone concentration, particularly measured as a bulk parameter outside the canopy. In the present case these techniques unified into a single linear relationship the yield-exposure data from the OTC and Non-Chamber treatments that had previously fallen on separate relationships when expressed as ozone concentration. Specification of transport resistances to several canopy locations should be required of all future OTC exposure studies. A catalog of transport parameters associated with contrasting canopy morphologies and OTC designs could be compiled to reduce the need for expensive micrometeorological measurements in each individual study, and to facilitate *post-hoc*, meta-analyses of all ozone response studies undertaken to date.

TABLE OF CONTENTS

DISCLAIMER	i
ACKNOWLEDGMENTS	ii
ABSTRACT.....	iii
TABLE OF CONTENTS	v
LIST OF FIGURES.....	vii
LIST OF TABLES	xv
I. INTRODUCTION	1
A. Geographic Background.....	1
B. Open top fumigation chambers	1
1. Bulk microenvironmental parameters.....	1
2. Within-canopy distribution of microenvironmental parameters.....	2
C. Ozone Uptake	4
1. Microenvironmental impact.....	4
2. Coupling of leaves to the environment.....	6
D. Effective Dose	7
E. Current Study.....	8
III. MATERIALS AND METHODS	9
A. Field Site.....	9
B. Data Collection, Storage, and Retrieval.....	10
C. Microenvironmental Measurements	10
1. Within-canopy.....	10
2. Above-canopy.....	11
D. Canopy Zone Designations.....	12
E. Additional Measurements	12
1. Within-canopy wind	12
2. Transpiration.....	12
3. Leaf area.....	13
4. Leaf water potential	13
5. Gas exchange measurements	14
F. Instrument Maintenance, Calibration, and Quality Assurance	14
G. Calculations	15
1. Gaseous flux and leaf surface concentrations.....	15
2. Environmental coupling.....	18
III. RESULTS AND DISCUSSION--ENVIRONMENTAL EXPOSURE	20
A. General Environmental Conditions and Canopy Effects	20
1. Wind.....	20
2. Light.....	20
3. Temperature	21
B. Effect of the OTC on Bulk Environmental Parameters.....	22
1. Temperature	22
2. Water vapor.....	22
3. Carbon dioxide.....	23

4. Ozone	23
C. Effect of the OTC on the Distribution of Microenvironmental Parameters.....	25
1. Cross-canopy gradients of heat and trace gases	25
2. Mapping the distribution of heat and trace gases.....	28
IV. RESULTS AND DISCUSSION--GAS TRANSPORT	31
A. Effect of Open-Top-Chambers on Water Transport (Transpiration).....	31
1. Water vapor pressure, gradients, conductances and fluxes.....	31
2. Liquid water gradients, conductances and fluxes	33
3. Calculated water vapor flux.....	34
4. Stomatal and Environmental regulation of water vapor fluxes.....	36
B. Effect of Open-Top-Chambers on CO ₂ Transport (Photosynthesis).....	38
1. CO ₂ concentration gradients, conductances and fluxes.....	38
2. Calculated carbon dioxide flux	39
C. Effect of Open-Top-Chambers on Ozone Transport (Leaf Uptake).....	41
1. Ozone concentration gradients and fluxes.....	41
2. Calculated ozone uptake	42
V. RESULTS AND DISCUSSION--MODELLING OZONE UPTAKE.....	44
A. Modelling Stomatal Conductance	44
1. Role of vapor pressure	44
2. Role of light.....	45
3. Environmental interactions	45
B. Ozone Uptake	46
1. Modelling O ₃ Flux	46
C. Application of the Flux Methodology to Plum Yield Data.....	48
VI. SUMMARY AND CONCLUSIONS.....	50
VII. RECOMMENDATIONS	52
VIII. REFERENCES.....	54
LIST OF INVENTIONS REPORTED AND PUBLICATIONS	61
GLOSSARY OF TERMS, ABBREVIATIONS, AND SYMBOLS.....	62
TABLES	65
FIGURES.....	82

LIST OF FIGURES

- Fig. 1. Effect of enclosure in an open-top-exposure chamber (OTC) on the bulk ozone concentration surrounding experimental plum trees, measured at location 3 in each canopy (see Fig. 8).
- Fig. 2. Effect of enclosure in an OTC on the relationship between ambient ozone and the physiologically relevant ozone concentration at the leaf surface, in two zones of the canopy differing in exposure.
- Fig. 3. Model relationship between total conductance and stomatal conductance to diffusive transfer of a trace gas from a leaf to the atmosphere, showing the large effect of the non-stomatal boundary layer conductance.
- Fig. 4. Photograph of a representative plum tree.
- Fig. 5. Photograph of the installation of data logging equipment, including several multiplexers, required to record signals from the large array of sensors.
- Fig. 6. Photograph of the tripod and horizontal booms to support the sampling tubing, thermocouples and signal cables within the canopy.
- Fig. 7. Photograph of the micrometeorological instruments deployed above the plum canopy.
- Fig. 8. Diagram of sensor locations and zone designations in the plum trees, showing that location 3 represents an ambient reference point.
- Fig. 9. Photograph of the air delivery system in the OTC, showing placement below the canopy, at the sides and center of the chamber. A) Prior to installation of the plastic chamber walls. B) Following installation of the plastic walls.
- Fig. 10. Photograph of a stem flow gauge mounted on a scaffold branch of a plum tree.

- Fig. 11. Photograph of the leaf area measurement performed following destructive harvest of a subsample of leaves.
- Fig. 12. Regression of leaf area (from destructive harvests) on measured leaf width (A) or leaf length (B).
- Fig. 13. Regression of leaf area (from destructive harvests) on product of leaf width x leaf length.
- Fig. 14. Diurnal pattern of above-canopy wind speed and direction averaged over the six days of intensive physiological measurements.
- Fig. 15. Diurnal pattern of within-canopy wind speed by zone averaged over the six days of intensive physiological measurements, measured by hot wire anemometers.
- Fig. 16. Diurnal pattern of above-canopy photon flux density averaged over the six days of intensive physiological measurements.
- Fig. 17. Diurnal pattern of within-canopy photon flux density (mean of two leaves per zone) by zone averaged over the six days of intensive physiological measurements, measured by photodiodes fixed to leaves.
- Fig. 18. Diurnal pattern of within-canopy photon flux density by zone averaged over the six days of intensive physiological measurements, measured with the quantum sensor attached to the gas exchange cuvette.
- Fig. 19. Diurnal pattern of leaf temperature (mean of two leaves per zone) by zone averaged over the six days of intensive physiological measurements.
- Fig. 20. Diurnal pattern of air temperature (mean of two leaves per zone) by zone averaged over the six days of intensive physiological measurements.
- Fig. 21. Diurnal pattern of leaf to air temperature difference by zone averaged over the six days of intensive physiological measurements.

Fig. 22. Diurnal pattern of ambient air temperature averaged over all sample dates and all nine canopy locations, outside (hollow circles) and inside (filled circles) the OTC .

Fig. 23. Diurnal pattern of H₂O vapor concentration (mole fraction) averaged over all sample dates and all nine canopy locations outside (hollow circles) and inside (filled circles) the OTC .

Fig. 24. Diurnal pattern of CO₂ concentration averaged over all sample dates and all nine canopy locations outside (hollow circles) and inside (filled circles) the OTC .

Fig. 25. Diurnal pattern of O₃ concentration averaged over all sample dates and all nine canopy locations outside (hollow circles) and inside (filled circles) the OTC .

Fig. 26. Diurnal pattern of ambient air temperature average over all sample dates at two contrasting canopy locations (A) inside and (B) outside the OTC.

Fig. 27. Diurnal pattern of ambient air temperature averaged over all sample dates at four pairs of contrasting locations demonstrating strictly vertical or horizontal gradients, outside the OTC.

Fig. 28. Diurnal pattern of ambient air temperature averaged over all sample dates at four pairs of contrasting locations demonstrating strictly vertical or horizontal gradients, inside the OTC.

Fig. 29. Diurnal pattern of H₂O concentration averaged over all sample dates at two contrasting canopy locations (A) inside and (B) outside the OTC.

Fig. 30. Diurnal pattern of H₂O vapor concentration averaged over all sample dates at four pairs of contrasting locations demonstrating strictly vertical or horizontal gradients, outside the OTC.

- Fig. 31. Diurnal pattern of H₂O vapor concentration averaged over all sample dates at four pairs of contrasting locations demonstrating strictly vertical or horizontal gradients, inside the OTC.
- Fig. 32. Diurnal pattern of seasonally averaged CO₂ concentration averaged over all sample dates at two contrasting canopy locations (A) inside and (B) outside the OTC.
- Fig. 33. Diurnal pattern of CO₂ concentration averaged over all sample dates at four pairs of contrasting locations demonstrating strictly vertical or horizontal gradients, outside the OTC.
- Fig. 34. Diurnal pattern of CO₂ concentration averaged over all sample dates at four pairs of contrasting locations demonstrating strictly vertical or horizontal gradients, inside the OTC.
- Fig. 35. Diurnal pattern of O₃ concentration averaged over all sample dates at two contrasting canopy locations (A) inside and (B) outside the OTC.
- Fig. 36. Diurnal pattern of O₃ concentration averaged over all sample dates at four pairs of contrasting locations demonstrating strictly vertical or horizontal gradients, outside the OTC.
- Fig. 37. Diurnal pattern of O₃ concentration averaged over all sample dates at four pairs of contrasting locations demonstrating strictly vertical or horizontal gradients, inside the OTC.
- Fig. 38. Midday ambient air temperature averaged over all sample dates from 1100-1400 PDT, at each of the nine canopy locations in the upper (A), mid (B) and lower (C) canopy inside and outside the OTC.
- Fig. 39. Response surface of midday ambient air temperature averaged over all sample dates from 1100-1400 PDT, at each of the nine canopy locations (data points) inside and outside the OTC.

- Fig. 40. Afternoon ambient air temperature averaged over all sample dates from 1400-1700 PDT, at each of the nine canopy locations in the upper (A), mid (B) and lower (C) canopy inside and outside the OTC.
- Fig. 41. Response surface of afternoon ambient air temperature averaged over all sample dates from 1400-1700 PDT, at each of the nine canopy locations (data points) inside and outside the OTC.
- Fig. 42. Midday H₂O vapor concentration averaged over all sample dates from 1100-1300 PDT, at each of the nine canopy locations in the upper (A), mid (B) and lower (C) canopy inside and outside the OTC.
- Fig. 43. Response surface of midday H₂O vapor concentration averaged over all sample dates from 1100-1300 PDT, at each of the nine canopy locations (data points) inside and outside the OTC.
- Fig. 44. Morning CO₂ concentration averaged over all sample dates from 900-1100 PDT, at each of the nine canopy locations in the upper (A), mid (B) and lower (C) canopy inside and outside the OTC.
- Fig. 45. Response surface of morning CO₂ concentration averaged over all sample dates from 900-1100 PDT, at each of the nine canopy locations (data points) inside and outside the OTC.
- Fig. 46. Midday O₃ concentration averaged over all sample dates from 1500-1700 PDT, at each of the nine canopy locations in the upper (A), mid (B) and lower (C) canopy inside and outside the OTC.
- Fig. 47. Response surface of midday O₃ concentration averaged over all sample dates from 1100-1300 PDT, at each of the nine canopy locations (data points) inside and outside the OTC.
- Fig. 48. Diurnal pattern of H₂O vapor pressure at the leaf interior, at the leaf surface, in the canopy air space within each zone, and in the ambient air in the canopy exterior, by zone.

- Fig. 49. Vapor pressure difference (V) from leaf interior to canopy exterior and from leaf interior to leaf surface, by zone inside and outside the OTC, averaged over the six days of intensive physiological measurements.
- Fig. 50. Diurnal pattern of hourly means of stomatal conductance determined from single leaf gas exchange measurements by zone averaged over the six days of intensive physiological measurements. Solid lines are from polynomial regression analysis.
- Fig. 51. Diurnal pattern of hourly means of xylem sap flow (transpiration) determined from heat balance stem flow gauges by zone averaged over the six days of intensive physiological measurements. Solid lines are from polynomial regression analysis.
- Fig. 52. Diurnal pattern of hourly means of water vapor flux (transpiration) calculated from water vapor gradients and diffusive conductances from the leaf interior to the ambient air by zone averaged over the six days of intensive physiological measurements. The similarity to Fig. 51 reflects the use of directly measured sap flow in calculating boundary layer conductances.
- Fig. 53. Cumulative xylem sap flow by zone averaged over the six days of intensive physiological measurements.
- Fig. 54. Diurnal pattern of liquid water flux (sap flow; transpiration) averaged over six days of intensive physiological measurements, inside and outside the OTC, averaged over both zones.
- Fig. 55. Diurnal pattern of the environmental decoupling coefficient (Ω) inside (A) and outside (B) the OTC by zone averaged over the six days of intensive physiological measurements.
- Fig. 56. Diurnal pattern of the environmental decoupling coefficient (Ω) by zone, demonstrating the impact of including (solid circle) or excluding (open circle) of radiative coupling.
- Fig. 57. Diurnal pattern of CO_2 concentrations at the leaf interior, at the leaf surface, in the canopy air space within each zone, and in the ambient air in the canopy exterior, by zone.

Fig. 58. Diurnal pattern of CO₂ gradients from leaf interior to canopy exterior and from leaf interior to the leaf surface by zone, inside and outside the OTC, averaged over six days of intensive physiological measurements.

Fig. 59. Diurnal pattern of hourly means of net CO₂ assimilation (photosynthesis) determined from single leaf gas exchange measurements by zone averaged over the six days of intensive physiological measurements. Solid lines are from polynomial regression analysis.

Fig. 60. Diurnal pattern of hourly means of net CO₂ assimilation (photosynthesis) determined from CO₂ gradients and diffusive conductances from the leaf interior to the ambient air, by zone averaged over the six days of intensive physiological measurements. The similarity to Fig. 59 reflects the use of single leaf measurements of CO₂ assimilation in calculating intercellular CO₂ concentration (C_i) and the resulting gradients for carbon flux.

Fig. 61. Diurnal pattern of net CO₂ flux (single leaf gas exchange, photosynthesis) averaged over six days of intensive physiological measurements inside and outside the OTC, averaged over both zones.

Fig. 62. Diurnal pattern of O₃ concentrations at the leaf surface, in the canopy air space within each zone, and in the ambient air in the canopy exterior, by zone. O₃ concentration at the leaf interior has been shown to be indistinguishable from 0 ppm.

Fig. 63. Diurnal pattern of O₃ gradients from leaf interior to canopy exterior and from leaf interior to the leaf surface, by zone inside and outside the OTC, averaged over the six days of intensive physiological measurements.

Fig. 64. Diurnal pattern of hourly means of O₃ flux (leaf uptake) determined from O₃ gradients and diffusive conductances from the leaf interior to the ambient air, by zone averaged over the six days of intensive physiological measurements. In the case of O₃ there is no alternative measurement of leaf uptake by zone, with which to compare these values.

- Fig. 65. Diurnal pattern of O_3 flux (uptake by leaves) averaged over six days of intensive physiological measurements inside and outside the OTC, averaged over both zones.
- Fig. 66. Apparent response of stomatal conductance to the single environmental parameter, vapor pressure difference, calculated from the leaf interior to the canopy exterior.
- Fig. 67. Apparent response of stomatal conductance to the single environmental parameter, vapor pressure difference calculated from the leaf interior to the leaf surface.
- Fig. 68. Apparent response of stomatal conductance to the single environmental parameter, above-canopy photon flux density.
- Fig. 69. Response of stomatal conductance to the composite environmental parameter, above-canopy photon flux density normalized by vapor pressure difference calculated from the leaf interior to the canopy exterior.
- Fig. 70. Response of stomatal conductance to the composite environmental parameter, above-canopy photon flux density normalized by vapor pressure difference calculated from the leaf interior to the leaf surface.
- Fig. 71. Relationship between plum yield in 1992 (Williams and DeJong, 1993) and 12 hour seasonal mean ozone concentration (A) or 12 hour seasonal mean ozone flux on a leaf area basis averaged over the entire canopy (B) calculated as in Table 16.

LIST OF TABLES

- Table 1. A comparison of bulk environmental modifications relative to ambient conditions, caused by enclosure of plants inside ozone exposure chambers of various designs, including those used in the present experiment.
- Table 2. Effect of open-top-chambers (OTC) on selected growth and yield parameters of plum trees in the present study (unpublished data from L.E. Williams and T.M. DeJong).
- Table 3. Effect of OTC on 12-hour seasonal mean ozone exposure (0800-2000, PDT) by canopy location, and by zone (ppm).
- Table 4. Mean daily diffusive conductances, gradients, and fluxes of H₂O vapor for each zone, and the effect of the OTC on the ratio of exterior to interior positions.
- Table 5. Mean midday values of transpiration, water potential, and hydraulic conductance for each zone, and the effect of the OTC on the ratio of exterior to interior positions .
- Table 6. Effect of OTC on mean daily stomatal, nonstomatal (boundary layer), and total conductance to H₂O, vapor pressure gradient, and water vapor flux (transpiration) averaged over 1100-1600 (PDT) and the six days of intensive physiological measurements.
- Table 7. Effect of OTC on the environmental decoupling coefficient, with radiative coupling (Ω_R) and without radiative coupling (Ω) averaged over 1000-1600 (PDT) and the six days of intensive physiological measurements.
- Table 8. Mean daily diffusive conductances, gradients, and fluxes of CO₂ for each zone, and the effect of the OTC on the ratio of exterior to interior positions.
- Table 9. Effect of OTC on mean daily stomatal, nonstomatal (boundary layer) and total conductance to CO₂ , CO₂ concentration gradient and net carbon assimilation rate (photosynthesis), averaged over 1100-1600 (PDT) and the six days of intensive physiological measurements.

- Table 10. Mean daily diffusive conductances, gradients, and fluxes of O_3 for each zone, and the effect of the OTC on the ratio of exterior to interior positions..
- Table 11. Effect of OTC on mean daily stomatal, nonstomatal (boundary layer) and total conductance to O_3 , O_3 concentration gradient and ozone flux (leaf uptake), averaged over 1100-1600 (PDT) and the six days of intensive physiological measurements.
- Table 12. Goodness of fit of contrasting models of stomatal conductance as a function of zone and a variety of individual, independent environmental parameters, inside and outside the OTC, separately and combined.
- Table 13. Contrasting models of stomatal conductance as a function of the composite environmental parameter, photon flux density (PPFD) normalized by vapor pressure gradient (V_a or V_s).
- Table 14. Contrasting models of stomatal conductance as a function of an additive combination of photon flux density and vapor pressure gradient.
- Table 15. Goodness of fit of contrasting models of ozone uptake as a function of stomatal conductance, of ambient ozone concentration, or as an additive function of both.
- Table 16. Application of the ozone flux model to the 1992 ozone exposure data of Williams and DeJong (1993).

I. INTRODUCTION

A. Geographic Background

The San Joaquin Valley (SJV) of California is a large geographic basin subject to high levels of solar radiation and increasing population and vehicular travel. Increasing emissions of hydrocarbons and oxides of nitrogen within the SJV, and the influence of growing metropolitan areas outside of the SJV, combined with limited air mass exchange, suggest that the SJV has the potential to surpass the Los Angeles (South Coast) Air Basin in air quality degradation (Howitt, 1990). Ozone generation and accumulation are of particular concern to agriculture and human health.

The SJV produces some 49% of the agricultural produce of California. Growth, development and yield of woody and herbaceous plants are adversely impacted by ozone (e.g., Reich and Amundson, 1985; Townsend, 1974). Current levels of ozone in the SJV account for crop yield reductions that approach or exceed 20% for many important commodities (Brewer and Ashcroft, 1982; Grantz et al., 1992; McCool et al., 1986; Olszyk et al., 1988). A recent study indicated large yield losses in newly introduced Pima cotton (Grantz and McCool, 1993). Seven of nine commercially important tree crops were significantly impacted by ozone (Retzlaff et al., 1991). Population and air quality trends indicate that future economic losses in the SJV may be considerably higher (Winer et al., 1990). Information on the ways in which atmospheric ozone penetrates plant canopies to cause these losses is lacking and necessary for modeling, regulatory and mitigation purposes.

B. Open top fumigation chambers

1. Bulk microenvironmental parameters

The experimental evidence for accepted ozone-yield reduction functions has been derived largely using open-top fumigation chamber (OTC) techniques, both in the SJV (e.g., grapes, Brewer and Ashcroft, 1983; plums, almonds and other tree crops, Retzlaff et al., 1991; cotton, Temple, 1988b; alfalfa, Temple et al., 1988a; tomatoes, Temple, 1990) and nationwide (Heck, 1989). Standardized OTC designs have represented a substantial contribution to the uniform assessment of ozone effects on plants. Some characteristics of these contrasting systems have been detailed (Bytnerowicz et al., 1986a,b, 1989; Fuhrer, 1994; Ham et al., 1993; Musselman et al., 1986; Weinstock et al., 1982). Small differences observed in relative humidity and temperature within and outside of OTCs have been considered explicitly and considered unimportant, relative to the benefits of the OTC protocol (Heck, 1989). However,

these chamber effects on bulk microenvironmental parameters can be large, typically including temperature increases of several °C (Albaugh et al., 1992; Brewer and Ashcroft, 1983). Yield differences between plants grown in ambient air-fumigated chambers and outside are typically non-significant (e.g., Mudd, 1991; Sanders et al., 1991; Williams et al., 1993) though effects on plant productivity have been noted (Fuhrer, 1994; Lewis and Brennan, 1977; Olszyk et al., 1992; Retzlaff et al., 1992).

Uniformity of exposure of each individual plant within an OTC is a well-recognized challenge (Heck, 1989) that has been largely solved through improved blower and air filtration technology. Any residual non-uniformity across experimental units, such as individual plants, appears as experimental error, and is successfully overcome statistically, through increased sample size. Systematic errors, such as incursion of ambient air through the open top of the OTC's may have little impact on interpretation of OTC results if they are consistent among treatments. For example, the factors causing depression of bulk O₃ exposure in the present study in plum trees exposed to ambient air inside relative to outside of the OTC (Fig. 1) were likely consistent across all ozone levels applied inside the OTCs, and thus did not compromise the the yield response functions generated by Williams and DeJong (1993). It has been the prevailing view (e.g., Heck, 1989) that such chamber effects are not important, even if they exist, because yield reduction data are expressed on a relative basis. This may be not entirely a valid assessment. These bulk measurements are typically made at reference points just above the plants and may not equally reflect the full ozone exposure of each canopy, as discussed below.

2. Within-canopy distribution of microenvironmental parameters

Potentially more significant is the alteration of ozone distribution rather than bulk concentration surrounding the canopy of each individual plant. Important aspects of ozone concentration, penetration and distribution within plant canopies are known to be altered by OTC techniques, but have not been adequately analyzed. OTC techniques may mask important effects of canopy structure on ozone resistance of different crops. Identical concentrations of ozone monitored above the canopy within and outside the OTC may result in different levels of ozone at leaf surfaces and different rates of uptake by leaves. These are caused by the forced ventilation of the OTC design, abolishing or reorganizing cross-canopy ozone gradients relative to distributions observed under the less disturbed canopy microenvironment outside the OTC. An additional cause is the introduction of ozone-rich air below the canopy which reverses the normal gradient from top to bottom. The potential ramifications of these alterations are not well understood (Unsworth et al., 1984), though they

are certain to be expressed differently in short-statured, dense canopies than in tall, rough tree canopies. Significantly, the National Crop Loss Assessment Network studies examined primarily short-statured, row crops. Even in managed pasture (Fuhrer, 1994), a very short-statured plant system, substantial effects of the OTC on coupling of the canopy to the atmosphere, gradients of environmental parameters, and effectiveness of stomatal control of ozone uptake were observed. Currently these OTC techniques are being extended to trees of horticultural and native species (e.g., Kats et al., 1985). In the present study we examine these issues in trees.

In OTC experiments for CO₂ exposure, design improvements led to achievement of ca 30 ppm differentials between the center of each chamber and the target, reference concentration, but a gradient of ca 100 ppm across the canopies within each OTC (Leadley and Drake, 1993). Windspeed was reduced relative to outside and was constant, with heating to ca 3°C above the outside canopy. OTC effects on plant growth were observed and attributed specifically to a large number of interacting microenvironmental parameters, and not to one or a few dominant factors. These authors conclude that greater turbulence within OTCs would represent the most significant remaining improvement in OTC design. In the present study, the presence of the OTC significantly altered the diurnal pattern of O₃ exposure at the leaf and its tracking of regional O₃ fluctuations (Fig. 2). These results are discussed further below. They are presented here to emphasize the potential importance of the problem addressed in this study.

In the early days of OTC design, low air flow rates were associated with gross underestimation of pollutant uptake (Roberts et al., 1987). Early chambers (Thomas, 1951; Katz and Lathe, 1939) achieved air exchanges of < 1/min. Use of these chambers led to gross underestimation of sensitivity (of various conifers to SO₂), because low wind speeds and inadequate turbulence reduced actual transport to the canopies, despite accurately measured bulk concentrations within each chamber.

Most considerations of chamber effects deal with light (quality and quantity), temperature (leaf and air), water (vapor loss and liquid supply) and air movement (linear velocity and volume exchange rate). These are the principal factors that define a field environment, and that must be approximated to assure a valid comparison between ambient chamber and "no-chamber" plants. The history of chamber technology has been reviewed by Roberts et al. (1987). More recent exposure chambers use 2-4 air changes per minute, and have reduced, but still potentially biologically meaningful, effects on canopy microenvironment. Wiltshire et al. (1992) have applied modern design principles to the problem of exposing large

trees, including ca four air changes per minute and removable chamber walls to reduce the duration and extent of the unavoidable elevation of temperature inside. Nevertheless, increased humidity and temperatures were observed. The chambers used in the current study are sufficiently advanced in this sense (Table 1). Nevertheless important differences were noted in growth and yield parameters of ambient-exposed trees grown inside and outside of the OTC (Table 2).

It is not surprising that the interaction of OTC design and canopy morphology should have a large impact on ozone distribution and uptake within the canopy. In outside trees a large range of factors, including leaf area and site location, uncoupled fluxes measured to individual leaves from both bulk ozone concentrations and from bulk (ground surface area) deposition velocity (Taylor and Hanson, 1994). Using potted tobacco plants inside and outside of an OTC demonstrated that visual damage was strongly related to ozone concentration inside but not outside, and that transformation of the exposure to a common flux basis led to consolidation of all data (collected inside and outside) into a single sigmoidal relationship (Grunhage et al., 1993).

C. Ozone Uptake

1. Microenvironmental impact

These localized environmental parameters control plant growth and development. They also impact ozone deposition to all external and internal plant surfaces through effects on leaf wetness (Grantz et al., 1994b) and aerodynamic resistances, laminar boundary layer resistances and stomatal resistances (Tingey and Taylor, 1982; Baldocchi et al., 1987). Modern exposure chambers typically achieve air velocities of $> 0.5 \text{ m s}^{-1}$ over the leaf surfaces (Roberts et al., 1987). A major recognition of the importance of air movement is the introduction of fans or stirring paddles as in the continuously stirred tank reactor (CSTR) of Heck et al. (1978).

Transport of water vapor, carbon dioxide and ozone between the bulk atmosphere, plant canopies and intercellular spaces appear to be regulated in a similar fashion. Recent demonstrations that ozone concentrations are reduced to near zero within leaves (Laisk et al., 1989) is further support for the analogy between transport of ozone and either water vapor or carbon dioxide. The high internal conductance for evaporation from cell walls, and widespread distribution of evaporation sites (Tyree and Yianoulis, 1980) is similar to the widespread distribution, high capacity and non-limiting conductance of antioxidant reactions that mediate ozone destruction within leaves in the model of ozone uptake of Hanson and Taylor (1990). This contrasts with the spatial separation for water and CO_2 (Taylor et al., 1989) and a

postulated separation for water and ozone (Taylor et al., 1982ab) based on solubility arguments. The relationship between water and ozone fluxes may not be fortuitous, as suggested (Taylor et al., 1989; Taylor and Hanson, 1994), if conductance for evaporation and for biochemical reduction of ozone are equally non-limiting to fluxes. Ozone is likely degraded at the cell wall, similar to evaporation, rather than at the cell membrane (Mudd, 1982; Chameides, 1989). Canopy conductance to ozone has been shown to be larger than for water vapor (Kaplan et al., 1988; Massman and Grantz, 1994). In both cases the cuticular conductance can generally be ignored (Taylor and Hanson, 1994; Gross and Wagner, 1992).

Canopy structure may influence ozone impact on specific plants in ways related to canopy transport processes. This has been recognized for some time (e.g., Bennett and Hill, 1975; Reich et al., 1990; Taylor et al., 1989). These effects may be incompletely expressed using OTC techniques. Inhibition of photosynthetic capacity has been demonstrated following exposure of individual leaves to ozone (Grantz et al., 1992; Reich, 1983; Reich and Amundson, 1985; Roper and Williams, 1989), and associated with accelerated senescence. Ozone depletion by canopy elements and effects on distribution and magnitude of the canopy scale of photosynthetic inhibition remain uncharacterized. Modeling efforts demonstrate that effects of canopy screening on photosynthesis may be quite significant (Reich et al., 1990).

Many early (Thomas, 1951; Katz and Lathe, 1939; Heck et al., 1968; Houston and Stairs, 1973; Roberts et al., 1987) chambers introduced air at the top. Subsequent designs used the rough equivalence of whole canopy deposition velocities inside and outside the chamber as an indication of adequate air movement within the chambers (Bennett and Hill, 1973; Unsworth and Mansfield, 1980). These design considerations have led to the current generation of open top chambers (e.g., those used in the current study), in which 2-3 air exchanges are introduced at the bottom and vented out the top, i.e., the reverse of the usual pattern of wind gust penetration from the top of the canopy. The result may be a pronounced inversion of the typical ozone concentration profile (Fig. 2).

The relationship between ozone at the leaf surface and ambient ozone concentration varied dramatically between inside and outside the OTC (Fig. 2). Outside the OTC, O_3 at the leaf surface remained roughly proportional to ambient ozone concentration, with small differences between zones within the canopy. Inside the OTC, ozone at the leaf surface remained relatively unchanged up to an ambient O_3 concentration of ca 80 ppb. Above this concentration, ozone at the leaf surface increased relative to that observed outside the OTC. This level of ambient O_3 concentration apparently reflected some threshold value above which ozone sinks associated with the chamber became saturated. Leaves in the interior of the tree

inside the chamber had higher $[O_3]$ at the leaf surface than did those at the exterior of the tree. Blower location or encroachment of ambient O_3 through the top of the chamber may have contributed to this.

The impact of localized concentrations of ozone within canopies is not limited to photosynthetic responses of leaves. Ornamental flowers may be devastated directly by contact with ozone (Los Angeles County Arboretum, unpublished). and postharvest quality of fruit may be similarly affected. Plums harvested at commercial maturity from the present experiment (Crisosto et al., 1993) exhibited greater rates of desiccation and greater responsiveness to exogenous ethylene stimulation of ripening when grown under high than low concentrations of ozone. Differences in wax and cuticle structure on fruits from the different treatments suggest, but do not prove, that local ozone concentration at the fruiting site within the canopy may be responsible.

2. Coupling of leaves to the environment

Aerodynamic and boundary layer resistances to gaseous transport can effectively uncouple individual leaves and fruits from pollution concentrations in the bulk atmosphere. This has been modeled (Jarvis and McNaughton, 1986) and demonstrated experimentally (Grantz and Meinzer, 1990; Meinzer and Grantz, 1989) for water vapor.

a. Redundant measures of transpiration. In these previous experiments we used micrometeorological techniques along with simultaneous single leaf measurements of gas exchange and stomatal conductance to obtain independent measures of transpiration at leaf and canopy levels in order to partition canopy structure and stomatal effects on gaseous transport in sugarcane (Meinzer and Grantz, 1989). Micrometeorological techniques are not feasible in small experimental plots, nor in OTC's. In the present study single stem measurements of water flux using stem-flow gauges and measurements of within-canopy gradients of trace gas concentrations were substituted for the micrometeorological measurements, as we had previously done in coffee hedgerows (Gutierrez et al., 1994). Measuring fluxes at these two levels of biological organization allows a determination of the effectiveness of stomatal closure in reducing ozone deposition by allowing calculation of the magnitude of aerodynamic and boundary layer conductances (Fig. 3). We examine the effects of canopy structure and fumigation protocol because experimental protocols such as OTC techniques that substantially reduce boundary layer thickness with fans or blowers unavoidably overestimate the significance of stomatal closure. This confounds the interpretation of studies in which drought induced stomatal closure has been found to confer protection against ozone damage (e.g., Temple, 1988; Temple et al., 1988a; Temple et al., 1988b).

The stem-flow gauges provide a total water flux for a single branch, corresponding to the sum of the transpiration of all leaves downstream of the site of gauge attachment. Individual gauges may be correspondingly summed to provide an estimate of total canopy transpiration. Orchard water requirements have been evaluated with these (Devitt et al., 1993), but air pollution effects have but rarely been investigated using them (e.g., van Wakeren et al., 1987).

In chambers, ozone uptake is easily uncoupled from ozone concentration, as is carbon assimilation from CO₂ concentration, by diurnal or experimental manipulation of temperature, VPD or humidity, through changes in stomatal conductance. Stomatal control of trace gas fluxes is substantial only when it represents the limiting resistance in the gas phase pathway. In the studies of Gross and Wagner (1992) use of bulk ozone concentration measured in the chamber was not a useful predictor of biological impact, specifically because of environmentally induced changes in stomatal conductance.

D. Effective Dose

Though bulk air concentrations of ozone represent an easily monitored exposure statistic and a convenient regulatory standard, use of such bulk values in secondary standards for plant protection relies on an implicit assumption that transport of ozone between the monitor height and leaf surfaces is comparable, in different species, different OTC designs, and in OTC and field environments. While differences between species of vegetation have been recognized as influencing the surface resistance for dry deposition of ozone on an airshed scale (e.g., Baldocchi et al., 1987; Grantz et al., 1994a; Weseley, 1989) these differences have not been widely considered in relating atmospheric concentrations to effective doses of ozone in different species and experimental conditions (Lefohn, 1992). An important conclusion is that secondary air quality standards may not lead to similar levels of protection for all crops and native species, even those for which similar dose response functions have been observed using OTC techniques.

The need to base exposure on plant uptake has been recognized for some time (Runeckles, 1974) but recent advances in instrumentation have made this more feasible. Development of methods to characterize the average concentration of ozone and water vapor at leaf surfaces within and outside of OTC's provides a protocol, based on the leaf surface as a reference point, for comparing different OTC experiments and for extrapolating OTC results to the field environment for regulatory purposes. Information on ozone concentrations at leaf surfaces also allows generalization of experimental results to other microenvironments in which similar concentrations at leaf surfaces are determined experimentally, or which can be back-

calculated from microenvironmental data and OTC design criteria. Specification of ozone concentration at the leaf surface normalizes experimental factors other than physiological parameters, between different exposure protocols. Ultimately, it is the flux to the leaf interior that must determine the magnitude of ozone damage (Tingey and Taylor, 1982), as discussed in detail by Taylor et al. (1982b, 1989). The concept of dose rather than exposure relates air quality physiological methods to the well-established methods of environmental toxicology.

E. Current Study

This report details measurements made in an open top chamber (OTC) investigation of plum trees, conducted over multiple years at the University of California Kearney Agricultural Center, in the central San Joaquin Valley. Measurements of yield, vegetative growth, reproductive development and photosynthetic rates have been reported as a function of ozone exposure (Williams et al., 1993). In the present study only equivalent trees growing in ambient air inside and outside of OTC's were heavily instrumented and sampled for two years. The approach has been to monitor the spatial distribution of trace gas concentrations within each canopy and to use gradients and fluxes of water, which can be measured as a vapor and as a liquid, to infer fluxes of CO₂ and O₃ in the open canopy without the potential artifacts of single leaf or branch enclosures. The objectives were to: 1) contrast the distribution of ozone and microenvironmental parameters within canopies of those trees exposed to ambient ozone, inside and outside of OTC's, and to contrast the factors controlling ozone transport in the two microenvironments, 2) determine ozone concentrations at leaf surfaces, allowing data from different OTC designs, field experiments, and single leaf chamber experiments to be compared on a compatible basis, 3) determine the effect of OTC protocols on partitioning of control of ozone deposition between stomatal and aerodynamic (boundary layer) factors, allowing evaluation of potential mitigation strategies, such as drought protection, against ozone damage, and 4) combine radiation, humidity, photosynthesis and stomatal conductance data with values for ozone concentrations at various canopy levels to model ozone uptake by leaves as a function of environmental condition and canopy position.

III. MATERIALS AND METHODS

A. Field Site

This study was conducted between 8 June 1992 and 17 September 1992 in an orchard of 4 year old plum trees (*Prunus salicina* cv. 'Casselman' on 'Citation' dwarfing rootstock) located at the University of California, Kearney Agricultural Center, Parlier, CA (Fig. 4). The orchard was located near Fresno, California, in the central San Joaquin Valley (36° 36' N, 119° 30' W).

The plum orchard was planted in April 1988 for a study previously funded by CARB, utilizing Open Top Chambers (OTC). Complete descriptions of the OTC protocol and horticultural measurements are contained in Williams et al. (1993). Trees were planted at 1.83 x 4.27 m spacing and irrigated twice weekly by low volume microfan sprinklers (ca 200 liters/tree/week). Groups of four adjacent trees were enclosed by individual OTCs and subjected to one of three ozone treatments. Additional groups of trees outside represented non-chamber controls.

The OTCs were ca 3 m tall, adequate to contain the pruned trees which had been grafted to a dwarfing rootstock (Citation). The OTC frames were constructed from extruded aluminum frames attached to redwood bases, both of which remained in place continuously from November 1988. The bases were 3 x 7 m, containing 4 trees.

The air distribution system within the OTC consisted of a blower mounted outside the chamber, capable of providing ca 133 m³ min⁻¹ of conditioned air. The air passed through 23 cm. diam. flexible plastic tubing (Arizona Bag and Plastic Co., Phoenix, AZ), with 8.5 x 8.5 cm. holes on the upward facing surface, spaced every 30 cm. There were 4 such tubes per chamber. Two were installed at 1.5 m height, along the chamber walls, and two at ca 2.0 m height, along each side of the main trunk of the trees (Fig. 9).

The ambient chamber studied in the present experiment received ambient air that passed only through a dust filter. The blowers were operated constantly from April to November.

Individual trees in two adjacent rows near the center of the orchard were selected for intensive within canopy micrometeorological and physiological investigation. One of the trees was located within ("IN") an OTC fumigated with ambient air. The other in an adjacent row, was located outside ("OUT") of the OTC in ambient air.

B. Data Collection, Storage, and Retrieval

Two tripods were positioned in the interrow area to support the data logging equipment (Fig. 5) and instruments such as a CO₂ and H₂O analyzer (Infrared Gas Analyzer, LI6252; LICOR, Inc. Lincoln, NE), and an ultraviolet spectrophotometric ozone analyzer (Model 1003 AH, Dasibi Corp., Glendale, CA). Additionally two 12 port sequentially sampling solenoid valves (Scanivalve Corp., San Diego, CA) sampled air from various canopy positions. All data were collected, and initial data reduction performed, using two data loggers (21X) with three attached analog multiplexers (AM416) (Fig. 5). Data were automatically transferred to solid state storage modules (SM192; all from Campbell Scientific, Inc., Logan, UT) for subsequent downloading to a personal computer for further reduction and analysis in the laboratory.

C. Microenvironmental Measurements

1. Within-canopy

An instrument tripod (CM10, Campbell Scientific) for mounting crossarms and sensors was positioned near each of the two trees used in the study (Fig. 6).

Three horizontal crossarms (Figs. 6, 7), extending from outside the canopy to within the canopy of the trees, were deployed at 1.5 m, 2.0 m, and 2.5 m above ground level. Sensors were placed at three positions across each of these arms, with specific sensor positions determined by canopy structure. For the tree outside the OTC, using the lowest, innermost position (location 7; see Figure 8) as a zero reference for measurement of horizontal distance, sensors on the lowest arm were placed at 0.0 m, 0.04 m, and 0.11 m. The middle arm had sensors at 0.01 m, 0.06 m, and 0.11 m. The upper arm had sensors at 0.02 m, 0.07 m, and 0.11 m. Within the OTC, using location 7 as reference, sensors on the lower arm were at 0.0 m, 0.03 m, and 0.12 m. The middle arm had sensors at 0.01 m, 0.02 m, and 0.12 m. The upper arm had sensors at 0.0 m, 0.03 m, and 0.12 m.

Thus microenvironmental sensors were located throughout the canopies of the trees inside and outside the open top exposure chamber (OTC), with location 3 (Fig. 8) approximating ambient conditions outside the canopy. Within canopy measurements were obtained at nine locations throughout the canopy of each tree (Fig. 8). At each of the nine grid locations within the canopy, ambient air temperature (T_a), PPFD, and air samples for determining concentrations of CO₂, H₂O, and O₃ were obtained.

Air temperature at each location was measured using a fine-wire type T thermocouple (TT-T-40, Omega, Inc., Stamford, CT) secured at the ends of the tubes used to obtain the

trace gas samples. Photosynthetically active radiation at each location inside the canopy was measured using a gallium arsenide phosphide (GAASP) photodiode (#G1118, Hamamatsu, Corp., Bridgewater, NJ). GAASP sensors were calibrated against the mean of two LICOR LI-190SA quantum sensors. Within canopy temperature and PPFD were measured every 2.5 s and recorded as 30 minute averages. Leaf temperature (T_l) was measured with a fine-wire type-T thermocouple appressed to the middle of the underside of one leaf per location, attached to the petioles with tape, and located within 5 cm of the thermocouples measuring T_a .

Concentrations of the three trace gases CO_2 , H_2O , and O_3 were determined simultaneously at each location, with the 18 (9 x 2 trees) grid locations sampled sequentially. Concentrations of CO_2 and H_2O were determined with a single IRGA and concentrations of O_3 with a single UV analyzer.

At each location, one of eighteen sampling tubes (3.2 mm i.d. polyethylene lined ethyl vinyl acetate tubing (Bev-A-Line IV, Cole-Parmer Instrument, Co., Chicago, IL) was secured. The 18 sections of tubing were of equal length (4.88 m). The sampling tubes were connected directly to the Scanivalve. The data logger controlled sequential sampling of the nine locations in each of the two canopies. Six of the 24 ports of the Scanivalve were not used. Gas flow proceeded from the sampling location to the Scanivalve, then to the ozone analyzer, then to the IRGA, and finally to a dual vacuum pump (Gast model RAA-V110-EB, Gast Mfg. Corp., Benton Harbor, MI) which aspirated the system. Each of the 17 sampling lines which were not involved with obtaining the current sample were continuously purged at a flow rate exceeding 1.2 l min^{-1} . Sampling flow rate was maintained at 2 l min^{-1} as measured by the rotameter attached to the ozone analyzer. For each location, 40 s were allowed to purge the instruments and sample tubes of the preceding sample, followed by 60 s of measurements at 5 s intervals. Data were averaged over the 60 s interval and output to the storage module. All 18 positions were sampled once per 30 minute cycle.

Ambient temperatures and concentrations of CO_2 , H_2O , and O_3 were recorded for 65 days during the period DOY 190 through DOY 267 (DOY 190, 198-224, 227-254, 259-267). Within canopy PPFD was recorded for 41 days of this period (DOY 227-267). Data are presented as averages of all days of measurement, over the hours specified in each figure or table.

2. Above-canopy

Some microenvironmental conditions were also monitored at 4 m above ground level in the interrow area (Fig. 7). Wind speed and wind direction were measured with a cup anemometer and wind vane (model 3301/3101-5 Wind Sentry set; R. M. Young Co., Traverse

City, MI). Photosynthetically active photon flux density (PPFD) was measured with a quantum sensor (LI-190SA; LICOR, Inc. Lincoln, NE), and total incoming solar (short wave) radiation was measured with a pyranometer (LI-200SA; LICOR). Sensors were interrogated every 5 s, and recorded as 30 minute averages.

D. Canopy Zone Designations

The nine canopy locations in each tree were combined into "zones" to provide four distinct and well-characterized parts of the canopies. Designation of these zones facilitated obtaining additional physiological (gas exchange) and sap flow measurements that were not feasible in all 18 locations. An interior ("INTER") zone and an exterior ("EXTER") zone, combined locations 1 and 4, and locations 2 and 5, respectively (Fig. 8). The zones in trees outside ("OUT") the OTC were designated, e.g., 'EXTEROUT' and 'INTEROUT', for the exterior and interior portions, respectively, of the outside tree. The zones inside ("IN") the OTC were designated 'EXTERIN' and 'INTERIN' for the exterior and interior portions, respectively, of the inside tree. For clarity, and because these four zones are better characterized with less variable averaged data than the individual 9 locations per tree shown in Fig. 8, all comparisons in the figures and tables are performed on the basis of the zones.

Air was delivered to the trees, after appropriate conditioning for ozone control, by a series of sheet metal and perforated plastic distribution tubes (Fig. 9 A), to the bottom and center of the tree canopies (Figs. 8, 9B). Each zone thus had a contrasting exposure to the ambient wind (OUTSIDE) or to the ducted air stream (INSIDE).

E. Additional Measurements

1. Within-canopy wind

At each of the two locations within each zone, a hot-wire air velocity transducer (FMA603V, FMA601V, FMA600V, or FMA600I; Omega Inc., Stamford, CT) was deployed to measure wind speed within the zone (Fig. 8).

2. Transpiration

Xylem sap flow (mol s^{-1}) associated with a scaffold branch within each zone was measured using replicated stem-flow gauges (Dynamax, Inc., Houston, TX), based on on Stem Heat Balance method. Within each zone, two stem flow gauges, one 10 mm gauge (SGA10) and one 19 mm gauge (SGB19), were used. The two gauges within a zone were placed either on separate branches, or the 10 mm gauge was placed downstream from (above) the 19 mm gauge.

The Stem Heat Balance method is based upon continuous heating of a stem section over a short vertical distance. Errors may result from uncontrolled sources of energy (heat) affecting thermocouple and thermopile voltage outputs. After the gauges were installed on the trees in this study, they were operated for four days with no power supplied to the heater to determine whether any substantial external source of heat was affecting the voltage output signals. The results were similar over the four days. A detailed evaluation of temperature gradients across the heater (stem ΔT) for each of the eight gauges indicated that there was little effect attributable to external sources of heat. Maximum stem ΔT was $< \pm 0.5^\circ \text{C}$. Software assigned a value of sap flow = 0 to observations with stem $\Delta T < 0.5^\circ \text{C}$. The output for these four days appropriately indicated no sap flow.

3. Leaf area

Estimates of total leaf area per zone were necessary to describe sap flow on a leaf area basis. Such units are also compatible with gas exchange measurements of water vapor flux. A manual but relatively quick and accurate method of estimating leaf area was required, since automatic canopy analyzers (e.g., LICOR LA1 2000) were impractical for use in these plum canopies without calibration, particularly in the OTC, and automatic leaf area meters require complete defoliation. Therefore a modified destructive harvest was employed. A number of leaves were collected from the plum trees, and their length (from leaf base to leaf tip) and their width (across the broadest part of the leaf) were measured. Actual areas of these individual leaves were then determined (Fig. 11) with a LI-3100 Area meter (LICOR, Inc., Lincoln, NE) (Fig. 11). Regressions of leaf area on leaf width and on leaf length were evaluated to determine if either dimension alone was sufficient for predicting leaf area. This was not successful due to pronounced curvilinearity (Fig. 12). Regression of area on leaf length multiplied by leaf width, however, resulted in an excellent regression statistic for predicting actual leaf area (Fig. 13).

For estimation of leaf area per zone, the length and width of each and every leaf of all sizes located downstream of each sap flow gauge was measured. The regression equation was then used to predict the actual leaf areas in the four zones. Sap flow on a per gauge basis was then transformed to a leaf area basis.

4. Leaf water potential

During three days of the study (DOY 238, 240, and 247), water potential measurements of exposed, transpiring leaves in each canopy zone ($n=4$ leaves/zone) were made at 1000 and at 1400 hours with a Scholander-style pressure vessel. Soil water potential in the root zone was taken to be near 0 Mpa, because of the frequent irrigation regime.

5. Gas exchange measurements

On six representative days of the study (DOY 205, 219, 238, 240, 247, 253), gas exchange measurements were conducted simultaneously in the canopies inside and outside the OTC, by two operators using two independent portable photosynthesis systems (LI 6200, LICOR Inc., Lincoln, NE). Standard operating procedures for calibration and operation of these instruments were followed, as recommended by the manufacturer. Values for stomatal conductance ($g_{s,v}$), net carbon assimilation (A), and intercellular CO_2 (C_i) were recorded, as well as data identifiers and Quality Control parameters (e.g., change in relative humidity in the leaf cuvette), for downloading to a personal computer for subsequent reduction and analysis in the laboratory.

Downstream of each of the sap flow gauges, four diverse but representative leaves were selected for gas exchange measurements, to sample the full range of variability in environment, leaf morphology and phenology exhibited in each zone. Microenvironments for individual leaves in each of the designated zones within the canopy were variable, ranging from fully shaded leaves in the cooler interior regions to fully sunlit leaves at the top of the zones. Leaf condition and morphology were also highly variable, with newly expanded leaves and leaves several months old existing simultaneously within any given zone. Eight leaves were sampled per zone, resulting in a diurnal course of 6-8 time points of 32 observations each, per day. Sampling leaves of all ages, covering the range of ambient environmental conditions to adequately represent gas exchange on a zone basis, resulted in some variability in measurements of stomatal conductance and carbon assimilation for particular zones and times.

As part of the Quality Control protocol, following completion of the 16 gas exchange measurements (8 leaves/zone x 2 zones/tree), the instrument operators and their assigned instruments inside the OTC exchanged places with those outside the OTC. This removed possible bias attributed to either instrument or operator.

Regression of conductance against time of day (see Fig. 50, below) was used to obtain a smoothed, diurnal time course of conductance for each of the four zones in the canopy for a representative, composite, day. The same procedure was used to provide a representative daily time course of carbon assimilation (see Fig. 59, below).

F. Instrument Maintenance, Calibration, and Quality Assurance

Inspection and maintenance of the large number of sensors and recording instruments was part of the daily Quality Assurance protocol. Each morning, the temperature readings

from the 18 thermocouples measuring ambient temperature were viewed in real time as a means of detecting thermocouple malfunction. The 12 leaf thermocouples were treated similarly, as well as being physically inspected to insure that contact with the underside of the leaf surfaces was maintained. Malfunctioning thermocouples were replaced immediately. Data from all other micrometeorological sensors were viewed in real time to detect malfunction.

The LI 6262 infrared gas analyzer was operated in absolute mode, with calibrations for CO₂ and H₂O performed as specified by the manufacturer, using a CO₂ reference gas of known concentration (503.1 ppm) and a LI-610 Dew Point Generator (LICOR, Inc.) for generation of a moist stream of air of known dew point. Calibrations were performed for CO₂ whenever the reading on the reference gas varied from the previous calibration by more than 0.5 ppm. Calibration for water vapor was more tedious and less precise than for CO₂, confounded by variable water vapor adsorption, temperature variations, and pressure effects introduced during calibration. Long equilibration times were required. Recalibration for water vapor was routinely performed twice weekly.

GAASP photosensors were calibrated against two factory-calibrated quantum sensors (above). Anemometers and net radiometers had all received factory calibration by the manufacturer.

G. Calculations

1. Gaseous flux and leaf surface concentrations

A general transport equation derived from Ohm's Law was used to describe the transport of several different species, with specific equations developed for heat, water vapor, CO₂, O₃, or other species of interest.

Utilizing the model for resistances in series, concentrations of H₂O vapor, CO₂, and O₃ at the leaf surface (e_s , C_s , and O_{3s} , respectively) were calculated assuming conservation of gaseous flux over the entire path being considered without appreciable flux divergences:

$$F = \Delta c_j / r_j \quad (1)$$

where F is the diffusive flux of the specific trace gas (j), Δc_j is the driving force or concentration gradient for H₂O, CO₂, or O₃ (V , ΔC , and ΔO_3 , respectively) based upon leaf interior concentrations (e_i , C_i , and O_{3i} , respectively) minus either concentrations at the leaf surfaces (e_s , C_s , and O_{3s} , respectively), within the canopy zones (V_z , ΔC_z , and ΔO_{3z} ,

respectively), or at the external ambient reference points (V_a , ΔC_a , and ΔO_{3a} , respectively), and r_j ($r_j=1/g_j$) is either the stomatal resistance to H_2O , CO_2 , or O_3 ($r_{s,v}$, $r_{s,c}$, and r_{s,O_3} , respectively; for use with stomatal conductance) or total (stomatal plus boundary layer) resistance to H_2O , CO_2 , or O_3 , to the canopy zone reference points ($r_{tz,v}$, $r_{tz,c}$, and r_{tz,O_3} , respectively) or to the external ambient reference point ($r_{ta,v}$, $r_{ta,c}$, and r_{ta,O_3} , respectively).

The resistances to gaseous transfer through the stomata, the leaf boundary layer and the aerodynamically structured canopy boundary layer may be considered to be in series. A simplified flux model, partitioning the gradients according to the ratio of resistances, may be employed to calculate the leaf surface concentration of any trace gas.

For water vapor flux, the general transport equation becomes:

$$r_j = V_j / E \quad (2)$$

Where r_j is total resistance to H_2O vapor incorporating both stomatal and nonstomatal components to either the within-canopy zone reference points ($r_{tz,v}$), or to the ambient reference point exterior to the canopy ($r_{ta,v}$). V_j represents the driving force, specified as the difference between saturation vapor pressure at leaf temperature and the vapor pressure measured at the same reference point used for determination r_j (V_z or V_a , mol/mol). E (flux) is transpiration on a leaf area basis ($mol\ m^{-2}\ s^{-1}$). Stomatal resistance was obtained as the inverse of measured values of stomatal conductance. Nonstomatal resistance was determined by subtracting stomatal resistance from total resistance. Total resistance was calculated from Eq. (2) using flux determined for each zone by stem flow gauges.

The laminar boundary layer conductance associated with individual leaves in each canopy zone was calculated from characteristic leaf dimensions (mean leaf width in each zone) and mean wind velocity in each zone.

Stomatal, nonstomatal, and total resistance values appropriate to CO_2 and to O_3 were converted from values appropriate to transfer of H_2O vapor by multiplying the resistance to water vapor by the ratio of diffusion coefficients of water vapor and the trace gas being considered:

$$r_i = r_{H_2O} (D_{H_2O} / D_i)^x \quad (3)$$

where r_i is resistance for the desired species (i), r_{H_2O} is resistance to H_2O vapor, and D_{H_2O} and D_i are the diffusion coefficients for the respective compounds as they diffuse in air (Jones,

1983). The value of x was taken as 1.0 for stomatal resistance and 0.67 for transport by diffusion through the quasi-laminar boundary layer (Jones, 1983).

To obtain total resistance to CO_2 and O_3 the nonstomatal and stomatal components for each gas were summed. Conductance values were obtained as the inverse of the sum. Leaf surface H_2O vapor pressure (e_s) was calculated as:

$$e_s = e_i - V_s \quad (4)$$

where e_i is saturation vapor pressure within the leaf based on leaf temperature, and:

$$V_s = r_s(E) \quad (5)$$

where E is transpiration on a leaf area basis, estimated by sap flow gauges and measured leaf areas above each gauge.

Flux of CO_2 (A) was calculated as the CO_2 gradient (ΔC) divided by the total resistance to CO_2 , ($r_{t,c}$) with the resistance term obtained from the total resistance to H_2O vapor according to Eq. (3). The CO_2 gradient was estimated by subtracting hourly average CO_2 concentration (measured in each zone as the average of concentrations prevailing one day prior and one day after each gas exchange measurement day) from intercellular CO_2 concentration. This method of estimating CO_2 concentration at each zone was necessary because human respiration during the gas exchange measurements influenced CO_2 concentration in the canopy on the actual days gas exchange measurements took place. Intercellular CO_2 concentration was calculated from the general transport equation as:

$$C_i = C_z - A/g_{s,c} \quad (6)$$

Where A and $g_{s,c}$ are the average, hourly net carbon assimilation rate and the stomatal conductance to CO_2 from single leaf gas exchange measurements, respectively, as measured on each of 6 days (LI 6200), and converted from water vapor using Eq. (3).

The calculation of leaf surface CO_2 concentration (C_s) utilized the same principles as Eq. (4).

O_3 flux (F_{O_3}) was computed using the calculated total resistance to O_3 (r_{tz,O_3}) multiplied by the O_3 gradient between leaf interior (concentration assumed zero) and each zone (ΔO_{3z}). Having obtained F_{O_3} and r_{tz,O_3} , calculations paralleling those for leaf surface water vapor pressure were used to determine leaf surface O_3 concentration in each zone.

2. Environmental coupling

Relative control of canopy water loss by stomata was estimated as a slightly modified version of the single leaf-canopy-atmosphere decoupling coefficient Omega (Ω), described by Jarvis and McNaughton (1986) and McNaughton and Jarvis (1983) as:

$$\Omega = (\varepsilon + 1) / (\varepsilon + 1 + [g_{ba,v} / g_{s,v}]) \quad (7)$$

with $\varepsilon = \Delta / \gamma$ (8)

and $g_{ba,v} = 1 / (1 / g_{la,v} - 1 / g_{s,v})$ (9)

and $g_{la,v} = E * P / V_a$ (10)

in which Δ is the slope of the saturation vapor pressure versus temperature relationship evaluated at air temperature (Penman, 1948), γ is the psychrometric constant, $g_{s,v}$ is stomatal conductance to water vapor on a leaf surface area basis, $g_{la,v}$ is total conductance to water vapor (stomatal and boundary layer components) on a leaf surface area basis, E is transpiration as measured by stem flow gauges on a leaf surface area basis, P is atmospheric pressure, and V_a is leaf to air vapor pressure difference evaluated at leaf temperature (saturation vapor pressure) and at the vapor pressure outside the canopy (ambient).

An additional calculation to quantify the importance of a stomatal feedback mechanism involving radiative coupling (decreased transpiration leading to increased leaf temperature and consequent increased outgoing long-wave reradiation following stomatal closure) was performed (Martin, 1989).

This was calculated as:

$$\Omega_R = \frac{\varepsilon + 1 + g_r/g_{ba,v}}{\varepsilon + 1 + g_{ba,v}/g_{s,v} + g_r/g_{s,v} + g_r/g_{ba,v}} \quad (11)$$

where:

$$g_r = \left(4\sigma T_a^3 / C_p \right) \quad (12)$$

in which g_r is in $\text{mol m}^{-2} \text{s}^{-1}$, σ is the Stefan-Boltzman constant in $\text{W m}^{-2} \text{K}^{-4}$, T_a is the air temperature at the ambient reference point converted to $^{\circ}\text{K}$, A is leaf area index, C_p is the specific heat of dry air at constant pressure in $\text{J mol}^{-1} \text{K}^{-1}$, P is atmospheric pressure in Pa, and R is the gas constant in $\text{Pa m}^3 \text{mol}^{-1} \text{K}^{-1}$. Eq. (11) has been modified by: 1) excluding a leaf area term (A , in Martin, 1989) because our conductance values are in molar units on a leaf area basis, and 2) correcting an error in Martin (1989) in which Eq. 12 was inappropriately scaled by the gas law term, P/RT_a .

Whole plant hydraulic conductance (L_E) was calculated as:

$$LE = \frac{E}{0 - \Psi} \quad (13)$$

where the liquid flux of water through a given scaffold branch in each zone (E) was determined by sap flow gauge, and the water potential gradient driving the flux from soil to leaf was taken as the transpiring leaf water potential with the assumption that the root environment was at 0 MPa. LE was additionally normalized to a leaf area basis (L_E/m^2) by dividing by the total leaf area downstream of the sap flow measurement.

Data presentation. Micrometeorological variables and concentrations of atmospheric trace gases (H_2O , O_3 , CO_2), recorded as 30-minute averages (see Methods), are presented as either 1) diurnal courses averaged over all 64 sampling days, 2) single averages of all measurements over the season, or 3) as partial diurnal patterns averaged over a several hour period on the days on which intensive physiological measurements were obtained. The presentation mode is specified in each case.

III. RESULTS AND DISCUSSION--ENVIRONMENTAL EXPOSURE

A. General Environmental Conditions and Canopy Effects

The summer growing season in the San Joaquin Valley is hot, dry and generally cloudless. The valley experiences among the lowest wind velocities of any comparably-sized area in the world.

1. Wind

Wind speed measured with a cup anemometer at 4 m above the ground generally increased from around 0.3 m s^{-1} in the early morning to around 1.6 m s^{-1} at 16:00 PDT (Fig. 14). In the late afternoon, wind speed was on the order of 1.2 to 1.6 m s^{-1} . The day to day variability of wind speed was quite small in the morning, but became larger in the afternoon.

Wind direction exhibited a consistent diurnal pattern, shifting from ESE (110°) in the early morning to WNW (300°) in the late afternoon (Fig. 14). The day to day variability of wind direction decreased with time of day, with variability small in the late afternoon when the strongest winds were experienced.

Within the canopy, air movement was measured using hot wire anemometers placed in each zone, perpendicular to the flow. These zones are used for all microenvironmental and physiological comparisons because the variability is reduced, due to averaging two of the 18 positions for each zone (see Fig. 8). Air movement inside the OTC, driven by the blowers and air distribution system, was quite consistent throughout the day, and completely uncoupled from ambient wind. Velocities were slightly higher, with larger day to day variability, in the exterior than interior zone (Fig. 15A,B).

Outside the OTC, wind speeds were lower than ambient (cf. Figs. 14,15) and more consistent in the interior than exterior zone (Fig. 15C,D). Within-canopy wind speeds were higher in the exterior zone, where they were closely coupled to ambient wind. There was little difference in wind speed between interior zones of the canopy outside and inside the OTC (cf. Fig. 15B, D), while wind speeds in the exterior zone outside the OTC (EXTEROUT) were greater than anywhere inside the OTC (Fig. 15A, C).

2. Light

Above the canopy, photosynthetically active photon flux density (PPFD) was measured using a quantum sensor (LiCor, Inc.) at 4 m above the ground. PPFD exhibited a typical "bell-shaped" diurnal time course (Fig. 16). The small error bars reflect the slight seasonal trend in solar angle during the measurement period as well as the occurrence of one cloudy afternoon.

PPFD incident upon leaves in each zone was measured with small, rigidly fixed photodiodes (Fig. 17), or with the quantum sensor attached to the gas exchange cuvette (LI-6200) during measurements (Fig. 18). Both inside and outside the OTC, these measures of PPFD exhibited more irregular patterns and lower magnitudes than PPFD above the canopy due to sporadic shading of sensors by leaves and branches and (inside the OTC) by the chamber framework.

It is important to note that the time of day at which maximal PPFD is observed in each canopy zone depends on leaf orientation and which side of an individual tree is sampled (cf. Figs. 17,18). However, both types of measurements indicate that EXTERIN and INTEROUT were relatively shaded, while INTERIN and (particularly) EXTEROUT were subject to greater than half-full sun.

3. Temperature

Leaf temperature (T_l) is determined by all components of the leaf and canopy energy balance. In the daytime this includes heating by radiation interception, and cooling by reradiation, evaporation, and convection. At night the cooling and heating processes reverse.

The presence of each leaf within a canopy, and the presence or absence of the OTC had large impacts on each of these processes. Leaf temperature (T_l) increased monotonically in all canopy zones until ca 16:00, when it reached a maximum and began to decline (Fig. 19). The differences in leaf temperature between the four zones were relatively small (see below), with greater differences within the canopy inside than outside the OTC. During the physiologically most active midday period the interior zones were warmer than exterior zones, and inside the OTC was warmer than outside.

Air temperature within the canopy zones exhibited the same diurnal course as leaf temperatures (Fig. 20), driven both by contact with the illuminated leaves, and by the general rise in temperature of the regional air mass.

The difference between air temperature, within each zone, and leaf temperature was always below 1°C (Fig. 21 A, B, C, D). In general, depression of leaf temperature below air temperature ($\Delta T < 0^\circ \text{C}$) suggests transpirational cooling in the absence of full, direct sunlight. In full sun, leaves of most species, particularly woody perennial species such as plum with relatively low levels of stomatal conductance, are warmer than air temperature. Specific diurnal patterns of ΔT (Fig. 21) reflect the side of the canopy, relative to solar position, in which measurements were made (as with PPFD), cf. Figs. 17,18) and are not generalizable as characteristics of the canopy zone.

B. Effect of the OTC on Bulk Environmental Parameters

To characterize the effect of enclosure within an OTC, on the microenvironment in which experimental plants grow and develop, measurements were made at each of nine locations within each canopy. These values were then averaged, both spatially and over the entire measurement period, to construct composite diurnal time-courses.

Most OTC exposure studies characterize the exposure inside and outside of the OTC using measurements taken at a single reference point near and usually above the canopy. Such measurements typically demonstrate modest differences in microenvironmental parameters between trees inside and outside the OTC. These differences in bulk parameters are typically larger (e.g., Fig. 1) than the canopy averages presented here (Figs. 22-25). Inversion of the typical vertical gradients in environmental parameters (see below) suggests that spatial averages may provide more meaningful information.

1. Temperature

Ambient air temperature inside and outside the OTC exhibited typical bell-shaped (daylight hours) diurnal cycles (Fig. 22) with minima near dawn and maxima near 16:00. Air temperature inside the OTC was generally higher than outside the OTC throughout the 24-hour period, with the largest differences coincident with the highest temperatures.

Maximum differences were somewhat less than 2°C, small relative to the entire diurnal range of temperatures (Fig. 22), but large enough to contribute to substantial differences in degree growing days, or other statistics commonly used to predict plant growth and development. Temperature differences in the OTC study of Brewer and Ashcroft (1982), also at the Kearney Agricultural Center, but using different chambers, were slightly greater than 2°C, based on single reference points.

Turbulent mixing of air near the plum canopy with the bulk atmosphere was inhibited inside relative to outside the OTC, while the plastic walls caused a partial greenhouse effect. This latter effect was particularly significant in sunlight, but also retarded long-wave infrared reradiation and resultant leaf cooling at night (Fig. 22).

2. Water vapor

Water vapor concentration (Fig. 23) increased as the sun rose, peaked near solar noon, and dropped to a low level in late afternoon. The increase in water vapor concentration in the morning reflected strong transpiration from the plum canopy. The afternoon decline reflected reduced solar radiation (Fig. 16) and consequent reduced transpiration (E ; see Fig. 51, below) associated with stomatal closure ($g_{s,v}$; see Fig. 50, below), while atmospheric turbulence and eddy transport of water vapor away from the surface into the deep mixed layer observed in daytime remained strong. As solar radiation further decreased, turbulent transport of water

vapor away from the surface may have slowed more than E (see Fig. 51, below), causing water vapor concentration to increase transiently between 18:00 and 20:00. The greatest decline occurred between midnight and 06:00, as transpiration ceased and condensation occurred.

The H_2O concentration inside the OTC was consistently higher than outside the OTC, with measured differences as large as 3 mmol mol^{-1} occurring during the daytime period. Inside the OTC the turbulent mixing of humid air near the canopy with the relatively dry air outside was impeded by the physical barrier of the chamber walls, despite the large infusion and distribution of ambient air by the blowers.

The consequences of increased humidity inside the OTC (ca 5%; Table 1) could range from increased leaf expansion and woody tissue growth and increased fruit expansion, to increased incidence or severity of leaf and fruit fungal infection, to reduced E and the resulting reduction in delivery of mineral nutrients to the foliage through the transpiration stream. These potential consequences are consistent with the available data from the present experiment on morphological attributes and xylem sap flow (Tables 2, 4).

3. Carbon dioxide

The daily pattern of CO_2 concentration was dominated by the diurnal courses of photosynthesis and respiration, occurring in the plum canopy as well as regionally throughout the agricultural San Joaquin Valley. CO_2 exhibited a rapid drop at sunrise followed by a more gradual decline through the late afternoon (Fig. 24). Renewal of CO_2 was rapid from 19:00 to midnight, with slower recovery continuing until sunrise. Reversal of source and sink for CO_2 between day and night, and the suppressed turbulent mixing of the bulk atmosphere with the air inside the OTC, resulted in higher CO_2 concentrations inside than outside the OTC during nighttime (reduced venting of respiratory CO_2), and lower concentrations inside than outside during daytime (reduced renewal of photosynthetically fixed CO_2). The small peak during the late morning hours was consistently observed, and may be due to local vehicle exhaust associated with early morning field crews at the Kearney Agricultural Center. The magnitude of the OTC effect on CO_2 concentration was small, and not likely to have significant physiological implications.

4. Ozone

Bulk ozone concentration increased rapidly in the morning both inside and outside the OTC, due to regional photochemistry and circulation patterns. Ozone reached average maxima in the mid-afternoon of about 0.08 ppm inside and 0.09 ppm outside the chamber (Fig. 25). After sunset, mean O_3 concentration rapidly decreased to around 0.02 ppm, and further to ca 0.01 ppm by dawn. The average O_3 concentration inside the OTC was consistently lower

than outside the OTC, with a maximum difference of approximately 0.01 ppm in mid-afternoon.

The reduction in O₃ concentration by the OTC is attributed to the numerous sinks for O₃ that exist in the distribution pathway between the ambient bulk atmosphere and the interior of the chamber, including the plastic ducting and chamber walls, the dust filters, and any dust, aerosols and other reactive materials that unavoidably collect on these surfaces. Turbulent mixing of the within-canopy air surrounding the canopy was less efficient inside than outside the OTC. A difference in ozone exposure of this magnitude is quite likely to have modest but significant effects on ozone response curves.

A two-way analysis of variance, with days and canopy positions as factors, indicated significant ($P < 0.05$) differences in ozone concentration between analogous canopy positions inside and outside the OTC. The 12-hr seasonal mean exposure, based on these bulk canopy estimates (averaged throughout the canopy), was more than 8 ppb greater outside than inside the OTC. This represents an additional fruit yield reduction of about 1 kg/tree, calculated from the response curve generated for this orchard by Williams et al. (1993). The difference in chamber ozone statistic generated from a single sampling point above the canopy (Williams et al., 1993) was only slightly larger in this particular study, at about 9 ppb.

C. Effect of the OTC on the Distribution of Microenvironmental Parameters

In this section we examine both the effect of the canopy itself and the presence of the OTC with its opening at the top and blowers at the bottom, on gradients of critical microenvironmental parameters across the canopy. These gradients are associated with a wide range of actual exposures in different portions of the canopy of individual leaves, fruiting sites, and growing points to air movement (Fig. 15), light (Fig. 17), temperature, humidity, CO₂ and ozone (below). Several presentations of these data (Figs. 26-47) are included to emphasize various aspects of the exposure contrasts, at the cost of a certain amount of intentional redundancy.

1. Cross-canopy gradients of heat and trace gases

Specific, preplanned comparisons were made between the upper, exterior and the lower, interior positions of each canopy. These were expected to be the most divergent canopy locations with respect to microenvironmental exposure. However, this was not always the case. Additional contrasts were made of strictly vertical or strictly horizontal gradients along imaginary planes through the canopy. In a later section, a 3-dimensional approach is taken.

a. Temperature. Differences in air temperature within the canopy between the upper, exterior, exposed location and the lower, interior and more sheltered location of the plum trees were generally small, both inside and outside the OTC (Fig. 26). During daytime, the ambient air temperatures at the upper, exterior, sunlit locations were slightly higher than those at the lower, interior, shaded locations. This pattern was reversed at night when outgoing long-wave reradiation cooled the exposed portion of the canopies. This difference was larger inside the OTC since turbulent mixing of air in the upper canopy with outside air was reduced.

Vertical or horizontal slices through the canopy outside the OTC revealed similar temperatures at the upper, exterior, the upper, interior, and the lower, exterior regions, all of which were greater than those in the lower, interior region (Fig. 27 A, B, C, D). Leaves in these former regions are exposed to a similar set of micrometeorological conditions (e.g., sunshine and turbulent mixing) which differs from those in the latter region.

Inside the OTC, these vertical or horizontal gradients were modified by the OTC effects. The lower, exterior and upper, exterior locations were warmer than the interior locations (Fig. 28-B,C), because of the stronger turbulent mixing in the canopy interior. Temperature at the upper, interior location was variable (Fig. 28-A,D), perhaps due to intermittent shading by the OTC frame.

b. Water vapor. The difference in water vapor concentration between upper, exterior and lower, interior locations was substantial (ca 1 mmol/mol, or 5-7%) during daylight hours, especially inside the OTC (Fig. 29). Significantly, the direction of the difference was inverted by the OTC. Inside the OTC, the H₂O concentration at the upper, exterior location was higher than at the lower, interior location, attributable to the stronger transpiration in the upper, exterior location and the introduction of relatively dry bulk atmospheric air directly into the lower canopy. Outside the OTC the pattern was reversed. More efficient mixing of the dry ambient atmosphere with the air near the upper, exterior region of the tree resulted in lower H₂O concentrations than in the lower, interior region, despite higher PPFD and $g_{s,v}$ (see Figs. 18,50).

Outside the OTC, the upper, interior location had the highest water vapor concentration, while the upper, exterior location generally had the lowest concentration (Fig. 30). Water vapor concentration in the lower, interior region was higher than in the lower, exterior region, the combined result of transpiration and turbulent mixing. The horizontal gradient in the upper canopy was the largest observed outside the OTC (Fig. 30A). Strong transpiration, the source of water vapor, was observed in the upper, exterior region, but the strong turbulent mixing in this region dominated rapidly removing water vapor to the bulk atmosphere.

Inside the OTC, the blower significantly influenced the distribution of water vapor (Fig. 31). All gradients were substantially reduced. The water vapor concentration at the upper level (reduced turbulence) was higher than at the lower level (greater turbulence) (Fig. 31-C,D), while the difference between interior and exterior regions was small (Fig. 31-A,B).

c. Carbon dioxide. Gradients in CO₂ across the canopy were relatively small (ca 2% at maximal and usually much less), but well established and stable under all conditions. Inside the OTC the upper, exterior part of the canopy exhibited lower CO₂ concentrations (Fig. 32A), but the differences were very small. Outside the OTC, the upper, exterior location had a slightly higher level of CO₂ concentration than the lower, interior location during daytime, but the situation was reversed during nighttime (Fig. 32B). Two factors account for this: (1) the canopy is a sink for CO₂ during the day, but a source during dark hours, and (2) the upper, exterior location is more open to the bulk atmosphere, and stronger turbulent mixing is expected there. Important exceptions to the general diurnal trends are observed at certain times (for example, between 9:00-10:30) because local effects such as shading limit photosynthesis and decrease the amount of CO₂ uptake at the lower, interior location.

Daytime patterns of CO₂ concentration indicate that significant differences exist between different canopy locations, particularly in the late morning. Outside the OTC, the CO₂ concentration was generally higher at lower levels than at upper levels (Fig. 33-C,D), and higher in exterior regions than in interior regions for most of the daytime period (Fig. 33-A,B). Leaves at upper levels are more directly exposed to sunlight and have a higher expected rate of carbon assimilation than those at lower levels, while interior regions are less exposed to turbulent mixing with the outside atmosphere, both yielding lower ambient CO₂ concentrations.

Inside the OTC, the distribution of CO₂ concentration is significantly altered, with CO₂ concentration generally highest at the upper, interior region and lowest at the upper, exterior region (Fig. 34). The high CO₂ concentration at the upper, interior region may reflect the encroachment of ambient CO₂ through the top of the chamber.

d. Ozone. Differences in O₃ concentration between the upper, exterior and the lower, interior locations were substantial (ca 9%), both inside and outside the OTC (Fig. 35). Differences were more pronounced outside the OTC during the afternoon (ca 8 ppb), when the atmospheric O₃ concentration levels were maximal. Outside the OTC, the upper, exterior region is more exposed to the bulk atmosphere, and to higher O₃ concentrations than the lower, interior region, which is sheltered by uptake of O₃ by the foliage above. Inside the OTC, the gradients were smaller but reversed. The blower delivers ambient air (with high O₃ concentration) into the OTC at the bottom, increasing the O₃ concentration in this region relative to levels in the more sheltered (by foliage from the blowers) upper, exterior region. Forced mixing within the canopies by the blowers reduces the O₃ concentration gradient.

In contrast to the distribution of water vapor, for which the canopy is a source rather than a sink, O₃ concentration outside the OTC was highest at the upper, exterior location, and lowest at the lower, interior location (Fig. 36). Averaged over all days of the study, the O₃ concentrations were significantly different between these two positions ($P < 0.05$). Maximum cross-canopy gradients generally appeared in the midafternoon when ambient O₃ concentration reached daily maxima.

Differences between different locations inside the OTC were not as clear (Fig. 37). The lower, interior region (near the blowers) exhibited the highest O₃ concentration over most of the daytime hours, while the upper, interior region had the lowest O₃ concentration.

Although ozone and carbon dioxide have a similar source (the bulk atmosphere) and sink (the canopy) during the day, their vertical concentration gradients are quite different. The O₃ sink influences O₃ concentration gradients more significantly than the CO₂ sink influences

CO₂ concentration distribution. This is likely associated with the substantial intracellular concentration of CO₂ ($C_i > \text{ca } 250 \text{ ppm}$; Fig; 57, below) relative to the near zero concentration of intracellular O₃ (Laisk et al., 1989).

2. Mapping the distribution of heat and trace gases

The cross-canopy gradients and the vertical or horizontal gradients examined in the preceding section represent specific subsets of the overall distribution of microenvironmental parameters throughout the canopies inside and outside the OTC. These measurements of a 9-point matrix over a vertical plane through the center of the canopy are considered in the following section. To clarify the distributional patterns the averages for each parameter are restricted to periods of 2-3 daylight hours. Full day means obscured the patterns.

a. Temperature. Air temperature is considered over two different 3-hour averaging periods. The near midday period, 11:00 to 14:00 exhibited a decrease in temperature down through the canopy, and a decrease from the center of the tree to its exterior margin (Figs. 38,39). In contrast, in late afternoon, 14:00 to 17:00, temperatures increased horizontally from center to margin and was less consistent inside than outside the OTC (Figs. 40,41). The reversal of the horizontal gradient is not significant, reflecting the placement of sensors along one side of the canopy, whereas the sun illuminated first one and then the other side.

Over both averaging periods (Figs. 38(A,B,C) and 40(A,B,C)) temperatures were greater inside than outside the OTC at each location. Standard errors were small and consistent over locations. These spatial maps allow a visualization of the higher air temperatures inside the OTC, and the more pronounced gradients across the canopy outside the OTC.

b. Water vapor. Water vapor concentrations, averaged from 1100-1300, PDT, over all sampling dates were consistently higher inside the OTC than in the corresponding locations outside the OTC (Fig. 42). H₂O concentration varied little from day to day, as shown by the small standard errors.

Outside the OTC, H₂O concentration decreased horizontally with distance from the interior of the tree at each observation height and generally decreased with height. Inside the OTC, concentration gradients were substantially reduced in both the horizontal and vertical directions. A slight trend toward increasing humidity with vertical height was apparent. There was little horizontal gradient. The contour plot of H₂O concentration inside the OTC was flat and well above the surface representing outside the OTC (Fig. 43).

c. Carbon dioxide. CO₂ concentrations outside the OTC were higher than inside the OTC at each location of the plum tree (Fig. 44-A,B,C). Outside the OTC, exterior regions had

consistently higher CO₂ concentrations than interior regions, with larger differences at upper levels than at lower levels (Fig. 45). Moreover, there was a significant CO₂ concentration gradient in the vertical direction, with CO₂ concentrations lower at upper levels. Reduced CO₂ concentration in the upper canopy reflects photosynthesis (CO₂ uptake) in this sunlit region, despite greater turbulent mixing. Emission of carbon dioxide from soil respiration may contribute to the high CO₂ concentration observed at the lower level. Small standard errors in these season-long averages (on the order of 1-2 ppm) indicate lack of large seasonal variation.

Inside the OTC, the chamber and blowers substantially affected the distribution of CO₂ concentration and resulted in reduced and inconsistent gradients in both the horizontal and vertical directions. The high CO₂ concentration in the upper, interior region inside the OTC may be due to the limited carbon assimilation rate there, as well as to the encroachment of ambient carbon dioxide through the open top of the OTC. The overall cross-canopy gradients (Fig. 45) were much more pronounced outside than inside the OTC, and the CO₂ concentration at all positions was greater outside than inside the OTC (Figs. 44, 45).

d. Ozone. The O₃ concentration (11:00-13:00) at each position of the tree was significantly ($p < 0.05$) higher outside the OTC than inside the OTC (Fig. 46 (A,B,C); Table 3). There was a consistent increase in O₃ concentration with distance away from the interior of the tree at each height outside the OTC, although the amount of increase was small when compared with the differences between inside and outside the OTC (Fig. 47). There was also a consistent vertical gradient outside the OTC, with O₃ concentration decreasing with depth through the canopy along each vertical plane.

Inside the OTC, the O₃ concentration gradients were very small and inconsistent, both horizontally and vertically (Fig. 47). An apparent anomaly is the depression in O₃ concentration at the upper, interior position inside the OTC. This reflects input of ozone laden air at the bottom of the canopy and removal of ozone by the foliage before the air mass arrives at the top of the canopy. It is noteworthy that entry of ambient air through the open top of the chamber did not substantially overcome this effect. The greater exposure to the bulk atmosphere, whether by blower or diffusion plus gust penetration, in a canopy region, the higher the O₃ concentration. The observed gradients must be viewed in the context of the open architecture pruning, which leads to higher ozone concentrations in the interior region of the outside tree than would otherwise be expected. Much greater gradients, inside and outside the OTC, would be expected in an unmodified, denser canopy.

Determination of ozone concentration, averaged over all sampling dates and over a 12-hour period (0800-2000, PDT) at each of 9 canopy locations, is a first step in approximating

seasonal ozone exposure by canopy zone (Table 3). Outside the OTC, ozone concentration was highest at location 3 (Fig. 8) and lowest at location 4, while inside the OTC, ozone concentration was highest at location 7, and lowest at location 1.

Environmental and physiological data from a selected few of the 9 locations within the canopies of the plum trees were combined to provide estimates of differences between generalized zones of the canopy in which detailed physiological measurements could be obtained. Two zones were designated for each INside or OUTside tree, one representing the INTerior of the canopy and one the EXTERior, resulting in four zones (2 trees x 2 zones/tree). The four zones were designated 'EXTERIN', 'EXTEROUT', 'INTERIN', and 'INTEROUT'. O₃ concentrations were higher at exterior zones than at interior zones for both inside and outside the OTC. Ozone concentrations were higher outside the OTC than inside the OTC for both interior and exterior zones (Table 3).

IV. RESULTS AND DISCUSSION--GAS TRANSPORT

A. Effect of Open-Top-Chambers on Water Transport (Transpiration)

The contrasting conditions observed in different locations or zones within the canopies have large impacts on the microenvironment of each zone, as well as on the transport of heat and trace gases. Each may be important. For example, temperature within the canopy may influence directly the rate of metabolic reactions, while influencing only indirectly the evaporation of water through effects on transport of heat energy to the leaves. In this section we consider fluxes of water vapor and liquid water by canopy zone, as a first step in characterizing transport conductances for exchange of water as well as CO_2 and O_3 between leaves and the atmosphere.

1. Water vapor pressure, gradients, conductances and fluxes

a. Concentrations and driving forces--role of the leaf surface. The flux of water vapor, transpiration (E), is the product of a concentration gradient and the conductance (inverse of resistance) to the flux. A difficulty in calculating water vapor loss from leaves using only porometric or gas exchange measurements of stomatal conductance, is in defining the appropriate end points for calculation of the water vapor concentration gradient.

Transpiration increases the water vapor concentration in the immediate vicinity of the leaves (Jarvis and McNaughton, 1986), altering the driving force (V_s) in water vapor pressure from leaf interior (e_i) to the leaf surface outside the stomatal pore (e_s), or V_z from e_i to to the canopy zone air space (e_z). Depending on highly variable conditions these driving forces may be more or less well represented by the conventionally cited V_a , calculated to an ambient external reference point above the canopy (e_a). Transpiration expressed only as a function of stomatal conductance (ignoring boundary layer and aerodynamic factors) is driven only by $e_i - e_s = V_s$, while the commonly cited $e_i - e_a = V_a$, when used as driving force with only stomatal conductance, grossly overestimates transpiration. The use of the leaf surface as a key reference point for trace gas concentrations is very useful when non-stomatal transport properties are unknown or variable (Ball, 1987). Under some conditions use of concentrations measured near the leaves in the various canopy zones can be substituted as approximate leaf surface concentrations.

Water vapor pressure, measured outside (e_a) and inside (e_z) the tree canopies, at the leaf surface (e_s) and within the leaf interior (e_i), exhibited (Fig. 48) the monotonic increase in each zone that drives E from the leaf through the canopy air spaces to the bulk atmosphere.

Vapor pressure outside the canopy of the outside tree (e_a ; dotted line in Fig. 48), measured at the ambient reference point, provides an identical baseline for each zone.

Vapor pressure in the zones varied somewhat, as expected from differences in transpiration and environmental exposure. Variations of e_z from the ambient baseline (e_a) were similar in diurnal pattern between zones but less similar in magnitude (Fig. 48). Within the OTC the exterior and interior zones exhibited smooth bell-shaped curves indicating high levels of humidification, slightly higher in the exterior zone. Outside the OTC, the exterior zone was nearly identical with the ambient reference (Fig. 48), and the interior zone exhibited only slightly elevated vapor pressures due to reduced air exchange caused by the exterior foliage. This range of vapor pressures resulted in a range of concentration gradients of water vapor (V) driving transpiration.

V_a , calculated as the difference between saturation vapor pressure of the intercellular space (e_i) and the ambient reference point external to the canopies (location 3, Fig. 8) did not vary substantially between zones. V_a exhibited a nearly linear increase through the course of the day (Fig. 49) responding to radiation and leaf temperature and to desiccation of the ambient air as turbulent mixing increased. The largest V_a reflected the warmest leaves, generally the interior canopy positions, though V_a was similar for all canopy positions (Fig. 49, upper).

The sources of water vapor, the leaf interior in each zone, exhibited varying temperatures and thus values of e_i (Fig. 48, solid lines). The gradient that drives E across the stomatal pore, V_s , therefore exhibited large differences between the two zones inside the OTC and the two zones outside (Fig. 49, lower), with larger values of V_s outside the OTC. The zonal patterns were also different. Inside the OTC, V_s remained relatively unchanged until after 1300, while outside the OTC, V_s more closely tracked V_a throughout the day. In both cases V_s was generally lower in the exterior than interior canopy zones.

The V_s calculation also differentiated the four canopy zones more clearly than did V_a . These differences were more pronounced inside the chamber than outside. This distinction between V_a and V_s may be important when OTC studies are characterized physiologically by single leaf measurements of gas exchange and stomatal conductance. The contrasting gradients for vapor transport obtained as V_s more closely relate single leaf measurements to actual values of E than do the more similar gradients obtained as V_a .

b. Stomatal conductance. Microenvironments for individual leaves in each of the canopy zones varied with position within the zone, ranging from fully shaded leaves in the cooler interior regions to fully sunlit leaves at the top or outside of the zone. Newly expanded

leaves and leaves several months of age existed simultaneously within each zone. Leaf condition, morphology and physiology were consequently as variable as the microenvironmental parameters.

Gas exchange measurements of stomatal conductance were obtained on leaves of all ages, covering the ranges of both ambient microenvironmental conditions and leaf morphology, to adequately represent the gas exchange of each zone. This environmental and leaf-to-leaf variability resulted in some variability in measurements of stomatal conductance and carbon assimilation. This adequately represented the true biological variation rather than experimental error.

Diurnal time courses of conductance were smoothed using a polynomial regression against time of day, to obtain a representative, composite diurnal course of conductance for each zone (Fig. 50). Coefficients of determination for these smoothing functions were in excess of 0.79 for all zones.

Differences in both diurnal trends and in magnitude of stomatal conductance were observed between zones within each canopy, and between inside and outside the OTC (Fig. 50). Inside the OTC the exterior zone exhibited the highest PPFD and lowest V_s and consequently the highest levels of stomatal conductance. Both are known as conditions conducive to high rates of stomatal gas exchange (Grantz, 1990). Stomatal conductance in the interior position inside the OTC, and comparable exterior position outside the OTC, were both considerably suppressed, by comparison. Outside the OTC the exterior position also exhibited larger stomatal opening than the interior position. The interior position outside was suppressed relative to the analogous position inside the OTC, reflecting the overall lower levels of humidity outside.

From the larger stomatal conductances alone (e.g., the daily means; Table 4), the erroneous conclusion could be drawn that rates of trace gas exchange were higher inside the OTC than outside. This is the reverse of the actual situation for water (Fig. 51, 54, below) as well as for CO_2 and O_3 (Figs. 61, 65, below). This reflects the greater coupling of the outside tree than the inside tree to the atmosphere, as shown by the lower Ω parameter (Fig. 55). This indicates less control of these fluxes by the stomata inside the OTC, in spite of their greater conductance. This is a key observation of the present study.

2. Liquid water gradients, conductances and fluxes

a. Concentrations and driving forces. The tree outside the OTC tended to exhibit slightly lower (drier, more negative) midday water potentials of transpiring leaves (Ψ) than the inside tree (Table 5). This is consistent with the greater mean rates of transpiration (E ; Table

5). Sap flow (directly measured transpiration rate) exhibited nearly bell-shaped curves in each zone, with maxima occurring in the early afternoon, near solar noon (Fig. 51). Midday maximal rates of E were greatest in the Exterior zone of the tree outside the OTC (Fig. 51C), also the location of the lowest values of Ψ (Table 5). Inside the OTC the zones were more similar, but the Interior zone exhibited a slightly higher midday maximum E than did the Exterior zone. E is used to calculate transport parameters (below). It is important that these data are internally consistent.

Cumulative sap flow during the day (0900-1600, PDT, Fig. 53) was also highest in the exterior zone outside the OTC (EXTEROUT), where radiation and turbulence were greatest, but lowest in this same exterior zone inside the OTC (EXTERIN), where PPFD was substantial but little wind movement occurred. These effects of wind movement on water vapor fluxes are reflected in non-stomatal, boundary layer conductance ($g_{ba,v}$; Table 4), which was also highest in EXTEROUT and lowest in EXTERIN, as discussed further below.

b. Liquid phase conductance. The water conducting capacity of the vascular system of the trees inside and outside the OTC reflect the long-term development of hydraulic architecture. Typically this hydraulic conductance (L) reflects the level of water use by the portion of the canopy supported by an individual branch. In the present study L is used to further document the differences in physiological performance between canopy zones inside and outside the OTC, and to support other measurements indicating differences in water fluxes.

Hydraulic conductance (L) was computed as transpiration (E), per branch and per leaf area, divided by Ψ , using data obtained between 1000 and 1400 PDT on DOYs 238, 240, and 247. This yielded two estimates of canopy hydraulic conductance (L_E and L_E/m^2 , respectively; Table 5).

The exterior part of the canopy outside the OTC exhibited higher values of L than all other canopy zones (Table 5), consistent with the higher maximal (Fig. 50) and average (Table 4) values of stomatal conductance and sap flow (Fig. 51; Tables 4,5). An alternative estimate of L , using $g_{s,v}$ instead of E revealed similar zonal rankings (not shown).

3. Calculated water vapor flux

a. Distribution of conductances. The redundant measurement of water fluxes, as a liquid and as a vapor, along with measurement of one of the conductances in the pathway for vapor loss (stomatal conductance), allows calculation of the boundary layer conductances. Comparison of the stomatal ($g_{s,v}$) and boundary layer ($g_{ba,v}$) conductances for water vapor (Table 4), and the total conductance for each zone ($g_{ta,v}$) allowed determination of the factors

controlling the zonal patterns of water flux. This information also allowed calculation of water vapor fluxes from measurements of e_i (from leaf temperature) and water vapor at the ambient reference point (Fig. 52).

In the case of water vapor, the redundancy of the measurement and the calculation of the flux insure that the calculated fluxes are identical with the measured sap flows (Fig. 51). However, this case is intended to be representative. The calculation method, and knowledge of the magnitudes of the various conductances in the gas phase pathway, also allow calculation of carbon dioxide and ozone fluxes by canopy zone (see below).

The patterns of boundary layer conductances (Table 4) reflect the differences in canopy exposure due to foliage and due to the effects of the OTC blowers. For example, the conductance of the boundary layer to the ambient reference point is much larger in the Exterior portion of the tree outside of the OTC, than in the Interior position (ca 23% greater; Table 4) and larger than corresponding values inside the chamber. Inside the OTC the Interior zone exhibited the larger boundary layer conductance to the ambient reference point (ca 40% larger than Exterior; Table 4). Conductances to the canopy zones, rather than to the ambient reference point were somewhat higher as expected. These values both confirm and explain the distribution of microenvironmental parameters observed in the two canopies and detailed in previous sections.

Both inside and outside the OTC the exterior position exhibited larger stomatal conductance. As a result, the fraction of the total vapor phase resistance ($1/\text{conductance}$) represented by the stomata was larger in the interior than exterior positions, and larger outside than inside the OTC. This latter observation reflects the additional inhibition of mixing with the bulk atmosphere represented by the chamber walls. Blower placement beneath the canopy inside the chamber, combined with the open architecture pruning protocol, resulted in greater boundary layer resistances (Table 4) and led to closer coupling of the canopy interior to the outside atmosphere than occurred outside (Fig. 55, below).

b. Effect of the OTC. Averaged over the six gas exchange days and both zones, water vapor flux was greater outside than inside the OTC (Fig. 54). Outside the OTC, the combination of substantially larger total conductance to H_2O ($g_{ba,v}$; Table 6) and only slightly smaller vapor pressure deficit (V_a), due to the generally lower leaf temperature (Fig. 19) outside the OTC relative to that inside the OTC, led to the higher rate of transpiration (E) during the physiologically active period from 1100-1600 (PDT).

This larger transpiration rate outside the OTC did not compensate for the greater removal of water vapor due to greater turbulent transport, so that water vapor concentration

was lower within the canopy zones outside than inside the OTC (Fig. 23). Using the within-canopy zones as the reference point for calculation of gradients and conductances (Tables 4, 6) reveals the lower levels of V_z and correspondingly larger levels of $g_{tz,v}$, relative to V_a and $g_{ta,v}$ that account for the observed water fluxes.

4. Stomatal and Environmental regulation of water vapor fluxes

The relative magnitudes of stomatal and boundary layer components of the total conductance reflect the effectiveness of stomatal control of transpiration and fluxes of other trace gases. One method of quantifying the effect of the OTC on canopy transpiration is by calculation of the dimensionless decoupling coefficient Omega (Ω) as described by Jarvis and McNaughton (1986) and McNaughton and Jarvis (1983). Ranging in value from 0 to 1, Ω describes the extent to which vapor pressure deficit at the leaf surface is decoupled from that in the bulk atmosphere. Values near 0 indicate that the saturation deficit (vapor pressure difference, V) of the ambient atmosphere is imposed at the leaf surface without adjustment due to local transpiration. Under these conditions, V drives transpiration and stomata exert primary control of water loss. Values near 1 indicate poor coupling to the atmosphere, with the local surface saturation deficit determined by local equilibration. Under these conditions, transpiration is governed primarily by receipt of net radiation.

Ω reflects the relative magnitudes of stomatal and non-stomatal conductances to H_2O vapor (see Eqs. 1, 5). Stomata exerted a much larger fraction of the total resistance to vapor flux outside the chamber (Table 4), suggesting that stomatal control of transpiration is larger than inside the OTC. Nonstomatal conductance to H_2O , with respect to an ambient reference point ($g_{ba,v}$) outside the OTC (Location 3, Fig. 8) was larger for leaves outside the OTC than inside the OTC (Table 6) while stomatal conductance to H_2O ($g_{s,v}$), was smaller outside the OTC (Table 6) yielding lower values for Ω outside than inside the OTC (Table 7). These values of Ω indicate that the tree outside the OTC was more tightly coupled to the changes in water vapor occurring in the ambient atmosphere than was the tree inside the OTC (Fig. 55). This is largely attributed to uncoupling of humidity by the presence of the OTC walls. The exterior zone of the tree inside the chamber (EXTERIN) had the highest values of Ω (least coupling; Fig. 55), and exhibited the lowest daily average of boundary layer conductances (Table 4). The outside tree exhibited smaller differences between zones for values of Ω (Fig. 55).

The original formulation of Ω (Jarvis and McNaughton, 1986) ignored the effect of stomatal closure on leaf temperature, and the resulting change in long wave re-radiation by the canopy. Martin (1989) described the importance of increased outgoing long-wave radiation,

due to increased leaf temperature resulting from stomatal closure and decreased transpiration. The effect of the OTC on water vapor concentrations and transpiration are reflected in values of Omega with (Ω) and without (Ω_R) radiative coupling (Table 7). Vegetative control of transpiration is thus determined by aerodynamic, physiological, and radiative controls. The effect of including the radiative coupling term in the Ω calculation was to decrease the value of Ω by a little over 10% (Fig. 56) in all zones.

The values of Ω observed for this tree crop seem relatively high, but low levels of coupling are consistent with the low wind conditions of the Central Valley. The plastic walls of the OTC serve to effectively decouple the tree from the ambient atmosphere. The degree of coupling did vary throughout the time course of the typical day, attributable to changes in both stomatal and boundary layer conductances and in resulting vapor pressure differences. Regression of Ω on estimates of V indicated a slightly negative linear response (not shown), indicating a shift from environmental to stomatal control of transpiration, as shown previously (Grantz and Meinzer, 1990).

B. Effect of Open-Top-Chambers on CO₂ Transport (Photosynthesis)

1. CO₂ concentration gradients, conductances and fluxes

The concentrations of CO₂ at various points between the bulk air and the sites of photosynthetic carbon fixation within the leaf varied considerably between the different canopy zones (Fig. 57). The concentrations in the canopy zone air spaces (C_z), and at the external ambient reference point (C_a) were measured directly (Fig. 57). Concentration within the leaf (C_i) and at the leaf surface (C_s) were calculated using information obtained from water vapor transport (above) and from measurements of single leaf CO₂ exchange (A).

Ambient CO₂ concentration exhibited a slight increase near 10:00 (Fig. 57; cf. Fig. 24), which was superimposed on the overall decrease in concentrations during the morning. This impacted the concentrations determined at the other locations. The concentrations within the canopy zones exhibited contrasting diurnal patterns, reflecting the different balance of photosynthetic consumption and turbulent renewal of CO₂ in each zone. Inside the OTC, C_z exhibited relatively smooth, bell-shaped functions. Outside the OTC, these patterns were somewhat more irregular, reflecting the inhibited mixing between the canopy zones, and more efficient overall mixing of the canopy with the outside air.

Values of C_i were considerably higher inside the OTC than outside. Outside the OTC, the levels of C_i were similar to those expected for plants such as plum that fix CO₂ using the C₃, Benson-Calvin Cycle (ca 230 ppm). Inside the OTC, the levels were uncommonly high, reflecting the greater humidity and consequent greater stomatal opening, and lower levels of PPFD-driven carbon assimilation (A). Intercellular CO₂ concentration reflects the balance between stomatal conductance for CO₂ and photosynthetic consumption of CO₂ at the individual leaf (Eq. 6). The values presented (Fig. 57) represent zonal averages of many leaves.

The concentration gradients (ΔC) defined by these prevailing concentrations (Fig. 57), varied considerably among the canopy zones, both when calculated from C_a to C_i (Fig. 58, upper) and from C_s to C_i (Fig. 58, lower). Outside the OTC, the Interior zone had larger gradients from C_s to C_i than the exterior zone in the morning, with the differences becoming smaller in the afternoon (Fig. 58, upper), due to somewhat higher wind speeds in the afternoon. Overall, boundary layer conductance was lower in the INTEROUT than in the EXTEROUT zone (Table 8).

Inside the OTC, the gradients were similar in pattern but showed greater differences in magnitude (Fig. 58, lower). The Interior of the tree exhibited a consistently greater

concentration gradient from both C_a to C_i and from C_s to C_i than the Exterior zones. As with the water vapor gradients, and in contrast with the outside trees, the interaction of the open-vase pruning technique and the blower placement effectively increased Interior zone boundary layer conductance above the level observed in the Exterior zone (Table 8). In the Exterior zone, the gradient across the stomatal pores (C_s to C_i) remained more constant throughout the day than in the Interior zone (Fig. 58, lower) while the gradient to the external atmosphere (Fig. 58, upper) showed a diurnal increase in the CO_2 concentration gradient for EXTERIN, but a general decline for INTERIN.

The rates of carbon flux (A) per individual leaf were measured directly using the transient gas exchange system (Fig. 59). As with $g_{s,v}$, A was smoothed over the course of a typical day using regression techniques, to provide an average, composite daily time course (Fig. 59; lines). Similar variability and zonal contrasts were observed as with $g_{s,v}$ (cf. Fig. 50). Single leaf A was highest in the Exterior position outside of the chamber, and similar in the other zones.

2. Calculated carbon dioxide flux

The concentration gradients and total conductances, appropriately transformed for CO_2 from water vapor (Table 8), allow calculation of CO_2 fluxes (A) in the absence of intensive physiological measurements. The values are not entirely independent of the single leaf measurements since C_i (one end of the gradient) was obtained from them. The calculation method, similar to that used for calculation of water fluxes (Fig. 52; above) illustrates the application of a general method that will allow calculation of fluxes of O_3 or other trace gases in OTC experiments.

The effect of the OTC on carbon dioxide fluxes was substantial, as noted above for water vapor. Averaged over the six gas exchange days, CO_2 concentration gradients outside the OTC were considerably larger than those inside the OTC, both from the leaf interior to the leaf surface and to the zone air space (Fig. 58; Table 9). The net carbon flux calculated from the gradients and stomatal conductance was also greater outside the chamber than inside (Fig. 61; Table 9).

Nonstomatal conductance to CO_2 ($g_{ba,c}$) outside the OTC was larger than inside the OTC, while stomatal conductance to CO_2 ($g_{s,c}$) inside the OTC was larger (Table 9). Overall, total conductance to CO_2 ($g_{tz,c}$, $g_{ta,c}$) was larger outside than inside the OTC. The net single leaf carbon assimilation rate outside the OTC ($A=7.9 \mu\text{mol m}^{-2}\text{s}^{-1}$) was considerably larger than inside the OTC ($A=4.9 \mu\text{mol m}^{-2}\text{s}^{-1}$; Table 9), thus the higher CO_2 concentration gradients

$(\Delta C_a, \Delta C_b)$ outside the OTC indicate more efficient turbulent transport of atmospheric CO_2 into the canopy, rather than a lower sink strength for CO_2 .

C. Effect of Open-Top-Chambers on Ozone Transport (Leaf Uptake)

1. Ozone concentration gradients and fluxes

Regional ozone concentrations increased diurnally with a late afternoon peak occurring near 16:00 PDT. Ambient concentrations during the experimental period ranged from a typical overnight minimum of ca 0.01 ppm (Fig. 25) to a daily maximum of nearly 0.1 ppm (Figs. 25; short dashed line, Fig. 62). The degree of air exchange between the within-canopy zones and the ambient atmosphere is reflected in boundary layer conductance (g_{bl,O_3} ; Table 10) and in the concentrations of ozone observed in the canopy zone airspaces (Fig. 62).

Outside the OTC, the ozone concentration in the Exterior zone was nearly indistinguishable from the ambient concentration while the Interior zone was somewhat depleted through uptake by the surrounding foliage (Fig. 62). Inside the OTC, both Interior and Exterior zonal concentrations were depressed below ambient levels, reflecting ozone degradation by the OTC air distribution system, and limited exchange with the atmosphere. The calculation of ozone gradients from leaf interior (concentration assumed zero; Laisk et al., 1989) to the Interior and Exterior zones of the canopy (Δ_{O_3Z}) indicate nearly identical mean daily gradients for the two zones within each tree, but larger gradients outside than inside (Table 10). This is reflected in the lower boundary layer conductances to the zones (g_{bz,O_3}) inside than outside the chamber (Table 10). The laminar boundary layer conductance adjacent to individual leaves in each canopy zone (g_{bl,O_3} ; Table 10), largely a product of turbulent wind speed within the canopy, was largest in the EXTEROUT zone and lowest in the INTEROUT zone. The two zones inside the OTC were intermediate and similar to each other. On average the outside tree had a greater g_{bl,O_3} . Total conductance to each zone was relatively similar (g_{tz,O_3} ; Table 10).

Had the air entering the zonal airspaces inside the OTC contained the same ozone concentration as the ambient air, e.g., by replacement of ozone losses during distribution, then a similar (within ca 6%; Table 11) ozone exposure of the leaves throughout the canopy would have occurred inside and outside of the chamber, based on the values of boundary layer conductance to the zones (Table 10).

If ambient levels of ozone had been imposed at the leaf surfaces by wind, as occurs more readily in trees growing outside, then the inside trees would have received a considerably greater dose of ozone. This can be seen by comparing the levels of stomatal conductance (greater on average inside the OTC; Tables 10, 11) and the levels of ozone gradients across the stomatal pores (greater on average outside; Fig. 63, lower). The ozone concentration at the

leaf surface exhibited contrasting diurnal patterns in the individual zones. Placement of the blower ducts, and prevailing stomatal conductances (Table 10), led to higher ozone concentrations at the leaf surface (O_{3s}) in the Interior than Exterior zone inside the OTC. These were not parallel to the trend in ambient ozone (Fig. 62), but rather reflected the combined time courses of both ozone concentration and stomatal and boundary layer conductances. As expected, the zones outside the OTC experienced higher ozone concentrations at the leaf surface than did the inside zones, where O_{3s} increased at a slower rate throughout the day than outside the OTC, remaining nearly unchanged throughout the morning, then increasing curvilinearly in the afternoon when ambient concentrations were highest. This sudden increase may reflect saturation of sinks (sites of ozone degradation) associated with the chamber itself (e.g., plastic walls, ducts, and adhering dust).

Gradients from the leaf interior to the leaf surface (Fig. 63, lower) exhibited greater differences between the zones, than did gradients from the leaf interior to the airspace within each zone (cf. Table 10) and much greater variability than the identical gradients for each zone to the ambient reference point (Fig. 63, upper). The gradients driving O_3 uptake across the stomatal conductance (O_{3s} to O_{3i}) were higher in the Interior than Exterior zone inside the OTC (Fig. 63, lower). The expected lower concentrations in the Interior of the tree due to filtering by the Exterior foliage, were not observed inside the OTC.

The implication of the above comparisons of fluxes, stomatal and non-stomatal conductances, and ozone concentrations, is that the relative comparability of yields and growth parameters in the ambient control and in the non-chamber ambient controls, frequently cited in OTC studies, may represent offsetting artifacts rather than evidence of the general comparability of the OTC treatment to natural conditions.

2. Calculated ozone uptake

Nonstomatal conductance to the ambient reference point (g_{ba,O_3}) was larger outside the OTC than inside the OTC, while stomatal conductance to O_3 (g_{s,O_3}) outside the OTC was smaller (Table 11). These gradients are reflected in the amount of ozone uptake by the trees inside and outside the OTC. The larger total conductance to O_3 (g_{tz,O_3} , g_{ta,O_3} Tables 10,11), combined with a larger or equal O_3 concentration gradient (ΔO_{3z} , ΔO_{3a} ; Fig. 63, upper; Tables 10, 11) yielded a ca 17% larger O_3 flux (F_{O_3}) by the entire canopy (Fig. 65; Table 11) outside the OTC. It is of interest that the stronger sink strength outside the OTC did not dominate the stronger turbulent transport of O_3 towards the canopy observed outside, so that a higher O_3 concentration within the canopy was maintained outside than inside.

The ozone fluxes calculated using the methods of this study were consistent with expected values in this area. The estimated F_{O_3} towards the canopy was 0.228 and 0.267 $\mu\text{g m}^{-2} \text{s}^{-1}$ (leaf area basis), for inside and outside the OTC, respectively. When multiplied by the estimated leaf area index of 4.5 for the plum canopy, the O_3 flux to the canopy (per ground area) was 1.05 (inside the OTC) and 1.23 (outside the OTC) $\mu\text{g m}^{-2} \text{s}^{-1}$, respectively. This flux is comparable to the dry deposition rate for O_3 measured during the California Ozone Deposition Experiment (Grantz et al., 1994a; Pederson et. al., 1995) over mixed deciduous orchards in the San Joaquin Valley, of 0.85 $\mu\text{g m}^{-2} \text{s}^{-1}$ (per ground area), measured using eddy covariance at 30 m height from an aircraft platform .

V. RESULTS AND DISCUSSION--MODELLING OZONE UPTAKE

Specification of the dose or uptake of ozone is likely to be superior to a simple exposure statistic when quantifying the effect of ozone on yield or growth suppression (LeFohn, 1992). However, uptake of ozone has been difficult to measure accurately on a single leaf basis, and the sampling of sufficient leaves to yield a representative estimate of canopy uptake has remained challenging. Regional airshed questions have traditionally been addressed through process-based modelling of ozone sources and sinks, including surface deposition components (Wesely, 1989; Pederson et al., 1995). These techniques could be of widespread utility in OTC studies as well.

Most of the ozone deposition to vegetated surfaces is associated with foliar uptake through the stomata (e.g., Grantz et al., 1994). As this is the component of ozone deposition that impacts photosynthetic function, it is considered to be the most important to ecological and agricultural investigations. Therefore, calculation of F_{O_3} in OTC studies will depend strongly on measurements or models of stomatal conductance.

A. Modelling Stomatal Conductance

Measurements made in this study afford the opportunity to evaluate stomatal responses in plum trees to key environmental stimuli measured within the canopy, and to determine how these responses may be modified by growth and development within the OTC and by position within the canopy. Responses to parameters measured outside the canopy are also likely to be altered by the sheltering effects of the OTC walls and the foliage surrounding Interior zones.

1. Role of vapor pressure

Plots of $g_{s,v}$ vs. V_a without consideration of zones showed a parabolic relationship (Fig. 66, top panel) with distinct lines apparent for each zone (Fig. 66, bottom panel). Apparently, $g_{s,v}$ increased with radiation until V_a increased sufficiently to stimulate stomatal closure. Due to the extreme non-linearity of these relationships (Fig. 66) linear regressions of $g_{s,v}$ on V_a (the commonly measured humidity parameter in OTC studies) were nonsignificant in all cases (Table 12).

Using V_s at the leaf surface, however, conductance was significantly ($p < .10$) and negatively related to vapor pressure difference when all zones were considered together (Fig. 67; Table 12). This is consistent with current understanding of stomatal response to V (Grantz, 1990). When analyzed within each zone, all zones except EXTEROUT yielded significant regressions, indicating that a significant amount of the apparent variability in stomatal conductance was attributable to V calculated at the leaf surface (Table 12). However, outside

the OTC, both zones exhibited a similar parabolic diurnal course to that observed using V_a (cf. Fig. 66, lower). Even though most of the stomatal response to V typically occurs below ca 2 kPa, (e.g., Grantz et al., 1987) detection of stomatal response to V under the hot, dry conditions of this study (V_s of 1 to 4 kPa) were still possible inside the OTC and in the interior of the tree outside the OTC.

These data suggest that the leaf surface is a useful reference point for characterizing the microenvironmental conditions that determine stomatal conductance, as well as the gradients that drive gas exchange and pollutant uptake.

2. Role of light

Regression of $g_{s,v}$ on above-canopy PPFD also accounted for a significant ($p < 0.05$) fraction of the variability in stomatal conductance when all zones of the canopy were considered together (Table 12; Fig. 68). When $g_{s,v}$ was regressed on PPFD by zone, a better fit was obtained for the zones inside the OTC (uncoupled from above-canopy radiation by the plastic walls of the OTC), while the regressions for the zones outside the OTC deteriorated (Table 12; Fig. 68). This reflects the offsetting interaction between the increased variability of the within-canopy measurements of PPFD and the more accurate rendering of PPFD incident upon the leaves.

3. Environmental interactions

PPFD was strongly correlated with V_a because of the negative association between PPFD and ambient vapor pressure (e_a), and positive association between PPFD and leaf temperature that tended to mask the true stomatal response to V (Grantz and Meinzer, 1990). Since PPFD and both measures of V were correlated, PPFD was normalized by V to provide the best means of evaluation of the effect of the contrasting references (ambient or leaf surface) for the V calculation.

Combining estimates of PPFD and V can yield successful models of conductance (Grantz et al., 1987). Regressing $g_{s,O3}$ on $PPFD/V_a$ yielded a significant ($p < 0.02$) regression when all zones were combined (Table 13), but the fit was poor. When evaluated by zone, the model worked well for the two zones in the outside tree, but resulted in insignificant regressions for the two zones inside the OTC. The relationship between $g_{s,v}$ and the composite parameter, above-canopy PPFD normalized by V_a , generated a poor relationship with wide scattering of points (Fig. 69, upper).

Substituting V_s for V_a , improved the fit for the regression over all zones combined, and the model provided highly significant regressions for each individual zone (Table 13). The relationship between $g_{s,v}$ and PPFD normalized by V_s (Fig. 70, lower) condensed the data into

a tight linear relationship (Fig. 70; upper). When resolved by zone (Fig. 70; lower), the individual relationships were highly significant, and similar to each other.

Regression of stomatal conductance on above canopy PPFD and V estimates may also be significant if additive models are employed. When applied within the individual zones, the two regressor model provides highly significant regressions with excellent fits with both estimates of V (Table 10). All coefficients for PPFD are positive, while all coefficients for V are negative, consistent with their respective roles as opening and closing stimuli for stomatal response (Grantz, 1990).

Other environmental variables may directly or indirectly affect stomata. Regression of $g_{s,v}$ on ozone concentration at the leaf surface (O_{3s}) was significant when all zones were considered together (see Table 12). Broken down by zone, however, regression of $g_{s,v}$ on O_{3s} was significant only for the interior zones of the trees, whether inside or outside the OTC. This is the same pattern that was observed for V_s . Ambient ozone concentration was thus ineffective in accounting for the variability observed in $g_{s,v}$. In the present experimental situation, it is likely that O_{3s} reflects, rather than controls, $g_{s,v}$ and leaf uptake.

B. Ozone Uptake

1. Modelling O_3 Flux

In section IV above the appropriate model of O_3 uptake was used to calculate fluxes (Figs. 64, 65; Tables 10, 11). The required parameters were obtained from direct measurements and inference from redundant measurements of water (liquid and vapor) fluxes. For general applicability to OTC studies an assessment of ozone concentration at or near the leaf surface (O_{3s}) and a measure of stomatal conductance (g_{s,O_3}) is sufficient to solve:

$$F_{O_3} = (g_{l,O_3})(\Delta O_{3,s}) \quad (14)$$

or else the more complete transport equation used in section IV (above) must be solved:

$$F_{O_3} = (g_{l,O_3})(\Delta O_{3,a}) \quad (15)$$

in which $O_{3,a}$ is the ozone concentration in the ambient atmosphere or above the canopy within the OTC, but:

$$g_{ta,O_3} = \frac{1}{\frac{1}{g_{s,O_3}} + \frac{1}{g_{ba,O_3}}} \quad (16)$$

and:

$$g_{ba,O_3} = \frac{1}{\frac{1}{g_{bl}} + \frac{1}{g_a}} \quad (17)$$

in which g_{bl} can be calculated from wind speed inside the canopy and leaf dimensions (as above). However, determination of g_{ta,O_3} requires additional information, in the present case derived from fluxes of water liquid and water vapor, but in field studies of extensive vegetation typically from direct micrometeorological measurements. Alternatively, ozone concentration at the leaf surface must be either approximated as ozone concentration measured within canopy zones, or it must be calculated from knowledge of the same transport parameters required above. This has proven to be a serious methodological limitation.

If dose is to be adopted as the standard for exposure specification, then some variant of these protocols will be required. Stomatal conductance alone was a poor predictor of ozone flux, both within each zone and when all zones were considered together (Table 15). Ambient ozone concentration was a better single predictor, and ozone flux could be predicted to some extent in all zones. Combining stomatal conductance and ambient ozone concentration into a single additive model yielded highly significant predictions of ozone flux within each zone and for all zones combined (Table 15). However, the goodness of fit masks the differences between zones and the effect of the OTC observed in the present study. Indeed, a test for homogeneity of slopes, (continuous-by-class effects, PROC GLM (SAS)), indicated that the response surfaces of the linear multiple regressions were not equal. Thus ozone flux, as influenced by $g_{s,v}$ and ambient O_3 concentration, varied significantly between different regions of the plum canopy.

One possibility that suggests itself is to catalog such transport properties for specific OTC designs, and canopy types within them, for use in subsequent exposure studies.

C. Application of the Flux Methodology to Plum Yield Data

Using the flux protocol developed in the preceding sections, it is possible to reanalyze the ozone-yield response curve developed by Williams et al. (1993) during the period of the present study. Ozone concentrations were reported for the bulk atmosphere inside each OTC, and for the comparable position outside (a non-chamber control). Whereas the previous analysis dealt exclusively with the ambient chamber and the outside (non-chamber) trees, the following treatment demonstrates that the method works as well for the range of ozone concentration exposures imposed in the larger study.

The ozone gradient between the canopy zones, Interior or Exterior, was relatively small (Table 10), though concentrations were quite different inside and outside the OTC. For the following calculation of fluxes on a leaf area basis in each of the chambers, we therefore assume that the reported 12 hour seasonal mean ozone concentrations in each chamber and in the non-chambered control (Williams et al., 1993), were equivalent to the concentrations in the zones of each tree (O_{3z} ; Table 16). Further, a boundary layer conductance from representative leaves to the ozone concentration in each zone (g_{lz,O_3}) was calculated as above, taking the average of the two zones ($0.22 \text{ mol m}^{-2} \text{ s}^{-1}$ inside each OTC; $0.37 \text{ mol m}^{-2} \text{ s}^{-1}$ for the outside tree; Table 10). Total conductance (g_{tz,O_3}) was then calculated from this boundary layer conductance and an estimate of stomatal conductance in each treatment (below), according to Eq. 9.

Stomatal conductance (predicted g_{s,O_3} ; Table 16) was calculated from net carbon assimilation (A) data presented by Williams et al. (1993) on a measurement day with significant treatment differences and with a ranking of non-chamber (our "outside") and ambient (our "inside") treatments consistent with the rankings from our independent and more extensive gas exchange measurements. In actuality the relative rankings were extremely similar (13% and 15% greater in the inside than the outside tree (ratio, Table 16). From the general proportionality of A and g_s (e.g., Wong et al., 1979) and the available data from the present study for g_{s,O_3} in the chambered and non-chambered ambient treatments (Table 16), a predicted g_{s,O_3} in each of the treatments of Williams et al. (1993) was calculated. Finally an average, canopy wide ozone flux per leaf area, over both of the zones defined in the present study, was calculated (F_{O_3} ; Table 16).

The yield for the non-chambered (outside) control trees was ca 19% higher inside than outside in 1992, the period of the present study (Table 2). The data from the outside trees did not fit on the ozone-yield loss relationship (Fig. 71A; replotted from Williams et al., 1993). As an illustration of the potential impact of consideration of the ozone fluxes rather than

exposures these data were plotted as a function of the ozone fluxes (Table 16) with considerable effect. The outlying data of the non-chambered trees became part of a very strong linear relationship ($r^2=0.99$) along with the data from the exposure chambers which had, at best, been characterized as a curve defined by three points (cf. Fig. 71A,B).

This is only a demonstration of the potential power of the process-based flux protocol. Yield and growth parameters were variable in the various years of this multi-year study and only one day of gas exchange data were used to calculate the stomatal component of total conductance in 1992. Not all available data were consolidated into such excellent relationships (Table 2). It is not considered that the flux approach will linearize all available ozone yield response data sets obtained using OTC techniques. But it will help to do so and to contribute an element of mechanistic rigor to the study of ozone effects on plants. The large data set in the current report, and the suggested calculation procedures, may contribute to the adoption of these protocols for all future ozone exposure studies.

VI. SUMMARY AND CONCLUSIONS

Trees of a commercial cultivar of plum were grown under commercial management protocols and pruned to an "open-vase" morphology. Trees were subjected to ambient air inside and outside of open top chambers (OTCs). Gas exchange and transpirational sap flow measurements were made in interior and exterior positions of trees both inside and outside of the chambers. Ozone, carbon dioxide, and water vapor concentrations, temperature and windspeed, were measured at a matrix of points throughout the canopies. Gradients of O_3 , H_2O , and CO_2 between leaves in various canopy positions and the surrounding air within the canopy, or between leaves and the ambient air outside the canopy, were calculated. Using this information, fluxes of trace gases were determined for interior and exterior positions, inside and outside the OTC.

General conclusions

- 1) The OTC substantially altered the growing environments of the plum trees, based on measured bulk parameters. Ozone concentration was lower inside the OTC than outside by about .01 ppm, while water vapor concentration was ca 3 mmol mol^{-1} higher inside the OTC than outside. Diurnal changes in ozone concentration at the leaf surface paralleled ambient ozone outside the OTC, but changes were delayed inside the OTC.
- 2) More uniform exposure to ozone of leaves throughout the canopy occurred inside than outside, particularly if equal concentrations of ozone were introduced into the canopy. Despite smaller values of stomatal conductance outside the OTC, total canopy ozone uptake was greater, because the O_3 concentration entering the canopy was greater, reflecting the much greater boundary layer conductance outside. Sufficient turbulence or open canopy structure would have imposed ambient ozone near the leaf surface, causing larger ozone doses inside than outside the OTC.
- 3) The gradients of trace gas concentrations horizontally and vertically across the canopies were minimized inside the OTC, and in some cases gradients were reversed, relative to outside trees.
- 4) OTC design and blower placement provided modest within-chamber turbulent mixing, though less than outside, and effectively decoupled the within-chamber trees from the bulk ambient atmosphere outside. Inside the OTC, wind speed generated by the blowers was consistent, averaging between 0.2 and 0.3 m s^{-1} , resulting in greater within-canopy turbulence relative to outside the OTC. Outside

the OTC, only the exterior of the tree was exposed to greater and substantially variable winds.

- 5) Stomatal control of transport was greater outside than inside the OTC, though both canopies were poorly coupled to the atmosphere under low wind, San Joaquin Valley conditions. Stomatal conductances to trace gases were smaller outside the OTC, while non-stomatal and total conductances were larger, relative to inside the OTC.
- 6) Stomatal conductance was well predicted by combinations of light (PPFD) and evaporative demand (V), particularly when V was referenced to the leaf surface rather than to a bulk reference point in the ambient atmosphere.
- 7) Ozone flux was readily modelled from measured or modelled stomatal conductance and any measure of non-stomatal conductance or calculation of ozone concentration at the leaf surface. Ozone exposure concentration or stomatal conductance alone were not adequate predictors of O_3 uptake (effective dose).
- 8) It is important to consider contrasting transport characteristics in different canopy zones. These are not necessarily vertical layers in OTC protocols nor in heavily managed canopies such as pruned orchards.
- 9) Expression of ozone exposure as a total canopy flux rationalizes measurements taken both inside and outside OTCs into a single response curve, that unifies data obtained using different exposure designs.

VII. RECOMMENDATIONS

The data presented in this report support several recommendations.

- 1) Ozone response functions must be based on actual ozone uptake (effective dose) rather than on exposure indices based on concentration measured at a convenient but poorly characterized reference point above the canopy.
- 2) Gas transport parameters to specific regions of plant canopies inside and outside of exposure chambers can be measured in a variety of ways. Once these transport resistances are known, routine measurement of ambient ozone concentration at a conventional reference point and modelled or measured stomatal conductance are sufficient to infer ozone uptake. Alternatively stomatal conductance and ozone concentration, nominally at the leaf surface, but approximated by measurements of ozone concentration in various positions within the canopy, can be used to infer ozone uptake. All future studies using exposure to ozone, whether using the open-top-chamber protocol, branch chambers, or open-field exposure systems, should be required to follow some protocol for specifying ozone dose.
- 3) To expedite analysis of future (and a retrospective analysis of past) open-top-chamber studies, transport parameters should be catalogued for a range of open top chamber designs during a study specifically devoted to this purpose.
- 4) A retrospective study should be undertaken using this information to attempt to reconcile past OTC exposure studies, non-OTC exposure studies, and regional studies of ozone deposition to vegetation. This will allow an integration of scale that has been lacking in ozone-plant effects research.
- 5) A direct test of the significance of these ideas should be conducted, using a combination of branch enclosure chambers within a larger open-top-chamber design with a tree crop such as plum, to test the significance of local ozone concentrations on fruit set and quality, and leaf photosynthetic function, separate from ozone effects on whole-canopy function.
- 6) A different direct test of the significance of these ideas should be conducted, using a resistant and a sensitive cultivar of a plant species that forms a dense and continuous canopy. Exposures to ozone should be administered in a variety of OTC designs and non-OTC exposure techniques, with turbulence deliberately varied using blower speed and windbreaks. Microenvironmental measurements, as

in the present study, should be obtained. The impact of resulting differences in ozone gradients and transport parameters should be tested as the resulting spatial distribution and canopy-averaged values of single leaf gas exchange, visual damage, biomass productivity and economic yield in the two cultivars.

VIII. REFERENCES

- Albaugh, T.J., F.L. Mowry and L.W. Kress. 1992. A field chamber for testing air pollution effects on mature trees. *Jour. Env. Qual.* 21: 476-485.
- Baldocchi, D.D., B.B. Hicks and P. Camara. 1987. A canopy stomatal resistance model for gaseous deposition to vegetated surfaces. *Atmospheric Environment* 21: 91-101.
- Ball, J.T. 1987. Calculations related to gas exchange. in *Stomatal Function*. E. Zeiger, G.D. Farquhar and I.R. Cowan (eds.). Stanford University Press. Stanford. Pages 445-476.
- Bennett, J.H. and A.C. Hill. 1973. Absorption of gaseous air pollutants by a standardized plant canopy. *Jour. Air Poll. Control Assoc.* 23:203-206.
- Bennett, J.H. and A.C. Hill. 1975. Interactions of air pollutants with canopies of vegetation. In *Response to Plants to Air Pollution Stress*. J.B. Mudd and T.T. Kozlowski (eds.). Acad. Press. New York. Pages 273-306.
- Brewer, R.F. and R. Ashcroft. 1982. The Effects of Ozone and Sulfur Dioxide on Alfalfa Yields and Hay Quality. Final Report on Contract A1-038-33. California Air Resources Board, Sacramento.
- Brewer, R.F. and R. Ashcroft. 1983. The effects of ambient air pollution on Thompson Seedless grapes. The effect of present and potential air pollution on important San Joaquin Valley crops: Grapes. Final Report on Contract No. A 1-132-33. California Air Resources Board, Sacramento.
- Bytnerowicz, A., D.M. Olszyk, P.J. Dawson, and L. Morrison. 1989. Effects of Air Filtration on Concentration and Deposition of Gaseous and Particulate Air Pollutants in Open-top Field Chambers. *J. Environ. Qual.* 18: 268-273.
- Bytnerowicz, A., D.M. Olszyk, G. Kats, P.J. Dawson, J. Wolf, and C.R. Thompson. 1986a. Characteristics of Air Exclusion Systems vs. Chambers for Field Air Pollution Studies. *J. Environ. Qual.* 15: 326-334.
- Bytnerowicz, A., D.M. Olszyk, G.Kats, P.J. Dawson, J. Wolf, and C.R. Thompson. 1986b. Crop Effects from Air Pollutants in air Exclusion Systems vs. Field Chambers. *J. Environ. Qual.* 15: 417-422.
- Chameides, W.L., 1989. The chemistry of ozone deposition to plant leaves: role of ascorbic acid. *Environ. Sci. Tech.* 23: 595-600.
- Crisosto, C.H., W.A. Retzlaff, L.E. Williams, T.M. DeJong, and J.P. Zoffoli. 1993. Postharvest Performance Evaluation of Plum (*Prunus salicina* Lindel., "Casselmann")

- Fruit Grown under Three Ozone Concentrations. *J. Amer. Soc. Hort. Sci.* 118(4):497-502.
- Devitt, D. A., M. Berkowitz, P.J. Schulte, and R.L. Morris. 1993. Estimating transpiration for three woody ornamental tree species using stem-flow gauges and lysimetry. *HortScience* 28(4):320-322.
- Fuhrer, J. 1994. Effects of ozone on managed pasture: I. Effects of open-top chambers on microclimate, ozone flux, and plant growth. *Environ. Poll.* 86(3): 297-305.
- Grantz, D.A. 1990. Plant response to atmospheric humidity. *Plant Cell and Envir.* 13: 667-679.
- Grantz, D.A. and P.M. McCool. 1993. Effect of ozone on Pima and Acala cottons in the San Joaquin Valley. In Herber, D.J. and D.A. Richter (eds.), *Proceedings of the 1992 Beltwide Cotton Conference*, Nashville, TN. National cotton council of America, Memphis, TN. Vol. 3: 1082-1084.
- Grantz, D.A., P.M. McCool, and C.L. Morrison. 1992. Effect of oxidant air pollution on crops in the San Joaquin valley: Sensitivity of pima and acala cottons to ozone. *Proc. 1992 Calif. Plant and Soil Conf., Decision-Making in an Uncertain Environment*, Fresno, CA, January 28-29, 1992. p. 44-48.
- Grantz, D.A. and F.C. Meinzer. 1990. Stomatal response to humidity in a sugarcane field: Simultaneous porometric and micrometeorological measurements. *Plant, Cell, and Environ.* 13: 27-37.
- Grantz, D.A., J.I. MacPherson, W.J. Massman, and J. Pederson. 1994a. Study demonstrates ozone uptake by San Joaquin Valley crops. *Calif. Agric.* 48(4): 9-12.
- Grantz, D.A., Zhang, X.J., W.J. Massman, G. den Hartog, H.H. Neumann and J.R. Pederson. 1994b. Ozone Deposition in Field-Grown Grape: Role of Stomatal Conductance and Surface Wetness under Non-Saturating Photon Flux Density in the San Joaquin Valley. *Atmospheric Environ.* In press.
- Grantz, D.A., P.H. Moore, and E. Zeiger. 1987. Stomatal responses to light and humidity in sugarcane: Prediction of daily time courses and identification of potential selection criteria. *Plant, Cell, and Environ.* 10: 197-204.
- Gross, K. and E. Wagner. 1992. Methodische probleme bei begasungsexperimenten mit ozon: Abhangigkeit des gaswechsels und der ozonaufnahme junger fichten von der lufttemperatur, der ozonkonzentration und der art der ozonherstellung. *Allg. Forst-u.J.-Ztg.* 163: 133-138.

- Grunhage, L., U. Dammgen, H-D. Haenel, H-J. Jager, A. Holl, J. Schmitt and K. Hanewald. 1993. A new potential air-quality criterion derived from vertical flux densities of ozone and from plant response. *Angew. Bot.* 67: 9-13.
- Gutierrez, M.V., F.C. Meinzer and D.A. Grantz. 1994. Regulation of transpiration in coffee hedgerows: covariation of environmental variables and apparent responses of stomata to wind and humidity. *Plant, Cell and Environ.* in press.
- Ham, J.M., C.E. Owensby, and P.I. Coyne. 1993. Technique for Measuring Air Flow and Carbon Dioxide Flux in Large, Open-Top Chambers. *J. Environ. Qual.* 22:759-766.
- Hanson, P.J. and G.E. Taylor. 1990. Modeling pollutant gas uptake by leaves: an approach based on physiochemical properties. In: R.K. Dixon, R. Meldahl, G. Ruark and W.G. Warren (Eds.) Process Modeling of Forest Growth Responses to Environmental Stress. Timber Press, Portland, OR. pp. 351-356.
- Heck, W.W. 1989. Assessment of crop losses from air pollutants in the United States. In J.J. MacKenzie and M.T. El-Ashry (eds.) *Air Pollution's Toll on Forests and Crops.* Yale University Press. New Haven.
- Heck, W.W., J.A. Dunning and H. Johnson. 1968. Design of a simple plant exposure chamber. National Center for Air Pollution Control. U.S.D.H.E.W., Wash., DC.
- Heck, W.W., R.B. Philbeck and J.A. Denning. 1978. A continuous stirred tank reactor (CSTR) system for exposing plants to gaseous air pollutants. USDA, ARS. Publ. No. ARS-5-181. Wash., DC.
- Houston, D.B. and G.R. Stairs. 1973. Genetic control of SO₂ and O₃ tolerance in eastern white pine. *Forest Science* 19:267-271.
- Howitt, R. 1990. In H.O. Carter and C.F. Nuckton (eds.) *California's Central Valley-- Confluence of Change.* University of California Agricultural Issues Center. p. 65.
- Jarvis, P.G. and K.G. McNaughton. 1986. Stomatal control of transpiration: Scaling up from leaf to region. *Adv. Ecol. Res.* 15:1-49.
- Jones, H.G. 1983. *Plants and microclimate: a quantitative approach to environmental plant physiology.* Cambridge University Press. Cambridge.
- Kaplan, W.A., S.C. Wofsy, M. Keller and J.M. da Coosta. 1988. Emission of NO and deposition of O₃ in a tropical forest system. *Jour. Geophysical Res.* 93:1389-1395.
- Kats, G., D.M. Olszyk, and C.R. Thompson. 1985. Open Top Experimental Chambers for Trees. *Journal of the air Pollution control Association.* APCA Note-Book. 35(12):1298-1301.

- Katz, M. and F.E. Lathe. 1939. Effect of sulfur dioxide on vegetation. Natl. Res. Council of Canada, Ottawa.
- Laisk, A., O. Kull and H. Moldau. 1989. Ozone concentration in leaf intercellular air spaces is close to zero. *Plant Physiol.* 90:1163-1167.
- Leadley, P.W. and B.G. Drake. 1993. Open top chambers for exposing plant canopies to elevated CO₂ concentration and for measuring net gas exchange. *Vegetatio* 104: 3-15.
- Lefohn, A.S. 1992. Surface level ozone exposures and their effects on vegetation. Lewis Publishers, Chelsea. 366 pages.
- Lewis, E. and E. Brennan. 1977. A Disparity in the Ozone Response of Bean Plants Grown in a Greenhouse, Growth Chamber or Open-Top Chamber. *Journal of the Air Pollution Control Association* 27(9): 889-891.
- McCool, P.M., R.C. Musselman, R.R. Teso and R.J. Oshima. 1986. Determining yield losses from air pollutants for California agriculture. *California Agriculture* 40: 9-10.
- McNaughton, K.G., and Jarvis, P.G. 1983. Predicting effects of vegetation changes on transpiration and evaporation. In *Water Deficits and Plant Growth*. Vol. VII. (ed. T.T. Kozlowski). pp. 1-47. Academic Press. New York.
- Martin, P. 1989. The significance of radiative coupling between vegetation and the atmosphere. *Agric. and Forest Meteorology*. 49:45-53.
- Massman, W.J. and D.A. Grantz. 1994. Estimating canopy conductance to ozone uptake from canopy scale evapotranspiration observations or by scaling up leaf stomatal conductance measurements: Does either method work? *Agric. and Forest Meteorol.* in press.
- Meinzer, F.C. and D.A. Grantz. 1989. Stomatal control of transpiration from a developing sugarcane canopy. *Plant Cell and Environ.* 12: 635-642.
- Mudd, J.B. 1982. Effects of oxidants on metabolic function. In: M.H. Unsworth and D.P. Ormrod (Eds.), *Effects of Gaseous Air Pollutants on Agriculture and Horticulture*. Butterworth Scientific, London, pages 189-203.
- Mudd, J.B. 1991. Field verification of yield losses from ambient ozone to cotton (*Gossypium hirsutum*) in the San Joaquin Valley. Final Report on Contract No. A833-105. California Air Resources Board.
- Musselman, R. C., P.M. McCool, R.J. Oshima, and R.R. Teso. 1986. Field chambers for Assessing Crop Loss from Air Pollutants. *J. Environ. Qual.* 15(2): 152-157.
- Olszyk, D.M., Cabrera and Thompson. 1988. California Statewide assessment of the effects of ozone on crop productivity. *Jour. Air Poll. Control Assoc.* 38: 928-931.

- Olszyk, D.M., B.K. Takemoto, G. Kats, P.J. Dawson, C.L. Morrison, J. Wolf Preston and C.R. Thompson. 1992. Effects of open-top chambers on 'Valencia' orange trees. *Jour. Env. Qual.* 21: 128-134.
- Pederson, J.R., A. Delany, S. Oncley, G. den Hartog, H.H. Neumann, R. Desjardins, D.A. Grantz, J.I. MacPherson, L.J. Mahrt, W.J. Massman, R. Pearson, Jr., P.R. Roth, P.H. Schuepp, R.H. Shaw and K.T. Paw U. 1995. California Ozone Deposition Experiment, Methods, Results and Opportunities. *Atmospheric Environment*. In press.
- Penman, H. L. 1948. Natural evaporation from open water, bare soil, and grass. *Proceedings of the Royal Society (London). Series A.* 193, 120-145.
- Reich, P.B. 1983. Effects of low concentrations of O₃ on net photosynthesis, dark respiration, and chlorophyll contents in aging hybrid poplar leaves. *Plant Physiol.* 73: 291-296.
- Reich, P.B. and R.G. Amundson. 1985. Ambient levels of ozone reduce net photosynthesis in tree and crop species. *Science* 230: 566-570.
- Reich, P.B., D.S. Ellsworth, B.D. Kloeppel, J.H. Fownes and S.T. Gower. 1990. Vertical variation in canopy structure and CO₂ exchange of oak-maple forests: influence of ozone, nitrogen, and other factors on simulated canopy carbon gain. *Tree Physiol.* 7:329-345.
- Retzlaff, W.A., L.E. Williams and T.M. DeJong. 1991. The effect of different atmospheric ozone partial pressures on photosynthesis and growth of nine fruit and nut tree species. *Tree Physiology* 8: 93-105.
- Retzlaff, W.A., L.E. Williams and T.M. DeJong. 1992. Photosynthesis, growth, and yield response of 'Casselman' plum to various ozone partial pressures during orchard establishment. *Jour. Amer. Hort. Sci.* 117: 703-710.
- Roberts, T.M., K.A. Brown and L.W. Blank. 1987. Methodological aspects of the fumigation of forest trees with gaseous pollutants using closed chambers. In *Air Pollution and Ecosystems*, P. Mathy (ed.). Proc. of Intl. Symp., Grenoble France, 18-22 May 1987. D. Reidel Publ. Co., Boston. pp. 338-360.
- Roper, T.R. and L.E. Williams. 1989. The effects of ambient and acute partial pressures of ozone on leaf net CO₂ assimilation of field-grown *Vitis vinifera* L. *Plant Physiol.* 91: 1501-1506.
- Runeckles, V.C. 1974. Dosage of air pollutants and damage to vegetation. 4:305-308.

- Sanders, G.E., A.G. Clark and J.J. Colls. 1991. The influence of open-top chambers on the growth and development of field bean. *New Phytol.* 117: 439-447.
- Taylor, G.E. and P.J. Hanson. 1994. Forest trees and tropospheric ozone: Role of canopy deposition and leaf uptake in developing exposure-response relationships. *Agric. Ecosys. and Environ.* In press.
- Taylor, G.E., P.J. Hanson and D.D. Baldocchi. 1989. Pollutant deposition to individual leaves and plant canopies: sites of regulation and relationship to injury. In: W.W. Heck, O.C. Taylor and D.T. Tingey (Eds.), *Assessment of crop loss from air pollutants.* Elsevier Applied Science, New York. pages 227-258.
- Taylor, G.E., S.B. McLaughlin and D.S. Shriner. 1982a. Effective Pollutant Dose. In *Effects of Gaseous Air Pollution in Agriculture and Horticulture.* 458-461.
- Taylor, G.E., D.T. Tingey and H.C. Ratsch, 1982b. Ozone flux in *Glycine max* (L.) Merr.: sites of regulation and relationship to leaf injury. *Oecol* 53: 179-186.
- Temple, P.J. 1988. Injury and yield responses of differentially irrigated cotton to ozone. *Agron. Jour.* 80: 751-755.
- Temple, P.J. 1990. Growth and yield responses of processing tomato (*Lycopersicon esculentum* Mill.) cultivars to ozone. *Environ. Exper. Bot.* 30: 283-291.
- Temple, P.J., L.F. Benoit, R.W. Lennox, C.A. Reagan and O.C. Taylor. 1988a. Combined effects of ozone and water stress on alfalfa growth and yield. *Jour. Envir. Quality* 17:108-113.
- Temple, P.J., R.S. Kupper, R.W. Lennox, and K. Rohr. 1988b. Physiological and growth responses of differentially irrigated cotton to ozone. *Environ. Poll.* 53: 255-263.
- Thomas, M.D. 1951. Gas damage to plants. *Ann. Rev. Plant Physiol.* 2:293-322.
- Tingey, D.T. and G.E. Taylor Jr. 1982. Variation in plant response to ozone: a conceptual model of physiological events. In: M.H. Unsworth and D.P. Ormrod (Eds.), *Effects of gaseous air pollutants on agriculture and horticulture.* Buttonworth Scientific. London. pp. 113-138.
- Townsend, A.M. 1974. Sorption of ozone by nine shade trees species. *J. Amer. Soc. Hortic. Sci.* 99: 206-208.
- Tyree, M.T. and P. Yianoulis. 1980. The site of water evaporation from sug-stomatal cavities, liquid path resistances and hydroactive stomatal closure. *Ann. Bot.* 46: 175-193.

- Unsworth, M.H., A.S. Heagle and W.W. Heck. 1984. Gas exchange in open-top field chambers--I. Measurement and analysis of atmospheric resistances to gas exchange. *Atmos. Env.* 18: 373-380.
- Unsworth, M.H. and T.A. Mansfield. 1980. Critical aspects of chamber design for fumigation experiments on grasses. *Env. Poll. (A)* 23:115-120.
- van Wakeren, H. Visser and F.B.J. Koops. 1987. Investigating Effects of Air Pollution by Measuring the Waterflow Velocity in Trees. Proceedings of an International Symposium held in Grenoble, France, 18-22 May 1987. 739-742.
- Weinstock, L., W.J. Kender and R.C. Musselman. 1982. Microclimate within open-top air pollution chambers and its relation to grapevine physiology. *Jour. Amer. Soc. Hort. Sci.* 107: 923-929.
- Weseley, M.L. 1989. Parameterization of surface resistances to gaseous dry deposition in regional-scale numerical models. *Atmospheric Environ.* 23: 1293-1304.
- Williams, L.E., T.M. DeJong, and W.A. Retzlaff. 1993. The Effect of Ozone on Photosynthesis, Vegetative Growth and Productivity of *Prunus salicina* In The San Joaquin Valley of California. Final Report on Contract A133-137. California Air Resources Board. Sacramento.
- Winer, A.M., D.M. Olszyk and R.E. Howitt. 1990. Air quality impacts on California Agriculture, 1990-2010. In H.O. Carter and C.F. Nuckton (eds.) *Agriculture in California--On the brink of a new millennium*. UC Agricultural Issues Center.
- Wiltshire, J.J.J., C.J. Wright and M.H. Unsworth. 1992. A new method for exposing mature trees to ozone episodes. *For. Ecol. and Manage.* 51: 115-120.
- Wong, S.C., I.R. Cowan and G.D. Farquhar. 1979. Stomatal conductance correlates with photosynthetic capacity. *Nature* 282: 424-426.

LIST OF INVENTIONS REPORTED AND PUBLICATIONS

Grantz, D.A. 1994. Paper presented at the 87th Annual Meeting of the Air and Waste Management Association, June 19-24, 1994, entitled, Ozone Uptake by San Joaquin Valley Crops. Paper No. 94-TA36.01 in the Preprint Volume. 15 pages.

Grantz, D.A., W.A. Retzlaff, L.E. Williams, and T.M. DeJong. 1992. Paper presented at the 89th Annual Meeting of the American Society for Horticultural Science 31 July-6 August 1992, entitled, Ozone Gradients, Photosynthesis and Yield in Plum. Abstract in Preprint Volume.

GLOSSARY OF TERMS, ABBREVIATIONS, AND SYMBOLS

<u>Symbol</u>	<u>Definition</u>
<u>Conductance</u>	
$g_{s,v}$, $g_{s,c}$, g_{s,O_3}	Stomatal conductance ($\text{mol m}^{-2} \text{s}^{-1}$) for H_2O , CO_2 , and O_3 , respectively.
$g_{bl,v}$, $g_{bl,c}$, g_{bl,O_3}	Leaf laminar boundary layer conductance ($\text{mol m}^{-2} \text{s}^{-1}$) for H_2O , CO_2 , and O_3 , respectively.
$g_{ba,v}$, $g_{ba,c}$, g_{ba,O_3}	Boundary layer conductance ($\text{mol m}^{-2} \text{s}^{-1}$) for H_2O , CO_2 , and O_3 , respectively, to the ambient reference point, location 3.
$g_{bz,v}$, $g_{bz,c}$, g_{bz,O_3}	Boundary layer conductance ($\text{mol m}^{-2} \text{s}^{-1}$) for H_2O , CO_2 , and O_3 , respectively, to within canopy zone.
$g_{ta,v}$, $g_{ta,c}$, g_{ta,O_3}	Total conductance ($\text{mol m}^{-2} \text{s}^{-1}$) for H_2O , CO_2 , and O_3 , respectively, to the ambient reference point, location 3.
$g_{tz,v}$, $g_{tz,c}$, g_{tz,O_3}	Total conductance ($\text{mol m}^{-2} \text{s}^{-1}$) for H_2O , CO_2 , and O_3 , respectively, to within canopy zone.
g_r	Long wave radiative transfer conductance ($\text{mol m}^{-2} \text{s}^{-1}$).
<u>Resistance</u>	
$r_{s,v}$, $r_{s,c}$, r_{s,O_3}	Stomatal resistance ($\text{m}^2 \text{s mol}^{-1}$) for H_2O , CO_2 , and O_3 , respectively.
$r_{bl,v}$, $r_{bl,c}$, r_{bl,O_3}	Leaf laminar boundary layer resistance ($\text{m}^2 \text{s mol}^{-1}$) for H_2O , CO_2 , and O_3 , respectively.
$r_{ba,v}$, $r_{ba,c}$, r_{ba,O_3}	Boundary layer resistance ($\text{m}^2 \text{s mol}^{-1}$) for H_2O , CO_2 , and O_3 , respectively, to the ambient reference point, location 3.
$r_{bz,v}$, $r_{bz,c}$, r_{bz,O_3}	Boundary layer resistance ($\text{m}^2 \text{s mol}^{-1}$) for H_2O , CO_2 , and O_3 , respectively, to within canopy zone.
$r_{ta,v}$, $r_{ta,c}$, r_{ta,O_3}	Total resistance ($\text{m}^2 \text{s mol}^{-1}$) for H_2O , CO_2 , and O_3 , respectively, to the ambient reference point, location 3.
$r_{tz,v}$, $r_{tz,c}$, r_{tz,O_3}	Total resistance ($\text{m}^2 \text{s mol}^{-1}$) for H_2O , CO_2 , and O_3 , respectively, to within canopy zone.
<u>Concentration</u>	
e_i , e_s , e_z , e_a	Water vapor pressure (kPa) in the leaf interior, at the leaf surface, within the canopy zone, and at the ambient reference point (location 3), respectively.

$O_{3i}, O_{3s}, O_{3z}, O_{3a}$	Ozone concentration (ppm) in the leaf interior, at the leaf surface, within the canopy zone, and at the ambient reference point (location 3), respectively.
C_i, C_s, C_z, C_a	CO ₂ concentration (ppm) in the leaf interior, at the leaf surface, within the canopy zone, and at the ambient reference point (location 3), respectively.

Gradients

V_s, V_z, V_a	Water vapor pressure gradient (mol mol ⁻¹) from leaf interior to the leaf surface, to within canopy zone, and to the ambient reference point (location 3), respectively.
$\Delta O_3, \Delta O_{3z}, \Delta O_{3a}$	Ozone concentration gradient (ppm) from leaf interior to the leaf surface, to within canopy zone, and to the ambient reference point (location 3), respectively.
$\Delta C, \Delta C_z, \Delta C_a$	CO ₂ concentration gradient (ppm) from leaf interior to the leaf surface, to within canopy zone, and to the ambient reference point (location 3), respectively.

Flux

E	Water vapor flux (transpiration) on a leaf area basis (mol m ⁻² s ⁻¹).
A	CO ₂ flux (assimilation) on a leaf area basis (μmol m ⁻² s ⁻¹).
F _{O₃}	Ozone flux on a leaf area basis (nanomol m ⁻² s ⁻¹).

Environmental and Physiological Parameters

T_a	Ambient air temperature (°C).
T_l	Leaf temperature (°C).
P	Atmospheric pressure (Pa).
Ω	Environmental decoupling coefficient (unitless).
Ω_R	Environmental decoupling coefficient including radiative transfer conductance (unitless).
γ	Psychrometric constant (Pa K ⁻¹).
Δ	Slope of the saturation vapor pressure versus temperature curve evaluated at air temperature.
ϵ	Dimensionless change of latent heat content relative to the change of sensible heat content of saturated air (=Δ/γ).
ψ	Transpiring leaf water potential (MPa).
L_E	Hydraulic conductance per scaffold branch (mmol s ⁻¹ MPa ⁻¹)

L_E/m^2	Hydraulic conductance per unit leaf area ($mmol\ m^{-2}\ s^{-1}\ MPa^{-1}$)
	<u>Other</u>
OTC	Open Top Chamber.
DOY	Day of Year.
PPFD	Photosynthetically active Photon Flux Density.

TABLES

Table 1¹. A comparison of bulk environmental modifications relative to ambient conditions, caused by enclosure of plants inside ozone exposure chambers of various designs, including those used in the present experiment.

	<u>Open top chamber</u> (Weinstock et al., 1987)	<u>Closed top chamber</u> (Roberts et al., 1987)	<u>Open top chamber²</u> (Williams et al., 1993)
Air changes	3.7	4	2
T air	+ 0.4 to - 3.7° C	+ 1° C	+1.5 to -0.4° C
T leaf	+ 1 to - 5° C	± 0	+1.1 to -0.7° C
RH	- 5 to - 10%	+ 5%	+1.2 to +5.4%
VPD	+ 5%	- 5%	-0.3 to -13.8%

1. Adapted from Roberts et al., 1987.
2. Used in the present study.

Table 2. Effect of open-top-chambers (OTC) on selected growth and yield parameters of plum trees in the present study (unpublished data from L.E. Williams and T.M. DeJong).

		1989	1990	1991	1992	1993
Cross-sectional area (cm ² /season)	In	17.6±1.3	30.5±1.0	25.3±1.1	22.6±1.5	na ¹
	Out	12.8±1.4	22.4±1.2	18.2±1.0	24.4±1.0	na
	Difference	+38%	+36%	+39%	-7%	
Fruit Yield (kg/tree)	In	na	6.3±0.5	15.9±1.3	23.7±1.7	14.5±1.3
	Out	na	5.5±0.6	15.8±1.7	19.9±1.5	20.1±1.4
	Difference	na	+14%	+1%	+19%	-28%
Fruit size (g/fruit)	In	na	63±1	84±2	80±2	88±1.7
	Out	na	58±1	75±1	78±2	83±0.3
	Difference	na	+9%	+12%	+2%	+6%
Fruit count (No./tree)	In	na	101±9	191±14	306±26	166±13
	Out	na	95±11	212±23	262±22	243±17
	Difference	na	+6%	-10%	+17%	-32%

¹na, not available

Table 3. Effect of OTC on 12-hour seasonal mean ozone exposure (0800-2000, PDT) by canopy location, and by zone (ppm).			
Outside the OTC		Inside the OTC	
Location	[O ₃]	Location	[O ₃]
1	.0655	1	.0557
2	.0669	2	.0573
3	.0673	3	.0574
4	.0638	4	.0581
5	.0660	5	.0583
6	.0668	6	.0581
7	.0641	7	.0584
8	.0653	8	.0580
9	.0660	9	.0583
Zone			
INTEROUT	.06464	INTERIN	.05691
EXTEROUT	.06645	EXTERIN	.05777

Table 4. Mean daily diffusive conductances, gradients, and fluxes of H₂O vapor for each zone, and the effect of the OTC on the ratio of exterior to interior positions.

Zone	$g_{s,v}$	$g_{bl,v}$	$g_{bz,v}$	$g_{tz,v}$	V_z	$g_{ba,v}$	$g_{ta,v}$	V_a	E
EXTERIN	0.22	0.83	0.21	0.11	.024	0.18	0.10	.027	2.6
EXTEROUT	0.19	1.12	0.54	0.14	.027	0.53	0.14	.027	3.8
INTERIN	0.16	0.80	0.40	0.11	.026	0.30	0.10	.029	2.9
INTEROUT	0.13	0.60	0.49	0.10	.027	0.43	0.10	.027	2.7
% Total Resistance									
EXTERIN	44.8	11.6	46.0	90.8	--	55.2	--	--	--
EXTEROUT	73.9	12.4	25.8	99.7	--	26.1	--	--	--
INTERIN	65.5	12.9	25.7	91.4	--	34.5	--	--	--
INTEROUT	77.2	16.6	20.2	97.5	--	22.8	--	--	--
Exterior/Interior									
Inside	1.37	1.04	0.52	1.00	0.92	0.60	1.00	0.93	0.90
Outside	1.46	1.87	1.10	1.40	1.00	1.23	1.40	1.00	1.41
$g_{s,v}$: Stomatal conductance (mol m ⁻² s ⁻¹); $g_{bl,v}$: Laminar leaf boundary layer conductance (mol m ⁻² s ⁻¹); $g_{bz,v}$: Boundary layer conductance from leaf to zone (mol m ⁻² s ⁻¹); $g_{tz,v}$: Total conductance to zone (mol m ⁻² s ⁻¹); V_z : Water vapor concentration gradient to zone (mol mol ⁻¹); $g_{ba,v}$: Boundary layer conductance to external, ambient reference point at location 3 (mol m ⁻² s ⁻¹); $g_{ta,v}$: Total conductance to ambient reference (mol m ⁻² s ⁻¹); V_a : Water vapor concentration gradient to ambient reference (mol mol ⁻¹); E: Water vapor flux (mmol m ⁻² s ⁻¹).									

Table 5. Mean midday values of transpiration, water potential, and hydraulic conductance for each zone, and the effect of the OTC on the ratio of exterior to interior positions.

Zone	E	Ψ	L_E/m^2	L_E
EXTERIN	2.1	-2.00	1.0	0.73
EXTEROUT	4.3	-2.16	2.0	2.07
INTERIN	2.5	-1.72	1.43	0.97
INTEROUT	2.3	-1.92	1.23	0.97
Exterior/Interior				
Inside	0.84	1.16	0.70	0.75
Outside	1.87	1.12	1.63	2.13

E: Transpiration ($\text{mmol m}^{-2} \text{s}^{-1}$); Ψ : Exposed leaf water potential (MPa); L_E/m^2 : Hydraulic conductance per unit leaf area ($\text{mmol m}^{-2} \text{s}^{-1} \text{Mpa}^{-1}$); L_E : Hydraulic conductance per scaffold branch ($\text{mmol s}^{-1} \text{MPa}^{-1}$).

Table 6. Effect of OTC on mean daily stomatal, nonstomatal (boundary layer), and total conductance to H₂O, vapor pressure gradient, and water vapor flux (transpiration) averaged over 1100-1600 (PDT) and the six days of intensive physiological measurements.

	$g_{s,v}$	%	$g_{ba,v}$	%	$g_{tz,v}$	%	V_z	$g_{ta,v}$	V_a	L_F/m^2	E
Inside OTC	.182	54.9	.221	45.2	.110	90.9	.025	.100	.028	1.2	.0027
Outside OTC	.153	75.8	.480	24.2	.118	98.3	.027	.116	.027	1.6	.0032

$g_{s,v}$: Stomatal conductance ($\text{mol m}^{-2}\text{s}^{-1}$); $g_{ba,v}$: Boundary layer conductance from leaf to ambient reference ($\text{mol m}^{-2}\text{s}^{-1}$); $g_{tz,v}$: Total conductance to zone ($\text{mol m}^{-2}\text{s}^{-1}$); V_z : Water vapor concentration gradient to zone (mol mol^{-1}); $g_{ta,v}$: Total conductance to ambient reference ($\text{mol m}^{-2}\text{s}^{-1}$); V_a : Water vapor concentration gradient to ambient reference (mol mol^{-1}); E: Transpiration ($\text{mol m}^{-2}\text{s}^{-1}$); L_F/m^2 : Hydraulic conductance per unit leaf area. % data represent the percentage of total resistance (inverse conductance, i.e., $1/g_t$) represented by each component resistance (i.e., $1/g_{s,v}$ etc.)

Table 7. Effect of OTC on the environmental decoupling coefficient, with radiative coupling (Ω_R) and without radiative coupling (Ω), averaged over 1000-1600 (PDT) and the six days of intensive physiological measurements.			
	Ω	Ω_R	% Reduction by R
Inside OTC	.76	.68	10.6%
Outside OTC	.56	.50	10.7%

Table 8. Mean daily diffusive conductances, gradients, and fluxes of CO₂ for each zone, and the effect of the OTC on the ratio of exterior to interior positions.

Zone	$g_{s,c}$	$g_{bl,c}$	$g_{bz,c}$	$g_{tz,c}$	ΔC_z	$g_{ba,c}$	$g_{ta,c}$	ΔC_a	A
EXTERIN	0.13	0.60	0.15	0.07	44.89	0.12	0.06	49.34	4.60
EXTEROUT	0.11	0.81	0.39	0.09	77.23	0.38	0.09	77.79	9.57
INTERIN	0.10	0.57	0.29	0.07	50.75	0.21	0.06	54.40	5.15
INTEROUT	0.08	0.43	0.35	0.06	71.88	0.31	0.06	73.79	6.32
% Total Resistance									
EXTERIN	48.8	10.8	42.7	91.4	--	51.2	--	--	--
EXTEROUT	76.9	11.0	22.8	99.7	--	23.0	--	--	--
INTERIN	69.2	11.5	23.0	92.2	--	30.8	--	--	--
INTEROUT	80.0	14.5	17.8	97.8	--	20.0	--	--	--
Exterior/Interior									
Inside	1.38	1.04	0.52	0.98	0.88	0.59	0.97	0.91	0.89
Outside	1.47	1.88	1.10	1.39	1.07	1.23	1.42	1.05	1.51
$g_{s,c}$: Stomatal conductance (mol m ⁻² s ⁻¹); $g_{bl,c}$: Laminar leaf boundary layer conductance (mol m ⁻² s ⁻¹); $g_{bz,c}$: Boundary layer conductance from leaf to zone (mol m ⁻² s ⁻¹); $g_{tz,c}$: Total conductance to zone (mol m ⁻² s ⁻¹); ΔC_z : CO ₂ concentration gradient to zone (ppm); $g_{ba,c}$: Boundary layer conductance to ambient reference (mol m ⁻² s ⁻¹); $g_{ta,c}$: Total conductance to ambient reference (mol m ⁻² s ⁻¹); A: CO ₂ flux (μmol m ⁻² s ⁻¹).									

Table 9. Effect of OTC on mean daily stomatal, nonstomatal (boundary layer) and total conductance to CO₂, CO₂ concentration gradient and net carbon assimilation rate (photosynthesis), averaged over 1100-1600 (PDT) and the six days of intensive physiological measurements.

	$g_{s,c}$	%	$g_{ba,c}$	%	$g_{tz,c}$	%	ΔC_z	$g_{ta,c}$	ΔC_a	A
Inside OTC	.111	58.6	.158	41.1	.071	91.5	47.8	.065	51.9	4.9
Outside OTC	.093	78.5	.344	21.2	.074	98.6	74.6	.073	75.8	7.9

$g_{s,c}$: Stomatal CO₂ conductance; $g_{ba,c}$: Boundary layer conductance from leaf to ambient reference (mol m⁻²s⁻¹); $g_{tz,c}$: Total conductance to zone (mol m⁻²s⁻¹); ΔC_z : CO₂ concentration gradient to zone (ppm); $g_{ta,c}$: Total conductance to ambient reference (mol m⁻²s⁻¹); ΔC_a : CO₂ concentration gradient to ambient reference (ppm); A: Net carbon assimilation rate from single leaf measurements (micromol m⁻²s⁻¹).

Table 10. Mean daily diffusive conductances, gradients, and fluxes of O₃ for each zone, and the effect of the OTC on the ratio of exterior to interior positions.

Zone	g_{s,O_3}	g_{bl,O_3}	g_{bz,O_3}	g_{tz,O_3}	ΔO_{3z}	g_{ba,O_3}	g_{ta,O_3}	ΔO_{3a}	F_{O_3}
EXTERIN	0.13	0.60	0.15	0.07	0.064	0.13	0.06	.073	4.69
EXTEROUT	0.12	0.81	0.39	0.09	0.071	0.38	0.09	.073	6.58
INTERIN	0.10	0.57	0.29	0.07	0.064	0.21	0.07	.073	4.83
INTEROUT	0.08	0.43	0.35	0.06	0.070	0.31	0.06	.073	4.56
% Total Resistance									
EXTERIN	48.8	10.8	42.7	91.4	--	51.2	--	--	--
EXTEROUT	77.0	11.0	22.9	99.8	--	23.1	--	--	--
INTERIN	69.1	11.5	23.1	92.2	--	30.9	--	--	--
INTEROUT	79.9	14.6	17.8	97.7	--	20.1	--	--	--
Exterior/Interior									
Inside	1.38	1.04	0.53	0.98	1.00	0.59	0.97	1.00	0.97
Outside	1.47	1.87	1.10	1.39	1.01	1.23	1.42	1.00	1.44
g_{s,O_3} : Stomatal conductance (mol m ⁻² s ⁻¹); g_{bl,O_3} : Laminar leaf boundary layer conductance (mol m ⁻² s ⁻¹); g_{bz,O_3} : Boundary layer conductance from leaf to zone (mol m ⁻² s ⁻¹); g_{tz,O_3} : Total conductance to zone (mol m ⁻² s ⁻¹); ΔO_{3z} : O ₃ concentration gradient to zone (ppm); g_{ba,O_3} : Boundary layer conductance to ambient reference (mol m ⁻² s ⁻¹); g_{ta,O_3} : Total conductance to ambient reference (mol m ⁻² s ⁻¹); F_{O_3} : O ₃ flux (nanomol m ⁻² s ⁻¹).									

Table 11. Effect of OTC on mean daily stomatal, nonstomatal (boundary layer) and total conductance to O_3 , O_3 concentration gradient and ozone flux (leaf uptake), averaged over 1100-1600 (PDT) and the six days of intensive physiological measurements.

	g_{s,O_3}	%	g_{ba,O_3}	%	g_{tz,O_3}	%	ΔO_{3z}	g_{ta,O_3}	ΔO_{3a}	F_{O_3}
Inside OTC	.111	58.6	.159	40.9	.071	91.5	.064	.065	.073	4.76
Outside OTC	.094	78.7	.345	21.4	.075	98.7	.071	.074	.073	5.57

g_{s,O_3} : Stomatal conductance; g_{ba,O_3} : Boundary layer conductance from leaf to ambient reference ($\text{mol m}^{-2}\text{s}^{-1}$); g_{tz,O_3} : Total conductance to zone ($\text{mol m}^{-2}\text{s}^{-1}$); ΔO_{3z} : Ozone concentration gradient to zone (ppm); g_{ta,O_3} : Total conductance to ambient reference ($\text{mol m}^{-2}\text{s}^{-1}$); ΔO_{3a} : Ozone concentration gradient to ambient reference (ppm); F_{O_3} : Ozone flux on a leaf area basis ($\text{nanomol m}^{-2}\text{s}^{-1}$).

Table 12. Goodness of fit of contrasting models of stomatal conductance as a function of zone and a variety of individual, independent environmental parameters, inside and outside the OTC separately and combined.						
Inside the OTC						
Independent regressor variable	Exterior of tree			Interior of tree		
	r^2	F	p	r^2	F	p
Above canopy photon flux (PPFD)	0.64	10.60	0.02¹	0.39	3.8	0.10
VPD to canopy exterior (V_a)	0.02	0.11	0.76	0.00	0.01	0.95
VPD to leaf surface (V_s)	0.52	5.30	0.07	0.93	55.10	0.00
Sap Flow (E)	0.13	0.91	0.38	0.14	0.99	0.36
Above canopy wind speed	0.02	0.09	0.77	0.02	0.10	0.77
O ₃ concentration canopy exterior ($O_{3,a}$)	0.05	0.32	0.59	0.00	0.01	0.95
O ₃ concentration at leaf surface ($O_{3,s}$)	0.06	0.37	0.56	0.45	4.83	0.07
Air temperature (T_a)	0.11	0.77	0.41	0.01	0.07	0.80
Outside the OTC						
Independent regressor variable	Exterior of tree			Interior of tree		
	r^2	F	p	r^2	F	p
Above canopy photon flux (PPFD)	0.03	0.2	0.67	0.06	0.41	0.55
VPD to canopy exterior (V_a)	0.28	2.39	0.17	0.17	1.22	0.31
VPD to leaf surface (V_s)	0.36	3.4	0.11	0.40	3.93	0.09
Sap Flow (E)	0.00	0.02	0.89	0.00	0.01	0.91
Above canopy wind speed	0.33	2.95	0.14	0.26	2.15	0.19
O ₃ concentration canopy exterior ($O_{3,a}$)	0.24	1.91	0.22	0.18	1.33	0.29
O ₃ concentration at leaf surface ($O_{3,s}$)	0.31	2.64	0.16	0.38	3.73	0.10
Air temperature (T_a)	0.14	0.98	0.36	0.09	0.62	0.46
All zones combined						
Independent regressor variable	r^2	F	p			
Above canopy photon flux (PPFD)	0.14	4.8	0.05			
VPD to canopy exterior (V_a)	0.02	0.55	0.47			
VPD to leaf surface (V_s)	0.42	19.50	0.00			
Sap Flow (E)	0.03	0.82	0.37			
Above canopy wind speed	0.02	0.75	0.39			
O ₃ concentration canopy exterior ($O_{3,a}$)	0.01	0.23	0.63			
O ₃ concentration at leaf surface ($O_{3,s}$)	0.22	9.80	0.00			
Air temperature (T_a)	0.00	0.008	0.93			

¹Bold text indicates significant relationships at $P \leq 0.10$.

Table 13. Contrasting models of stomatal conductance as a function of the composite environmental parameter, photon flux density (PPFD) normalized by vapor pressure gradient (V_a or V_s)				
PPFD normalized by V_a to the ambient reference				
Zone	r^2	F	p	Equation
EXTERIN	0.03	0.16	0.70	$g=0.1779+.00005(PPFD/V_a)$
EXTEROUT	0.61	9.51	0.02	$g=.0890+.0002(PPFD/V_a)$
INTERIN	0.04	0.28	0.62	$g=0.132+.00004(PPFD/V_a)$
INTEROUT	0.53	6.83	0.04	$g=0.064+.0001(PPFD/V_a)$
All Zones	0.13	4.57	0.04	$g=.106+.0001(PPFD/V_a)$
PPFD normalized by V_s to the leaf surface.				
Zone	r^2	F	p	Equation
EXTERIN	0.86	31.08	0.003	$g=.0876+.0001(PPFD/V_s)$
EXTEROUT	0.69	13.62	0.01	$g=.0877+.0001(PPFD/V_s)$
INTERIN	0.98	252.24	0.0001	$g=.0351+.0002(PPFD/V_s)$
INTEROUT	0.83	30.06	0.0015	$g=.0405+.0001(PPFD/V_s)$
All Zones	0.70	63.0	0.0001	$g=.071+.0001(PPFD/V_s)$

Table 14. Contrasting models of stomatal conductance as a function of an additive combination of photon flux density and vapor pressure gradient.				
PPFD and V_a to the ambient reference.				
Zone	r^2	F	p	Equation
EXTERIN	0.98	111.0	0.0001	$g=0.0284+0.0002PPFD-0.0423V_a$
EXTEROUT	0.98	137.9	0.0001	$g=0.1483+0.0001PPFD-0.0528V_a$
INTERIN	0.98	119.4	0.0001	$g=0.0483+0.0002PPFD-0.0390V_a$
INTEROUT	0.99	418.1	0.0001	$g=0.0899+0.0001PPFD-0.0371V_a$
All Zones	0.52	15.77	0.0001	$g=.0766+.0002PPFD-.0459V_a$
PPFD and V_s to the leaf surface.				
Zone	r^2	F	p	Equation
EXTERIN	0.97	87.9	0.0001	$g=0.0888+0.0001PPFD-0.0703V_s$
EXTEROUT	0.95	49.6	0.0005	$g=0.1572+0.0001PPFD-0.0620V_s$
INTERIN	0.98	105.7	0.0001	$g=0.1561+.0001PPFD-0.0537V_s$
INTEROUT	0.92	28.1	0.0019	$g=0.1166+0.0001PPFD-0.0348V_s$
All Zones	0.72	36.6	0.0001	$g=.1312+.0001PPFD-.0589V_s$

Table 15. Goodness of fit of contrasting models of ozone uptake as a function of stomatal conductance, of ambient ozone concentration, or as an additive function of both.

Zone	$\frac{g_{s,v}}{r^2}$	$\frac{[O_3]}{r^2}$	$g_{s,v} + [O_3]$		
			r^2	F	p
EXTERIN	0.29	0.88	0.99	233.6	0.0001
EXTEROUT	0.002	0.69	0.95	53	0.0004
INTERIN	0.16	0.79	0.98	102.2	0.0001
INTEROUT	0.0003	0.79	0.95	49.3	0.0005
All Zones	0.08	0.52	0.65	26.9	0.0001

Table 16. Application of the ozone flux model to the 1992 ozone exposure data of Williams et al. (1993).							
Treatment	Predicted						
	A ¹	g_{s,O_3}^2	$^3g_{s,O_3}$	g_{bz,O_3}^2	g_{tz,O_3}^2	O_{3z}^4	$F_{O_3}^5$
Inside-charcoal	10.8	-	0.142	0.22	0.086	0.027	2.32
Inside-Ambient	8.7	0.115	0.114	0.22	0.075	0.045	3.38
Inside-2x Ambient	4.6	-	0.060	0.22	0.047	0.087	4.09
Outside-Ambient	7.7	0.100	0.101	0.37	0.079	0.054	4.27
Inside/ Outside	1.13	1.15	-	-	-	-	-

¹ From Williams et al. (1993), ca. DOY 238, when significant treatment differences in A were observed, with a ranking of gas exchange performance similar to that consistently observed in the present study in the same trees over the same time period.

² From Table 10, average of both zones of the Inside/Outside tree.

³ Stomatal conductance calculated assuming a constant ratio of A: g_{s,O_3} , using the mean value of $g_{s,O_3} = 0.1075$.

⁴ From Williams et al. (1993), assuming that their 12 hour seasonal mean ozone concentrations are equivalent to the zone concentrations in the present study.

⁵ Calculated as $F_{O_3} = (g_{tz,O_3})(O_{3z})$, an application of Eq. 1.

FIGURES

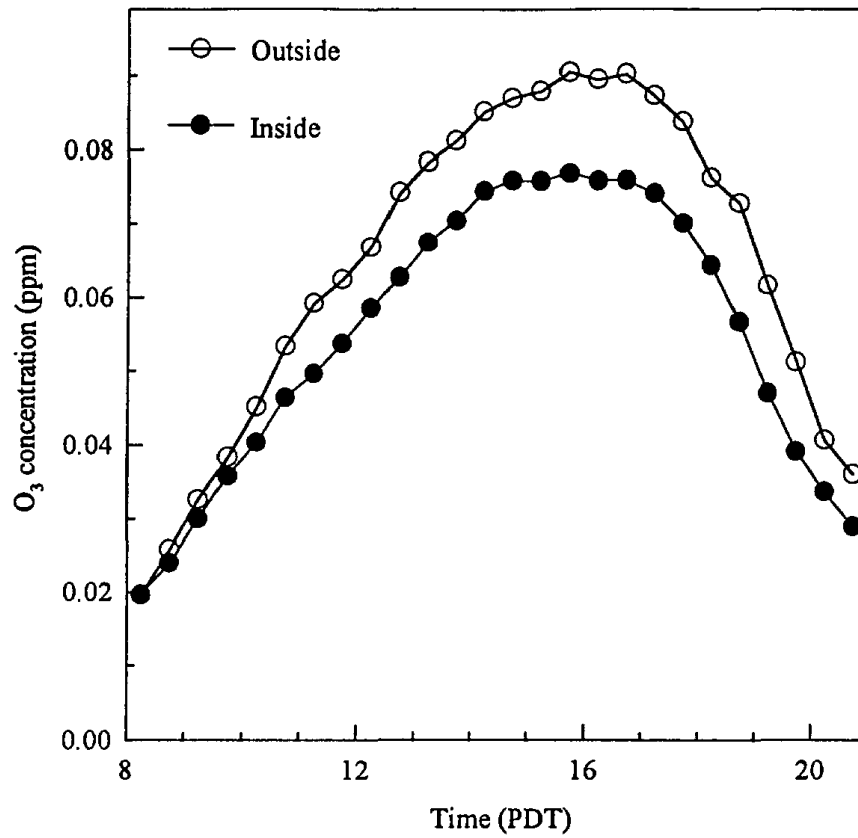


Fig. 1. Effect of enclosure in an open-top-exposure chamber (OTC) on the bulk ozone concentration surrounding experimental plum trees, measured at location 3 in each canopy (see Fig. 8).

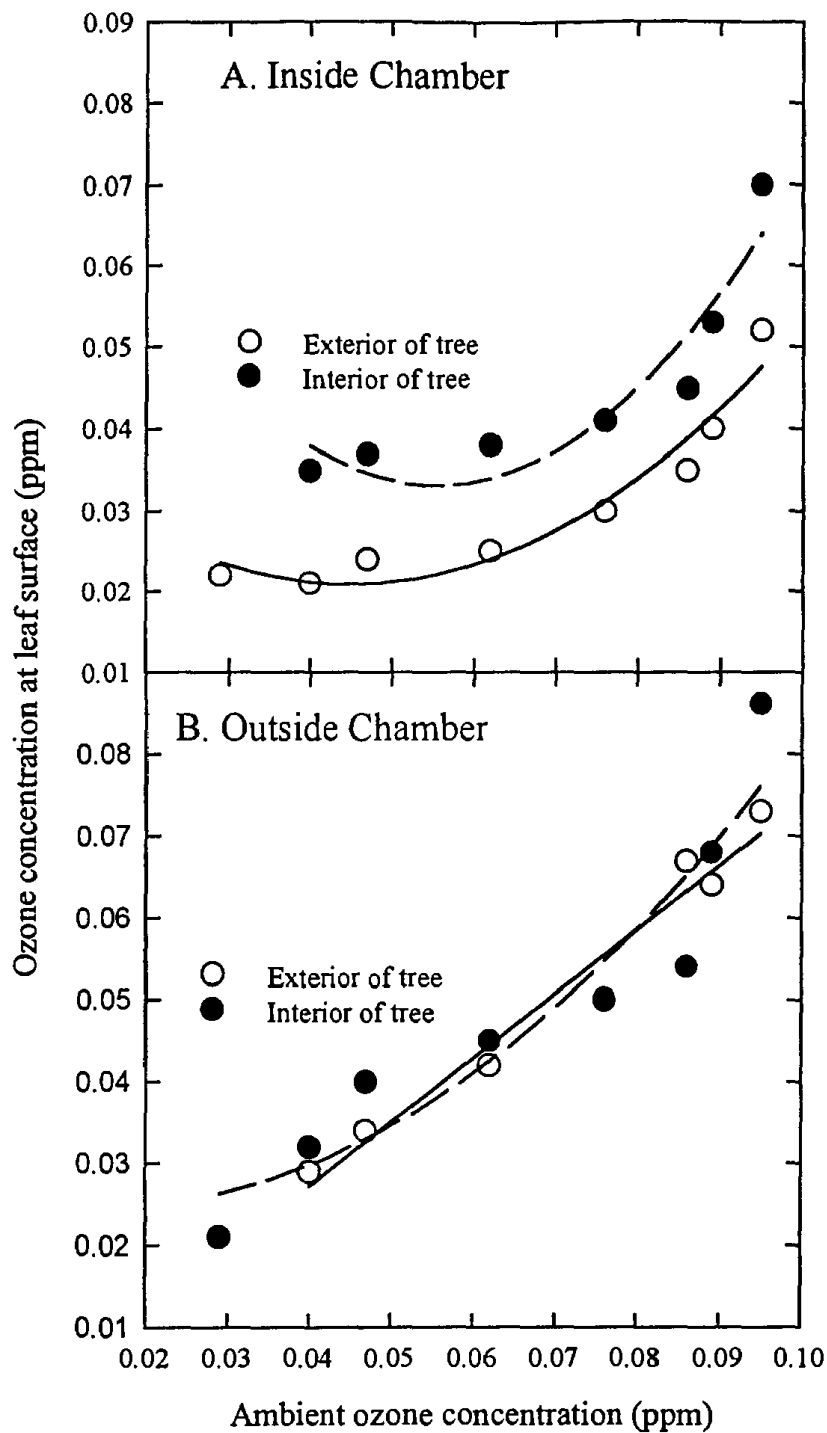


Fig. 2. Effect of enclosure in an OTC on the relationship between ambient ozone and the physiologically relevant ozone concentration at the leaf surface, in two zones of the canopy differing in exposure. Interior data are averages of locations 1 and 4, and exterior data are averages of locations 2 and 5 (see Fig. 8).

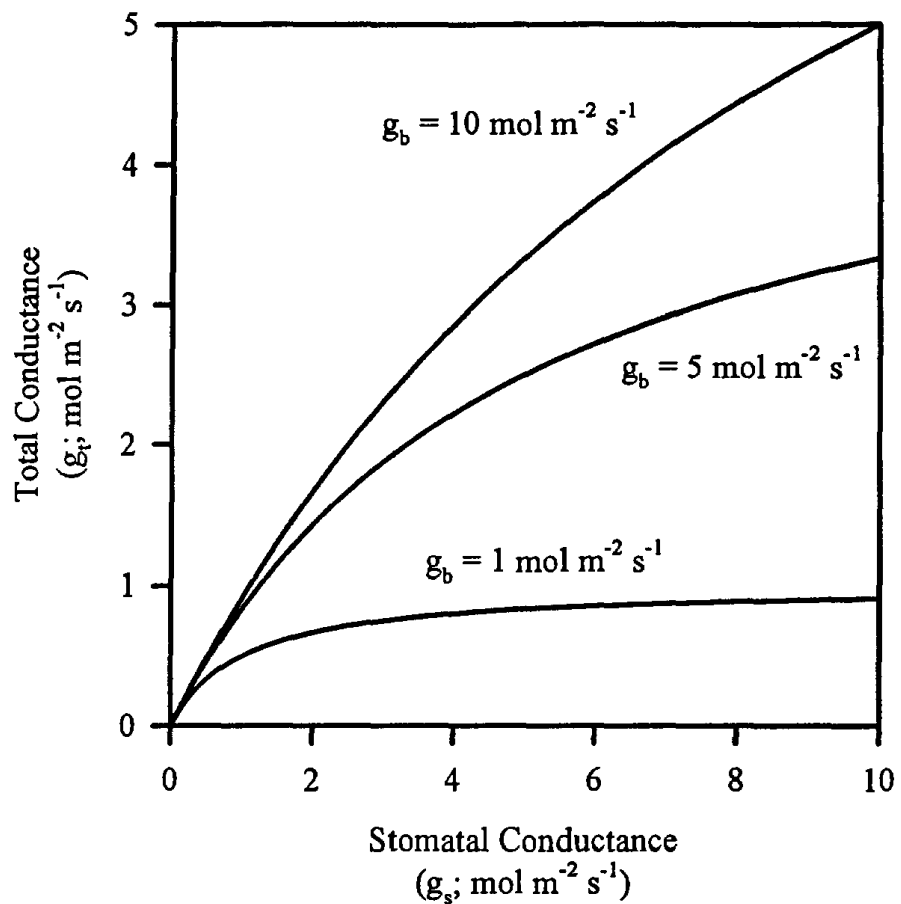


Fig. 3. Model relationship between total conductance and stomatal conductance to diffusive transfer of a trace gas from a leaf to the atmosphere, showing the large effect of the non-stomatal boundary layer conductance.

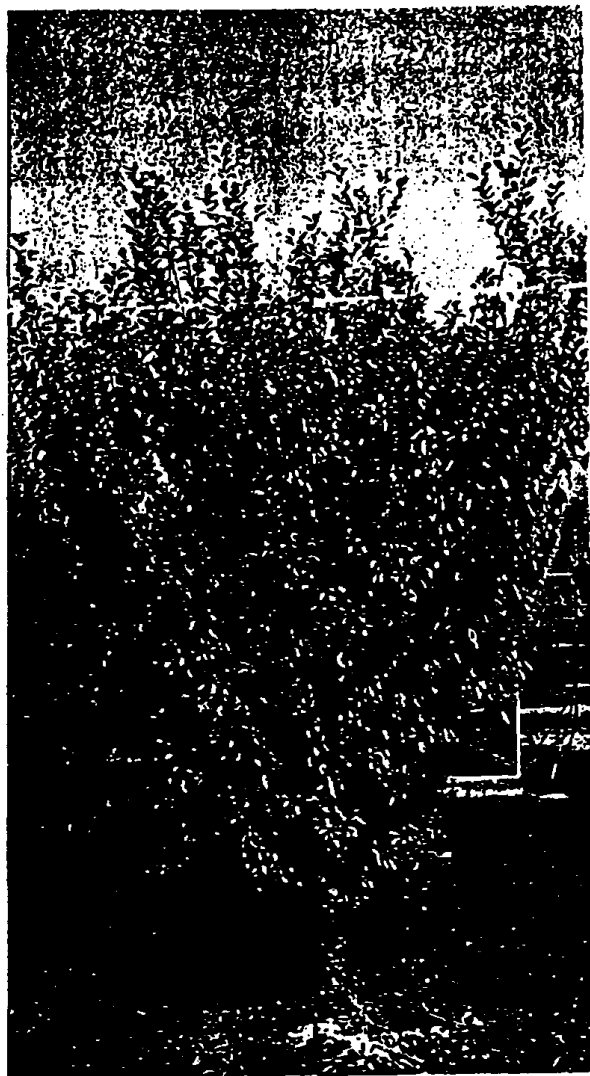


Fig. 4. Photograph of a representative plum tree.

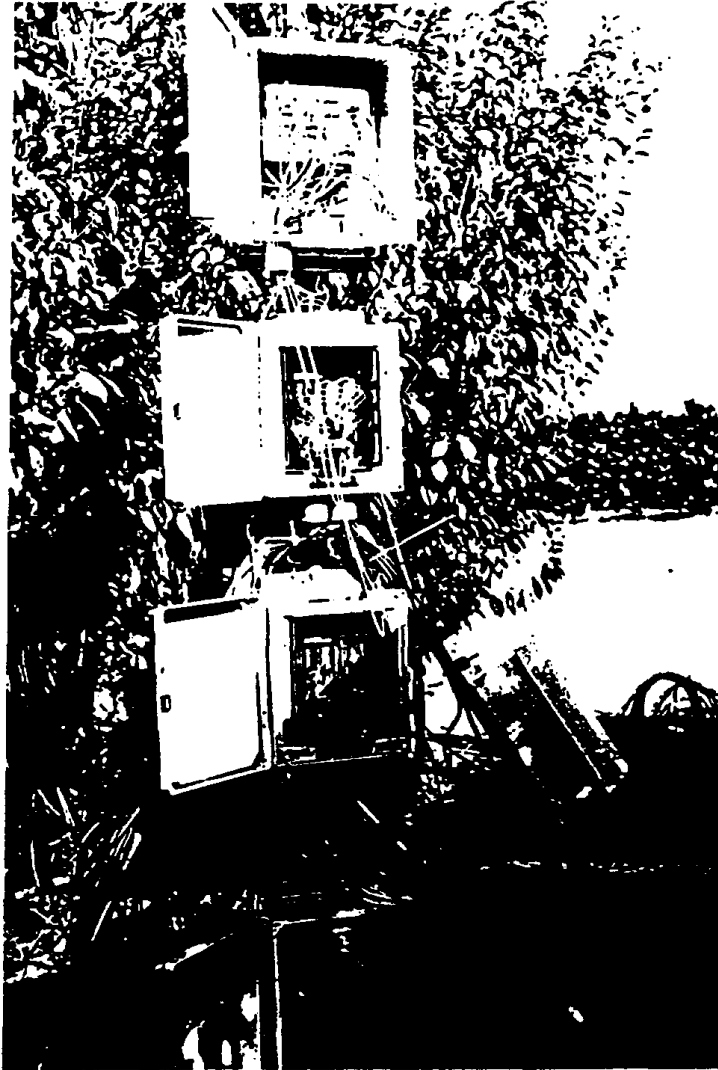


Fig. 5. Photograph of the installation of data logging equipment, including several multiplexers, required to record signals from the large array of sensors.

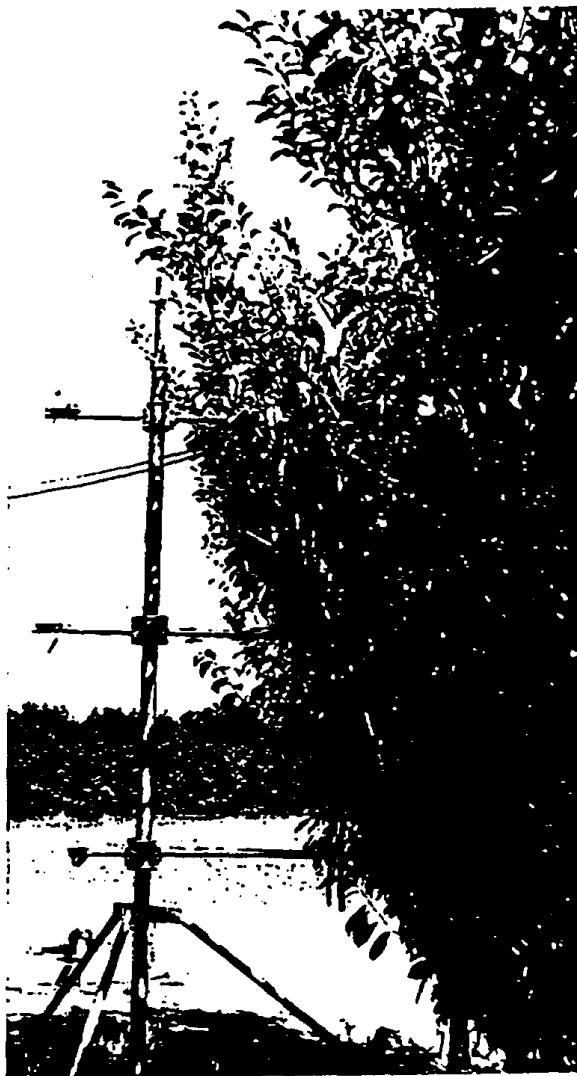


Fig. 6. Photograph of the tripod and horizontal booms to support the sampling tubing, thermocouples and signal cables within the canopy.

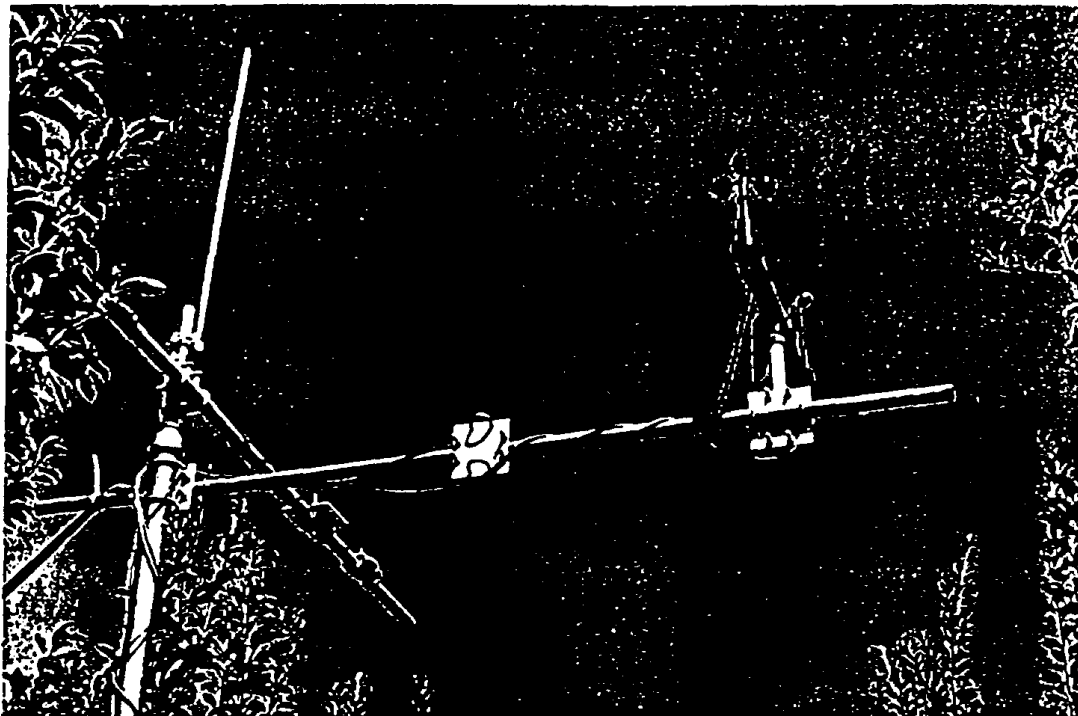


Fig.7. Photograph of the micrometeorological instruments deployed above the plum canopy.

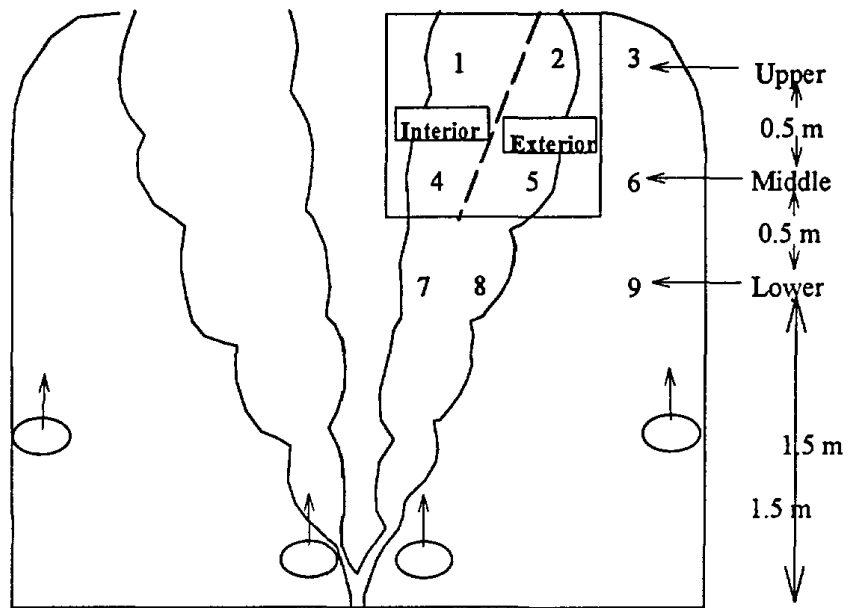


Fig. 8. Diagram of sensor locations and zone designations in the plum trees, showing that location 3 represents an ambient reference point.

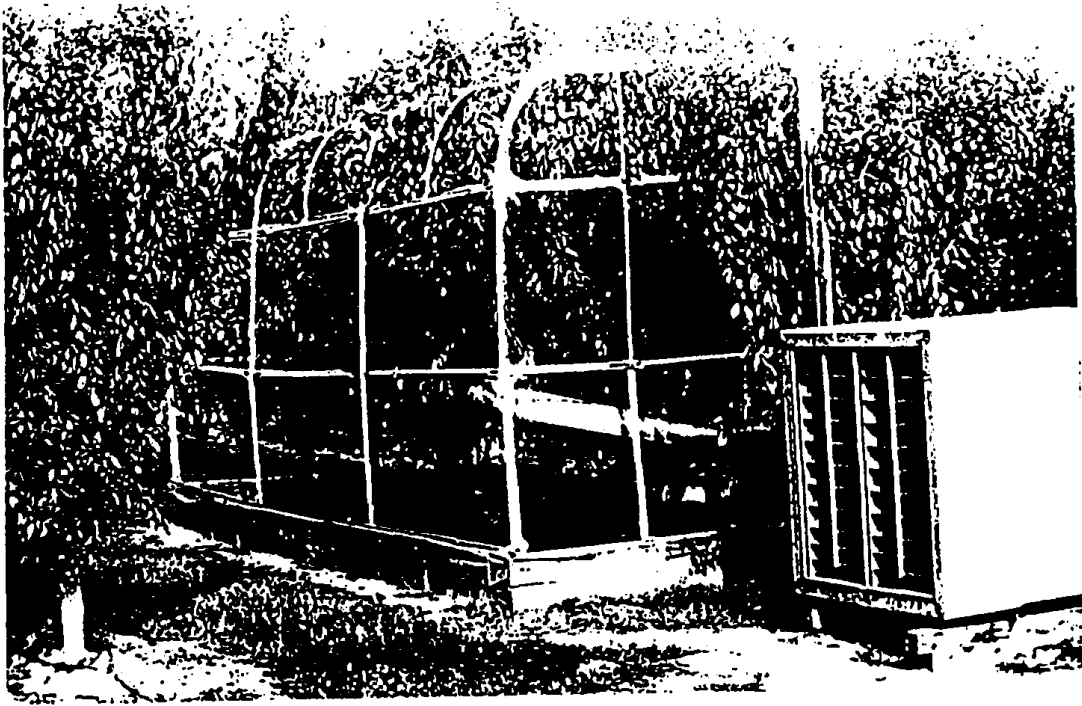


Fig. 9. Photograph of the air delivery system in the OTC, showing placement below the canopy, at the sides and center of the chamber. A) Prior to installation of the plastic chamber walls. B) Following installation of the plastic walls.



Fig. 10. Photograph of a stem flow gauge mounted on a scaffold branch of a plum tree.



Fig. 11. Photograph of the leaf area measurement performed following destructive harvest of a subsample of leaves.

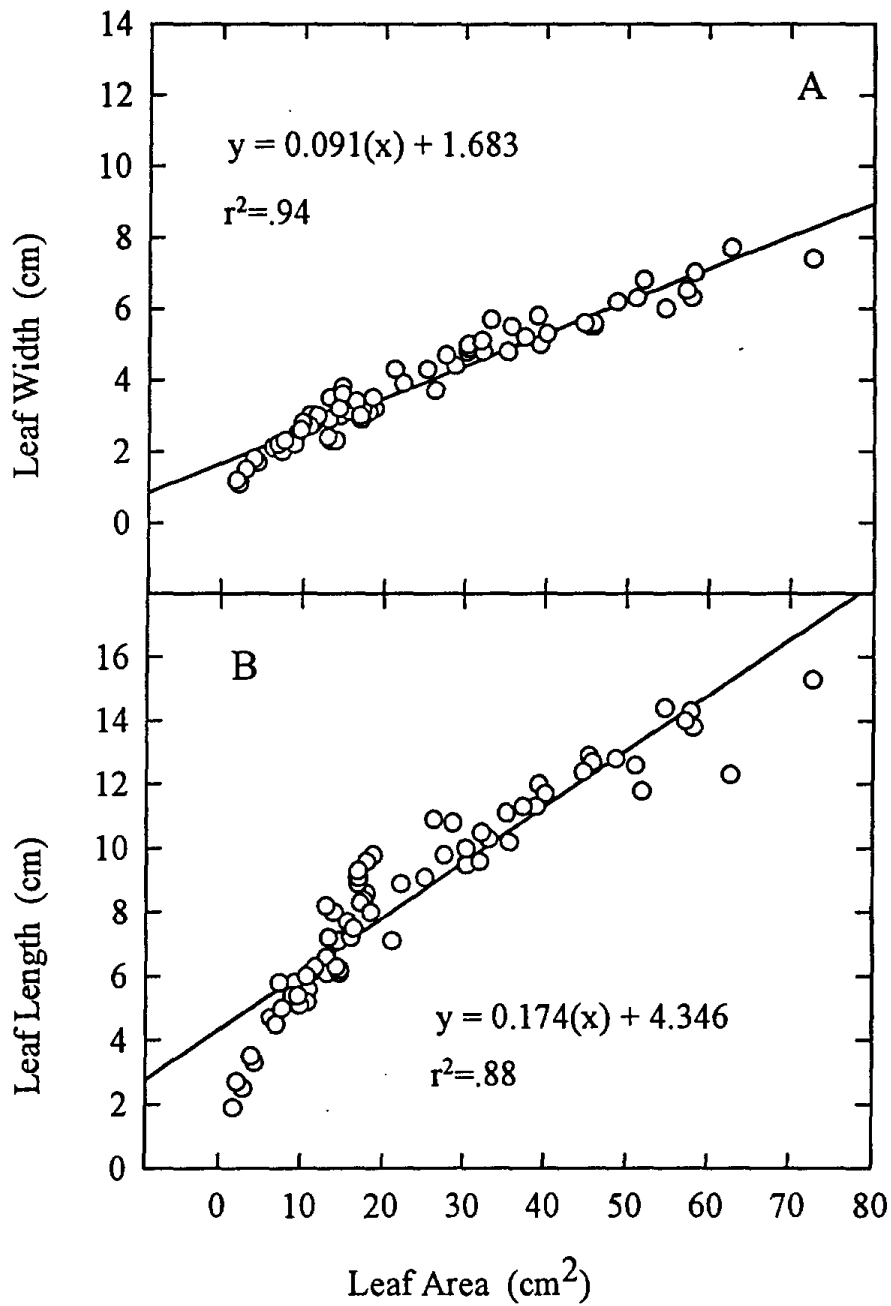


Fig. 12. Regression of leaf area (from destructive harvests) on measured leaf width (A) or leaf length (B).

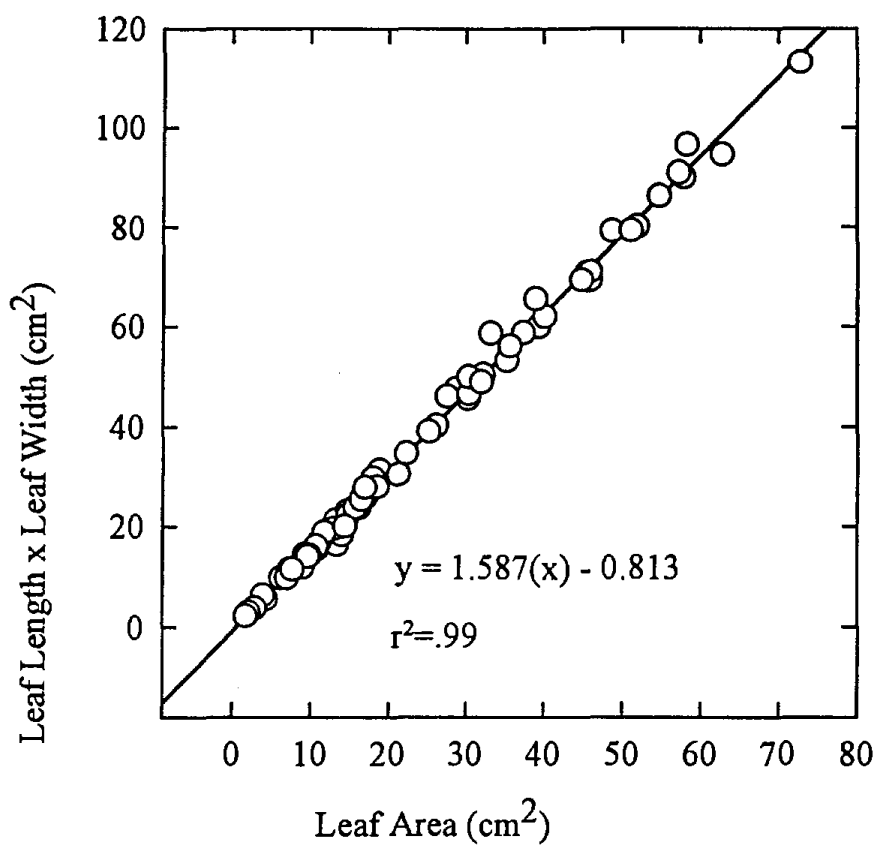


Fig. 13. Regression of leaf area (from destructive harvests) on product of leaf width x leaf length.

TIMECOURSES OF WIND SPEED AND WIND DIRECTION
AVERAGED FROM FIVE GAS EXCHANGE DAYS. DATA
COLLECTED AT A HEIGHT OF 4 m ABOVE THE GROUND.

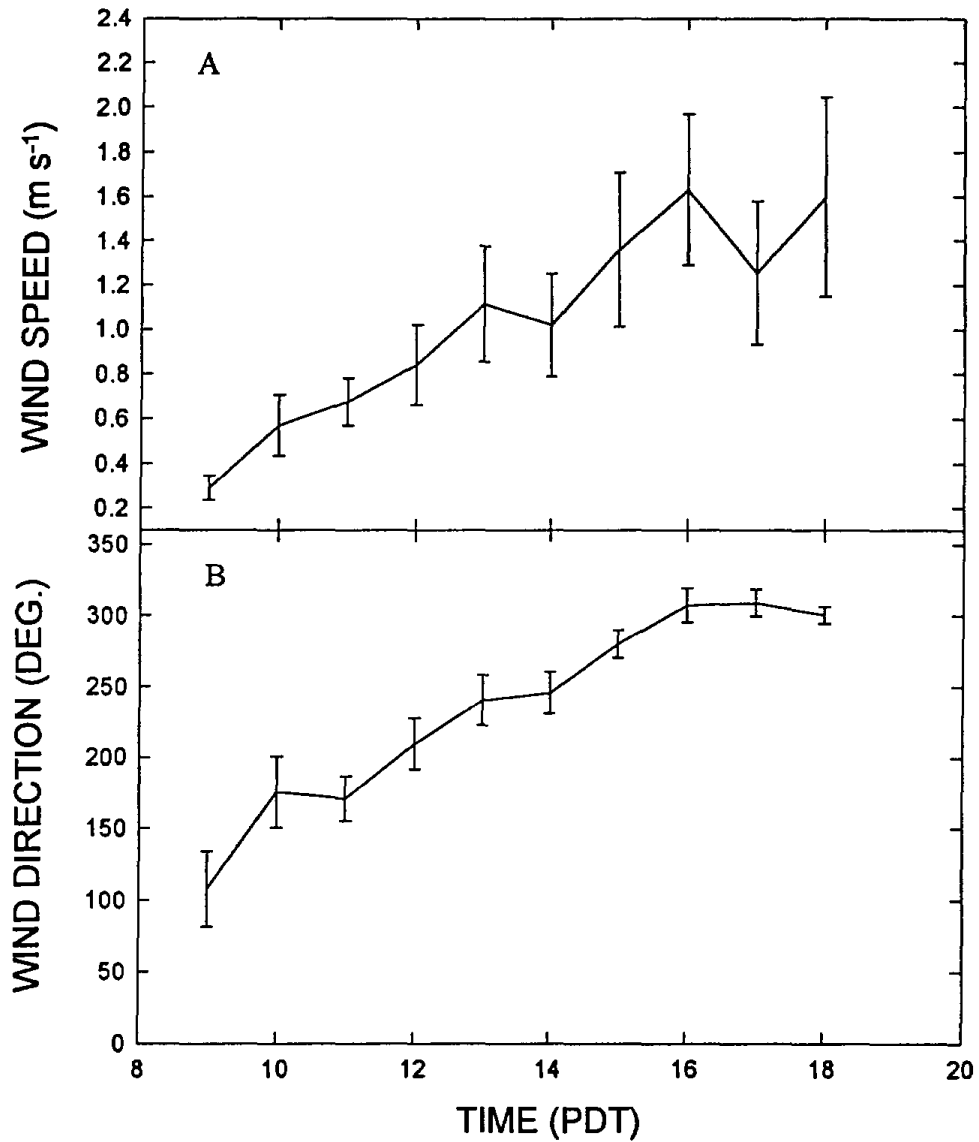


Fig. 14. Diurnal pattern of above-canopy wind speed and direction averaged over the six days of intensive physiological measurements.

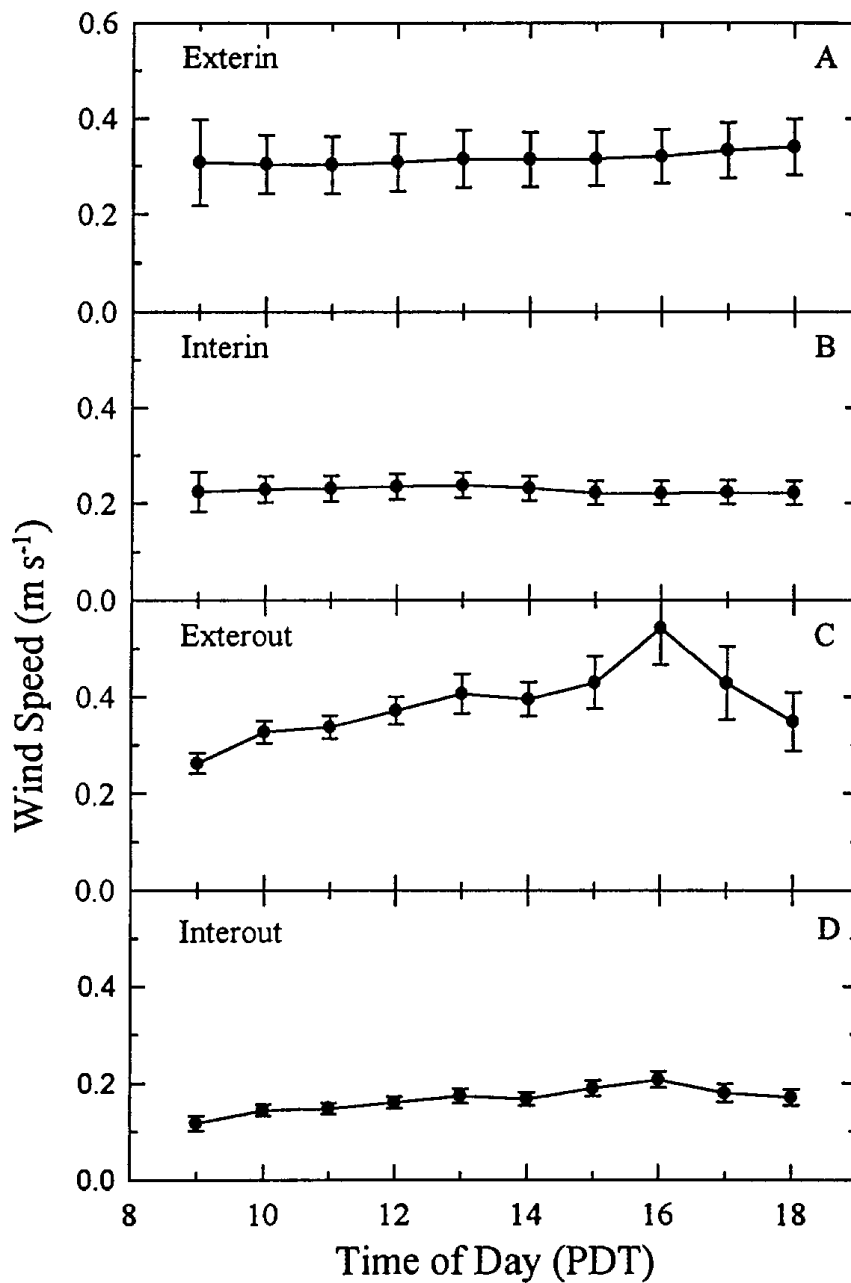


Fig. 15. Diurnal pattern of within-canopy wind speed by zone averaged over the six days of intensive physiological measurements, measured by hot wire anemometers.

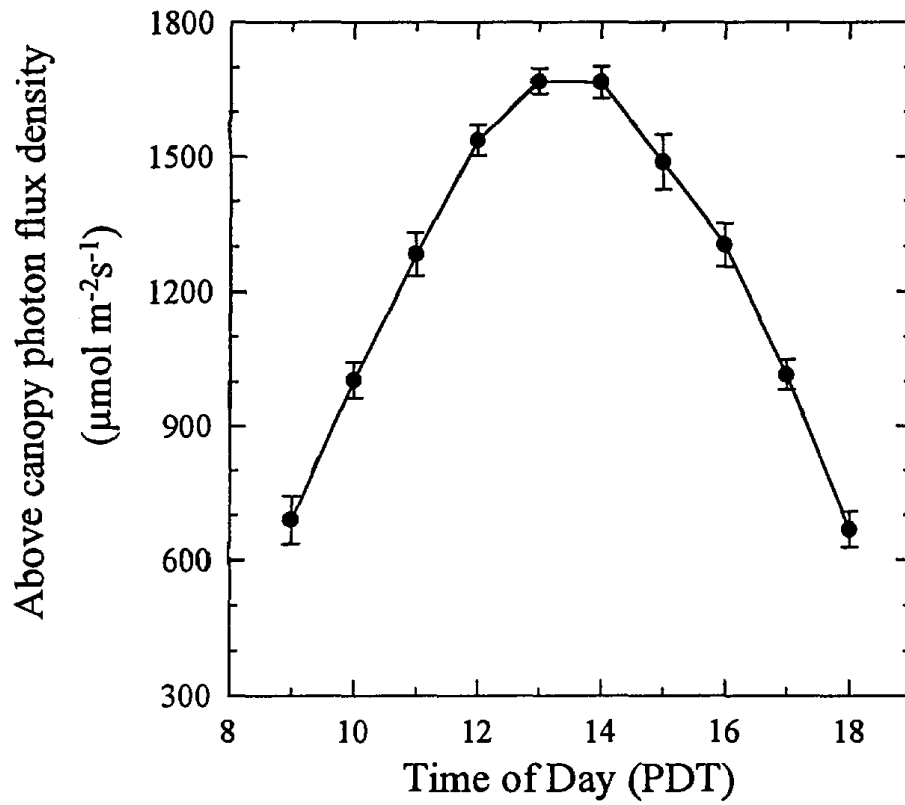


Fig. 16. Diurnal pattern of above-canopy photon flux density averaged over the six days of intensive physiological measurements.

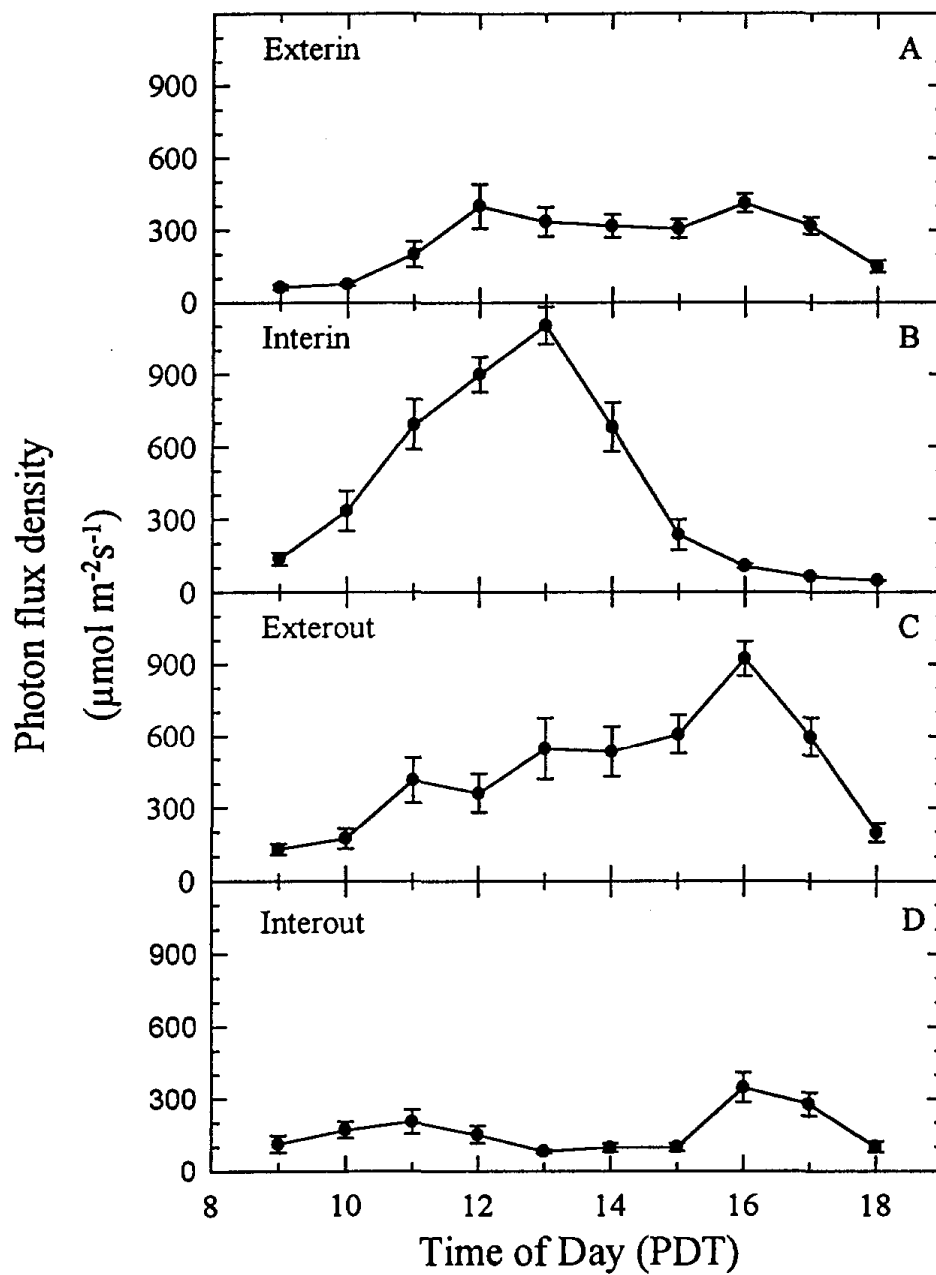


Fig. 17. Diurnal pattern of within-canopy photon flux density (mean of two locations per zone) by zone averaged over the six days of intensive physiological measurements, measured by photodiodes.

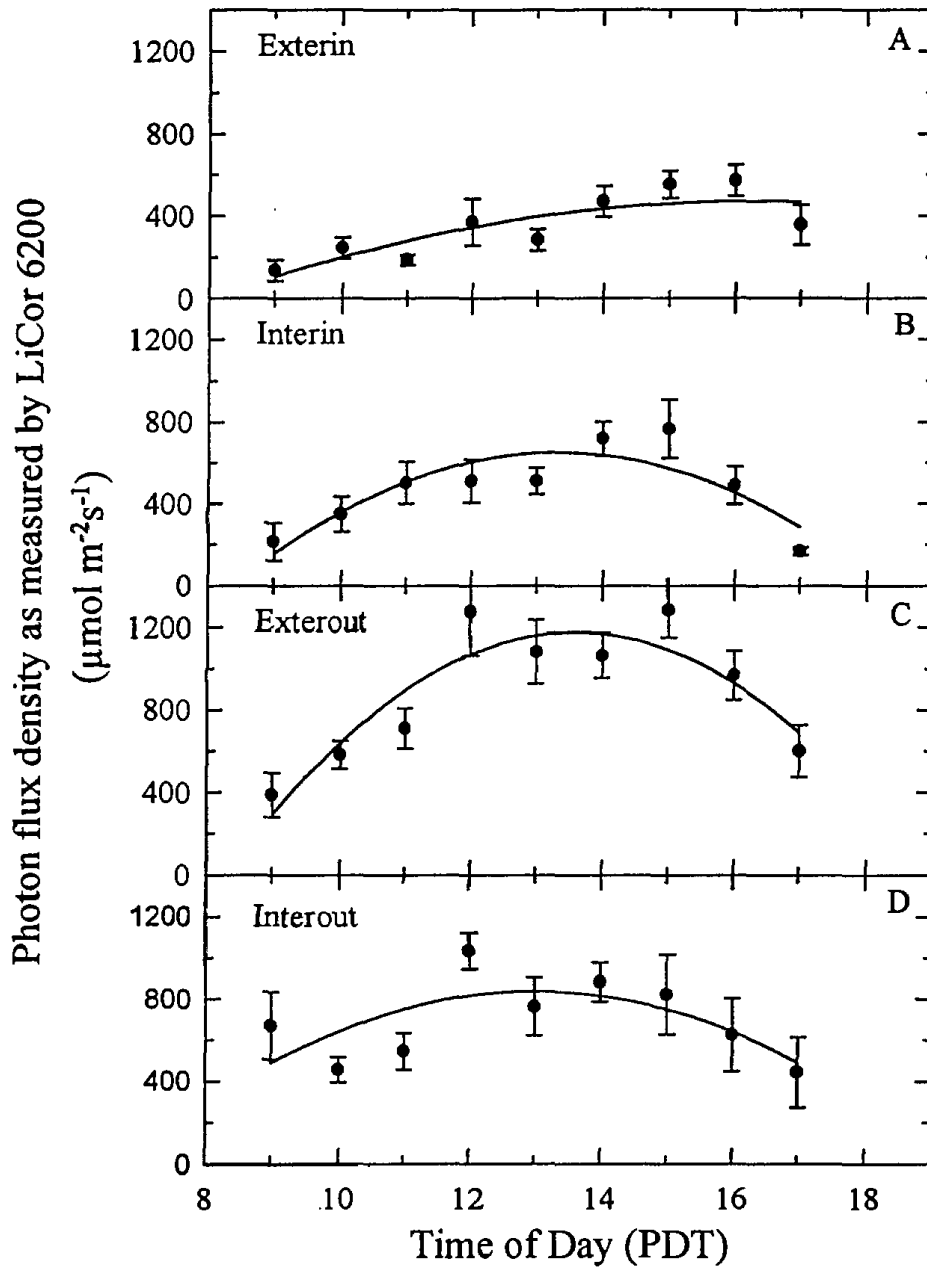


Fig. 18. Diurnal pattern of within-canopy photon flux density by zone averaged over the six days of intensive physiological measurements, measured with the quantum sensor attached to the gas exchange cuvette.

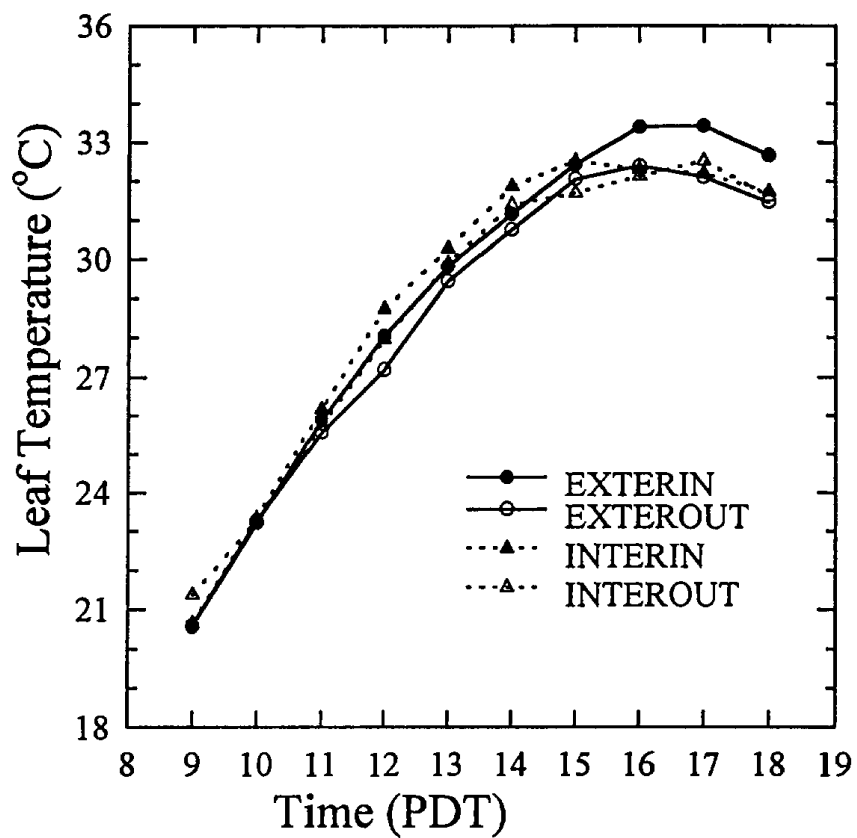


Fig. 19. Diurnal pattern of leaf temperature (mean of two leaves per zone) by zone averaged over the six days of intensive physiological measurements.

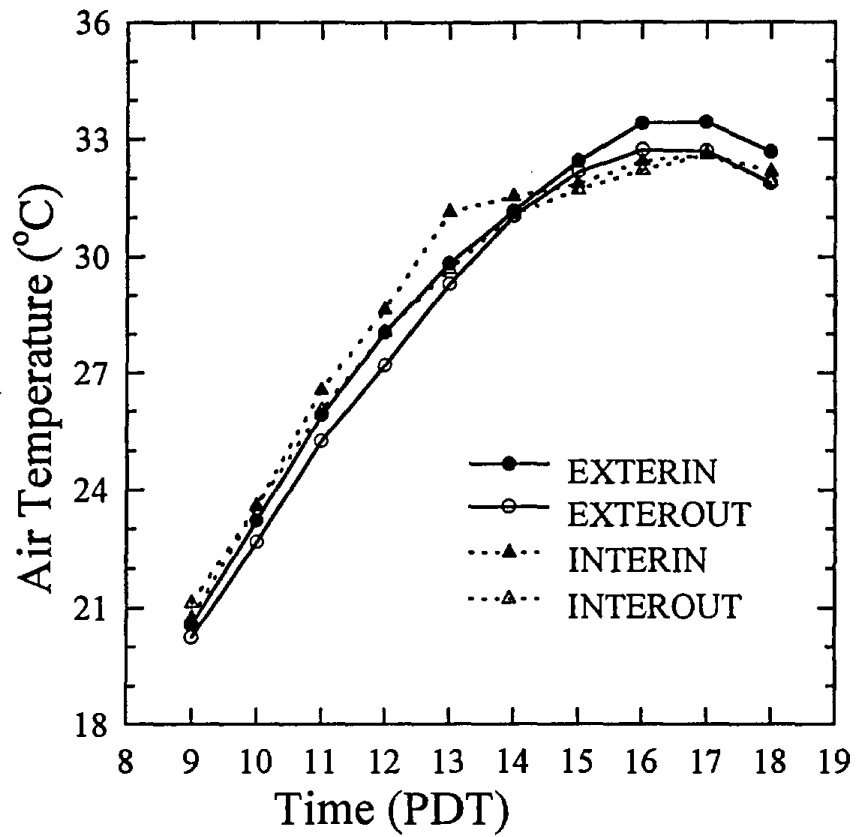


Fig. 20. Diurnal pattern of air temperature (mean of two locations per zone) by zone averaged over the six days of intensive physiological measurements.

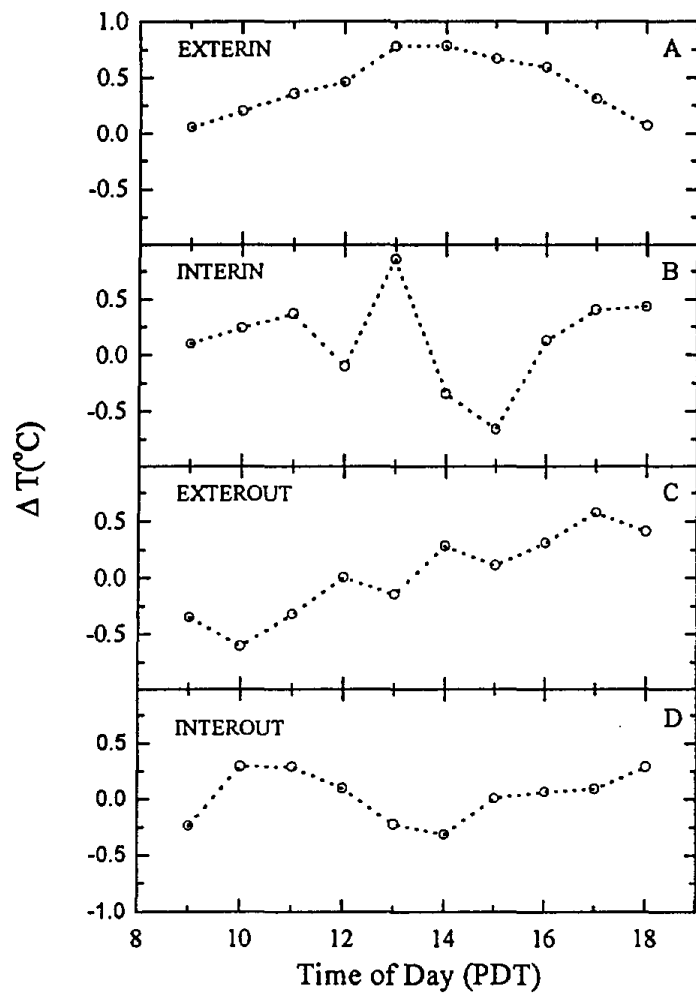


Fig. 21. Diurnal pattern of leaf to air temperature difference by zone averaged over the six days of intensive physiological measurements.

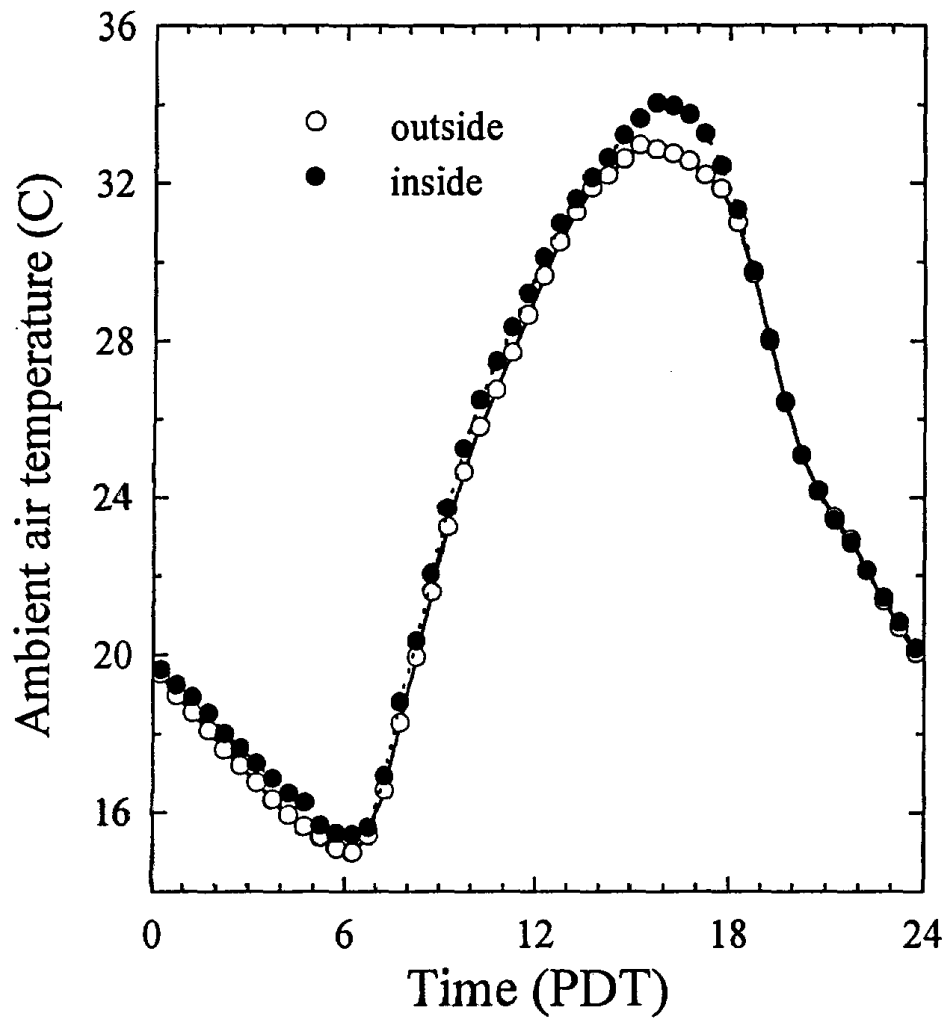


Fig. 22. Diurnal pattern of ambient air temperature averaged over all sample dates and all nine canopy locations, outside (hollow circles) and inside (filled circles) the OTC .

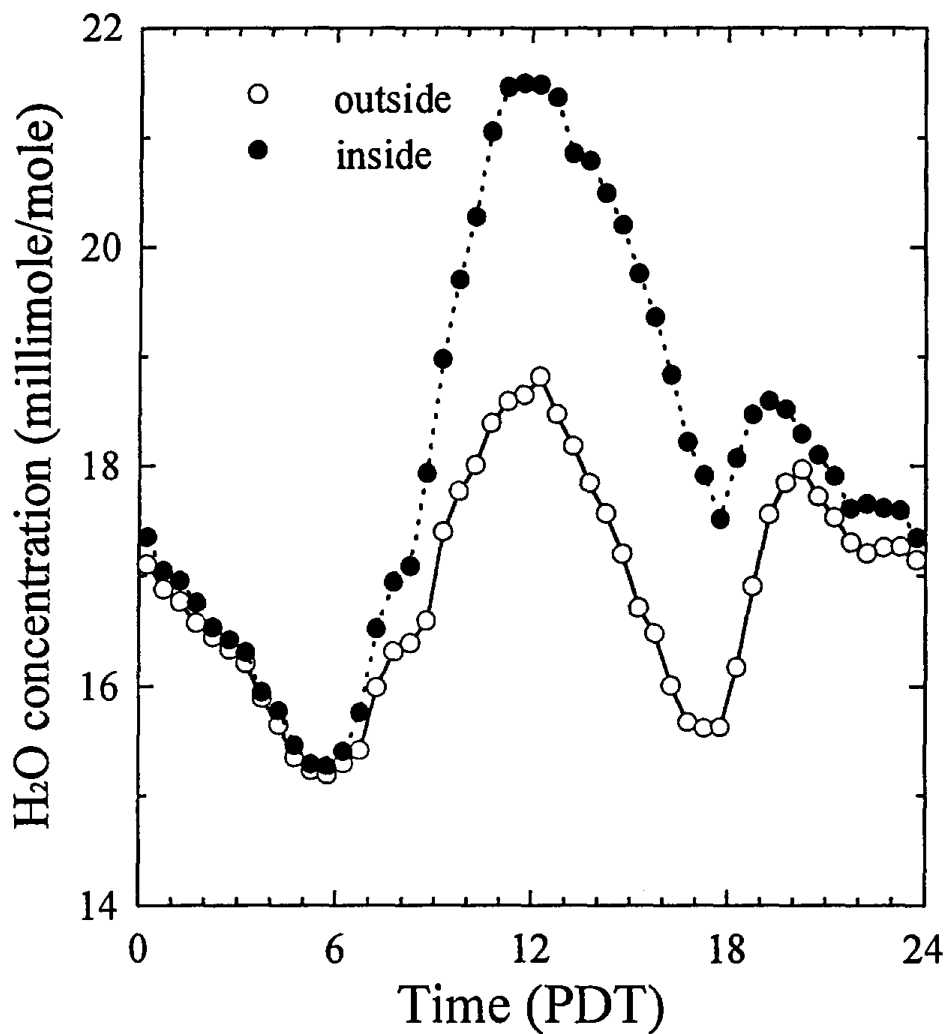


Fig. 23. Diurnal pattern of H₂O vapor concentration (mole fraction) averaged over all sample dates and all nine canopy locations outside (hollow circles) and inside (filled circles) the OTC .

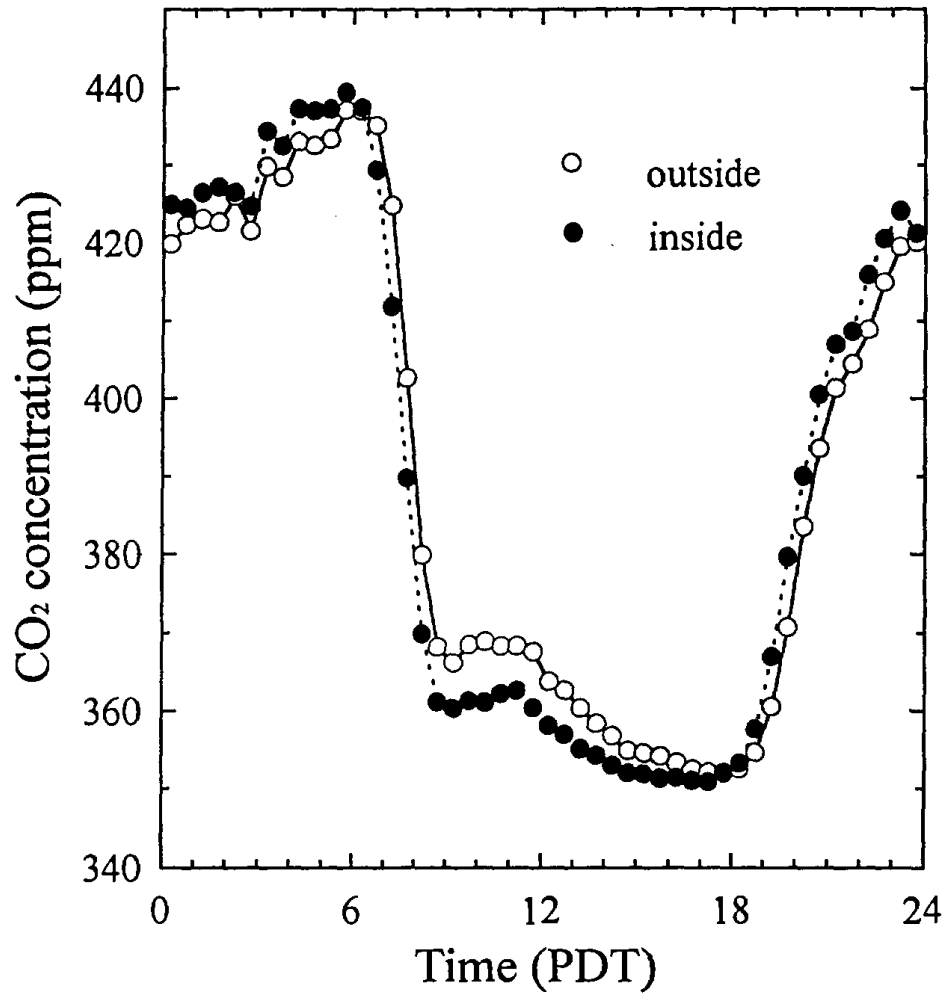


Fig. 24. Diurnal pattern of CO₂ concentration averaged over all sample dates and all nine canopy locations outside (hollow circles) and inside (filled circles) the OTC .

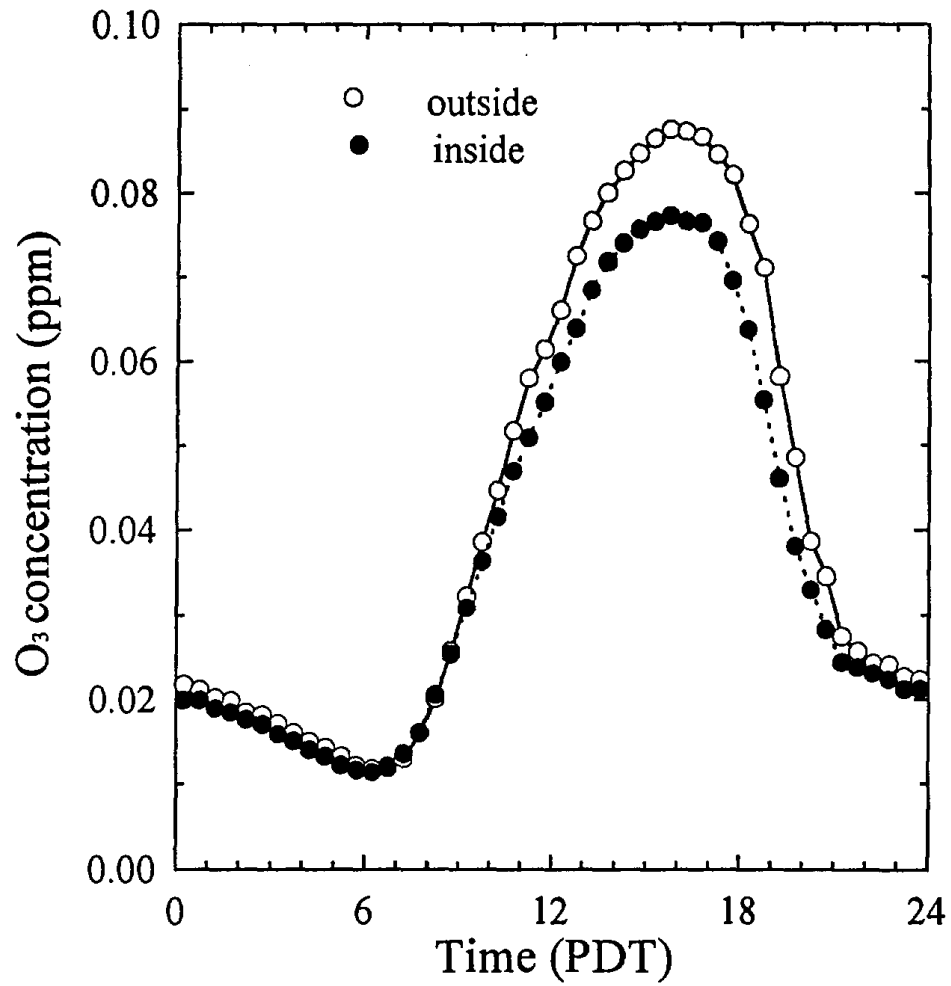


Fig. 25. Diurnal pattern of O₃ concentration averaged over all sample dates and all nine canopy locations outside (hollow circles) and inside (filled circles) the OTC .

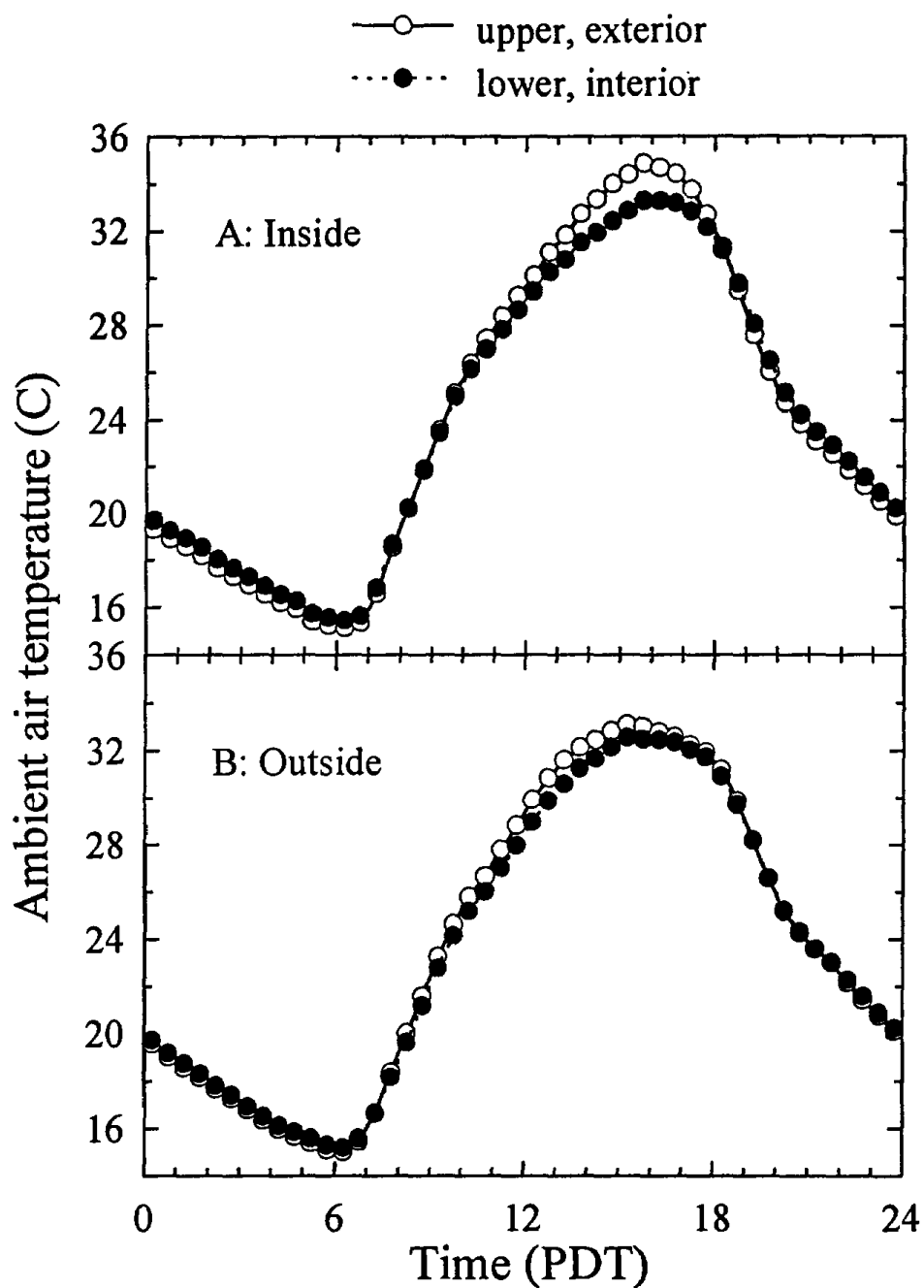


Fig. 26. Diurnal pattern of ambient air temperature averaged over all sample dates at two contrasting canopy locations (A) inside and (B) outside the OTC.

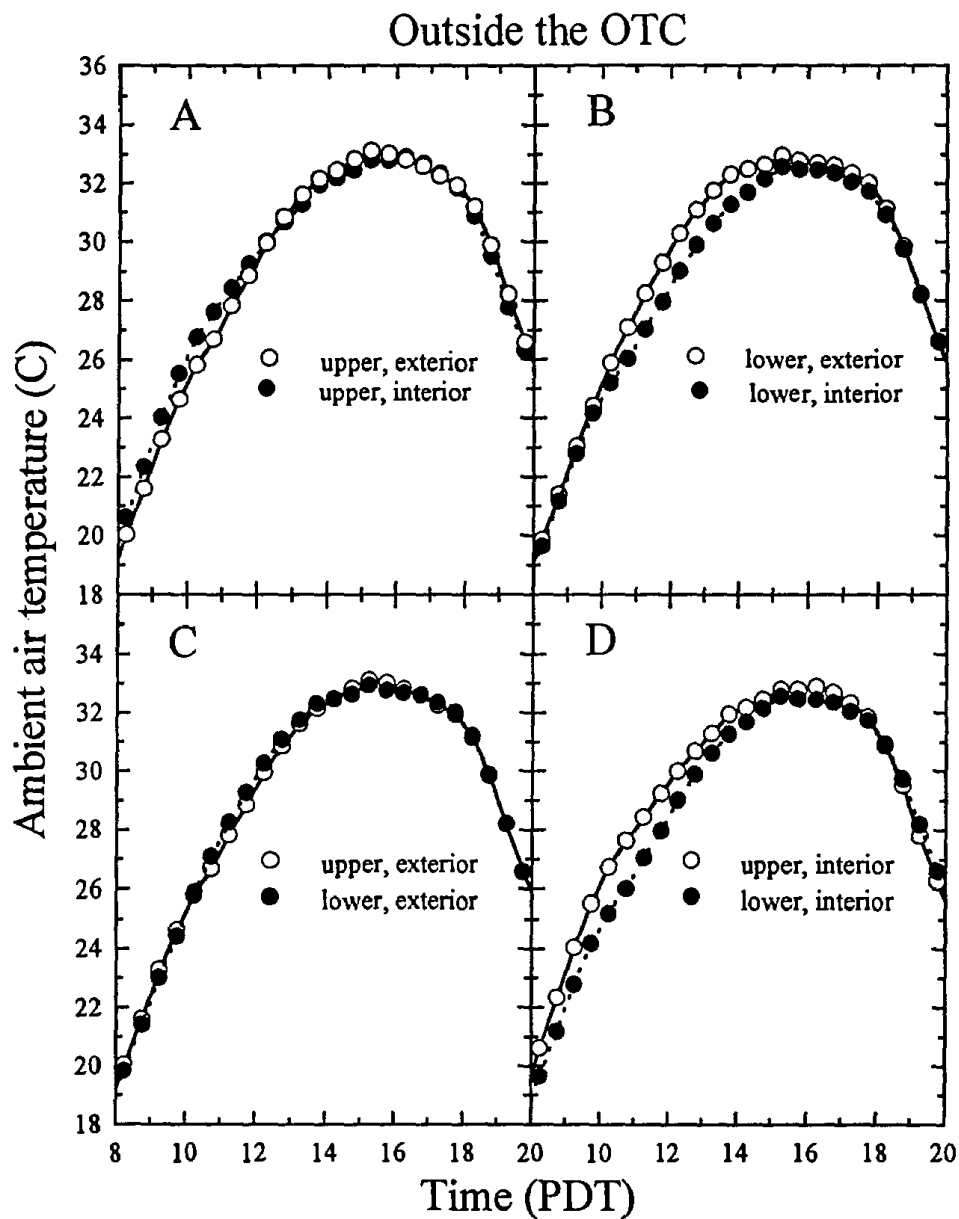


Fig. 27. Diurnal pattern of ambient air temperature averaged over all sample dates at four pairs of contrasting locations demonstrating strictly vertical or horizontal gradients, outside the OTC.

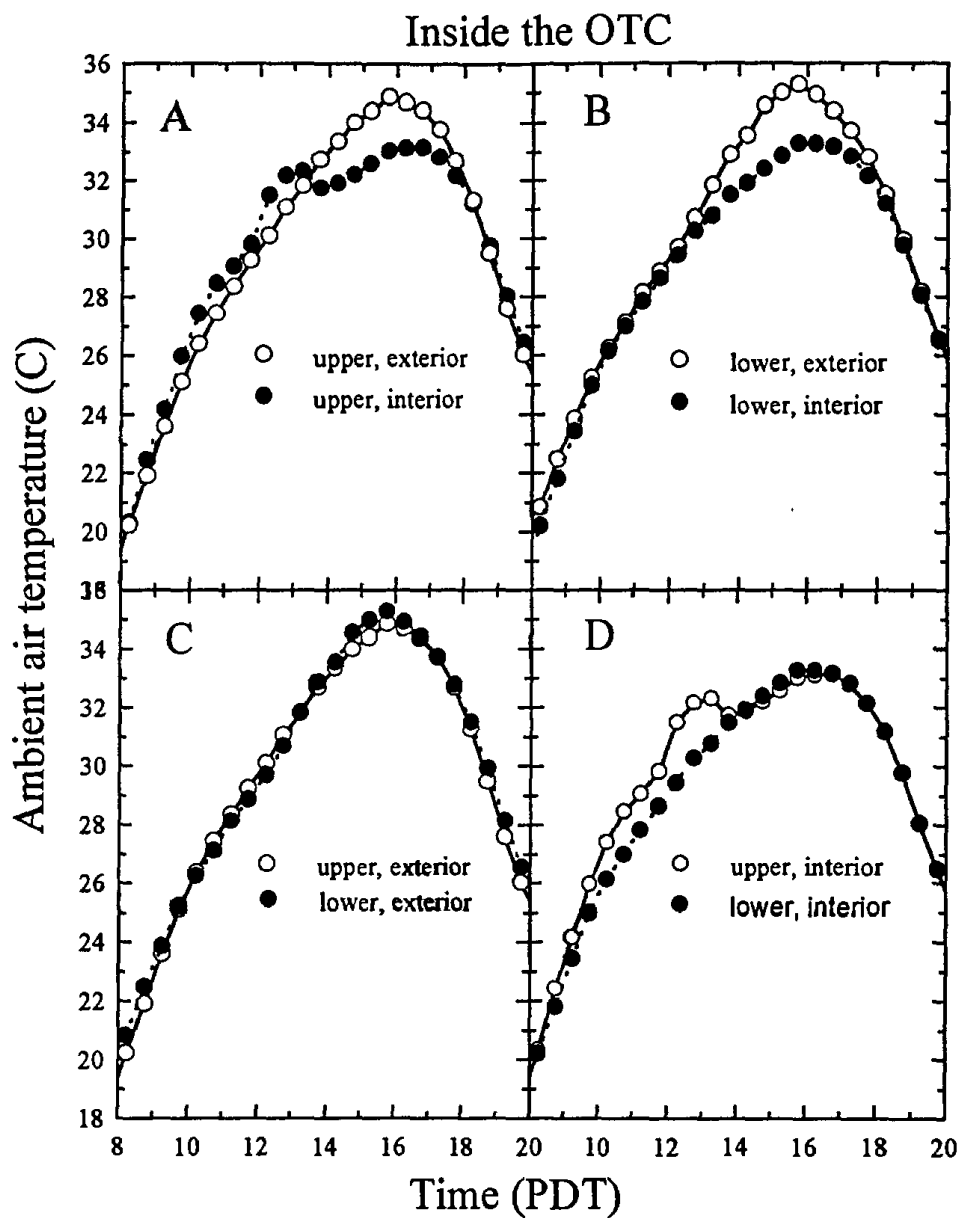


Fig. 28. Diurnal pattern of ambient air temperature averaged over all sample dates at four pairs of contrasting locations demonstrating strictly vertical or horizontal gradients, inside the OTC.

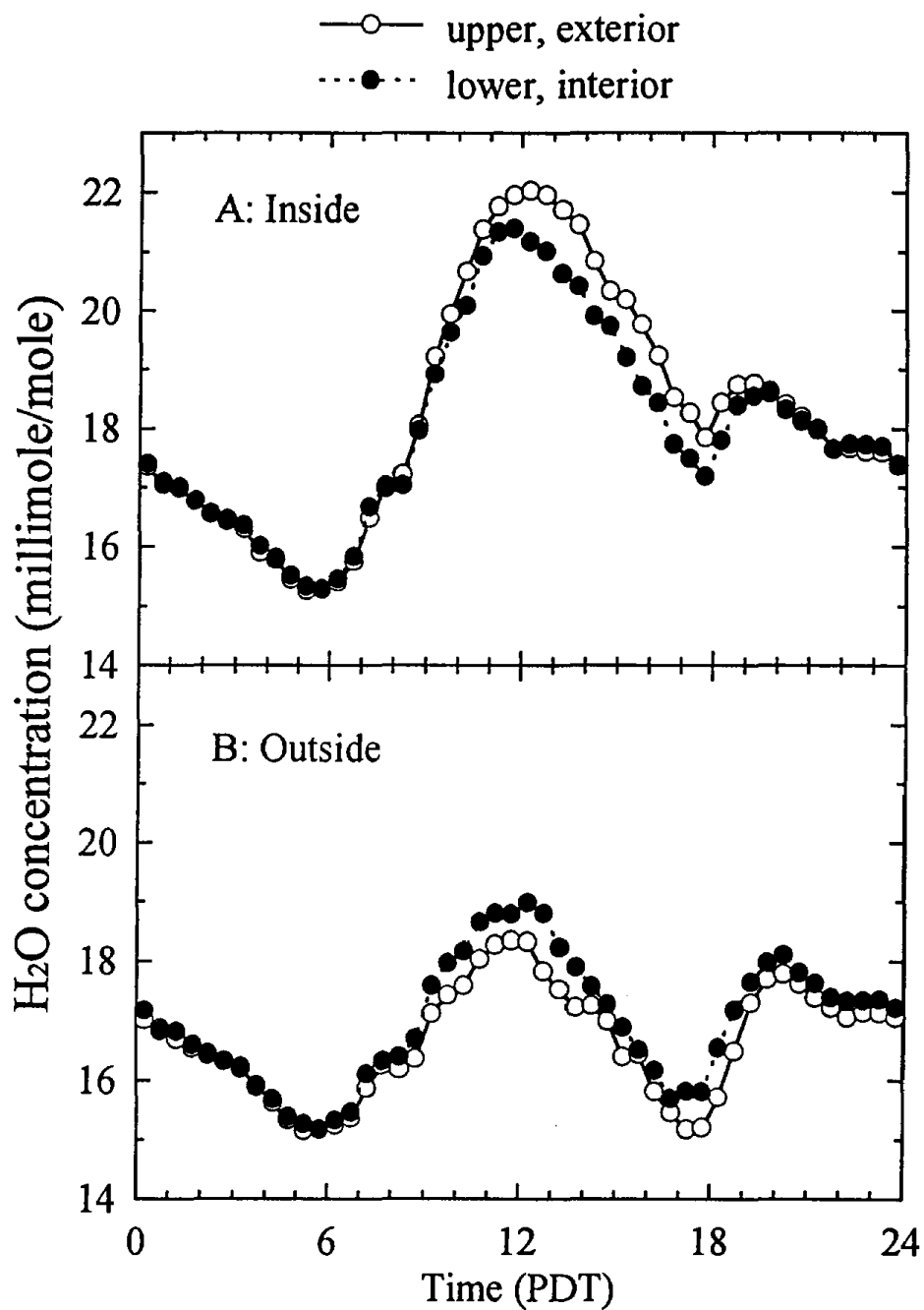


Fig. 29. Diurnal pattern of H₂O concentration averaged over all sample dates at two contrasting canopy locations (A) inside and (B) outside the OTC.

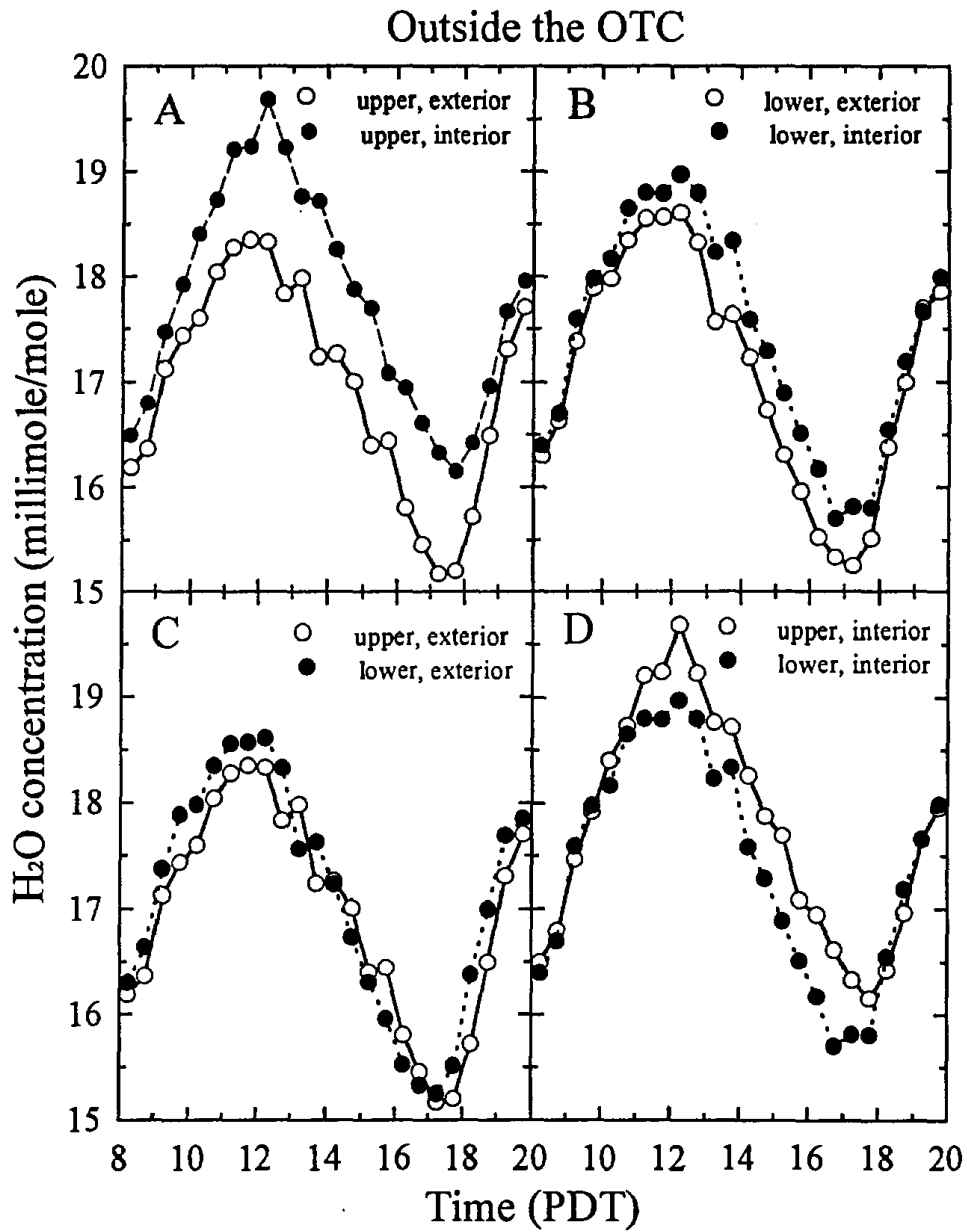


Fig. 30. Diurnal pattern of H₂O vapor concentration averaged over all sample dates at four pairs of contrasting locations demonstrating strictly vertical or horizontal gradients, outside the OTC.

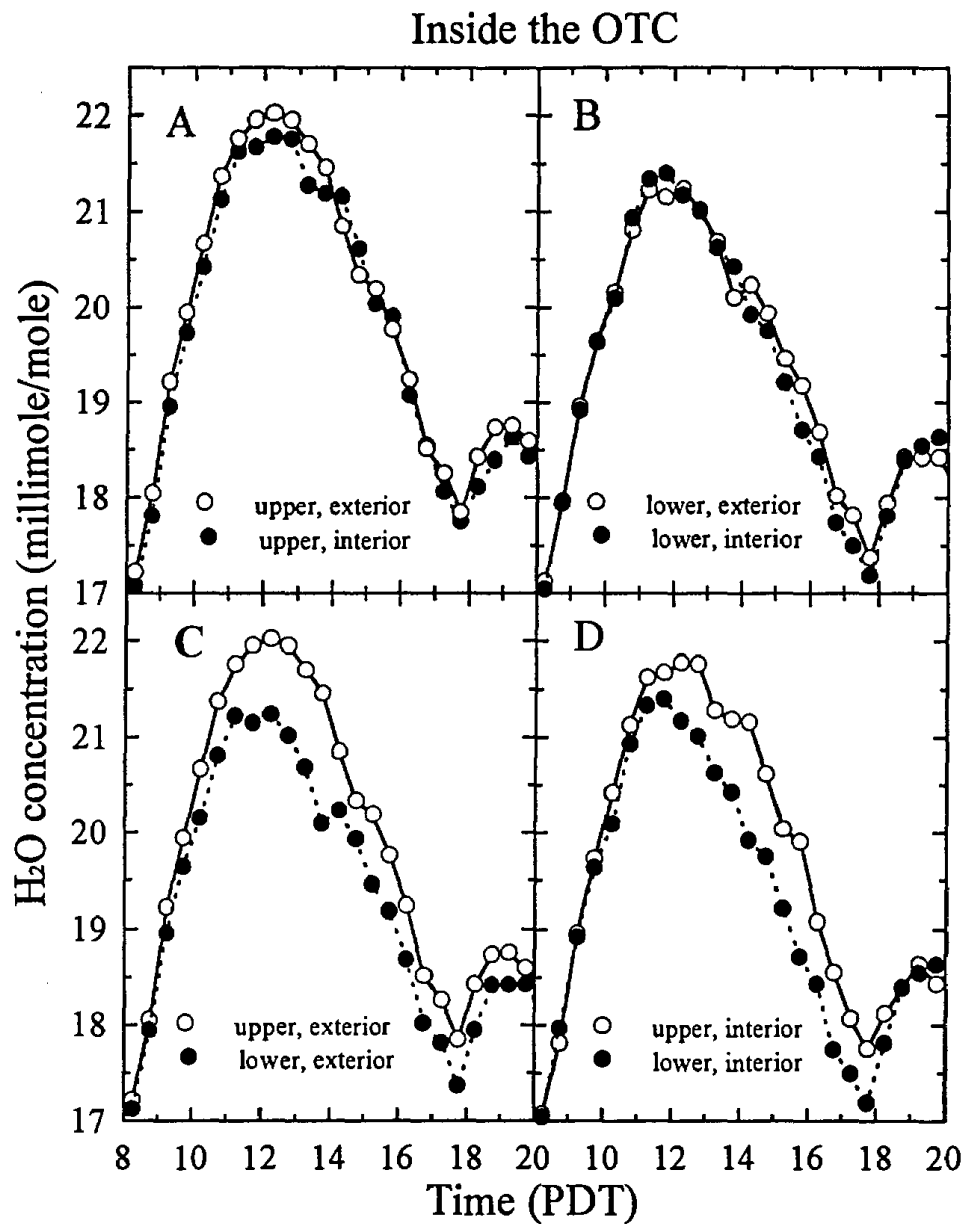


Fig. 31. Diurnal pattern of H_2O vapor concentration averaged over all sample dates at four pairs of contrasting locations demonstrating strictly vertical or horizontal gradients, inside the OTC.

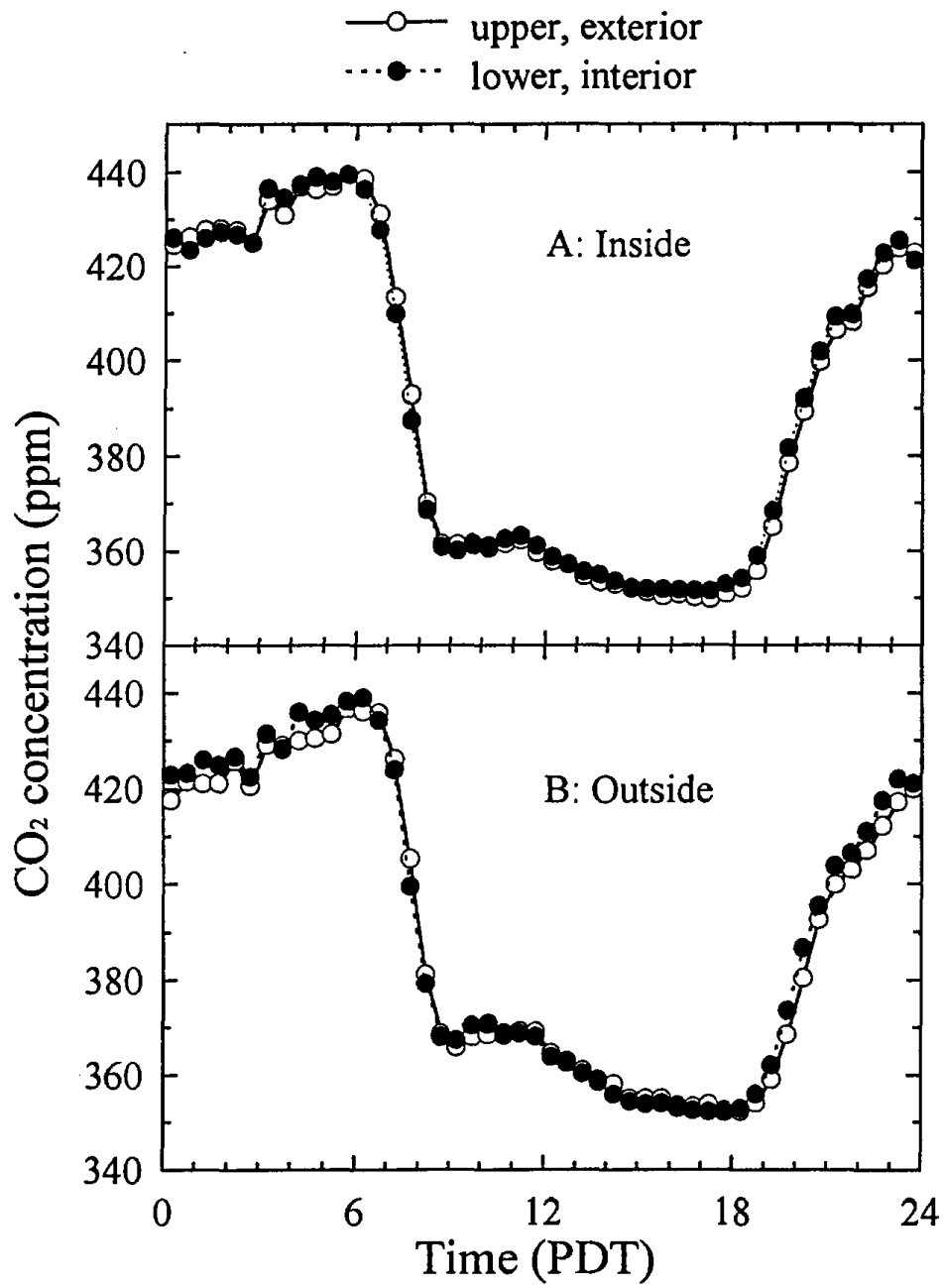


Fig. 32. Diurnal pattern of seasonally averaged CO₂ concentration averaged over all sample dates at two contrasting canopy locations (A) inside and (B) outside the OTC.

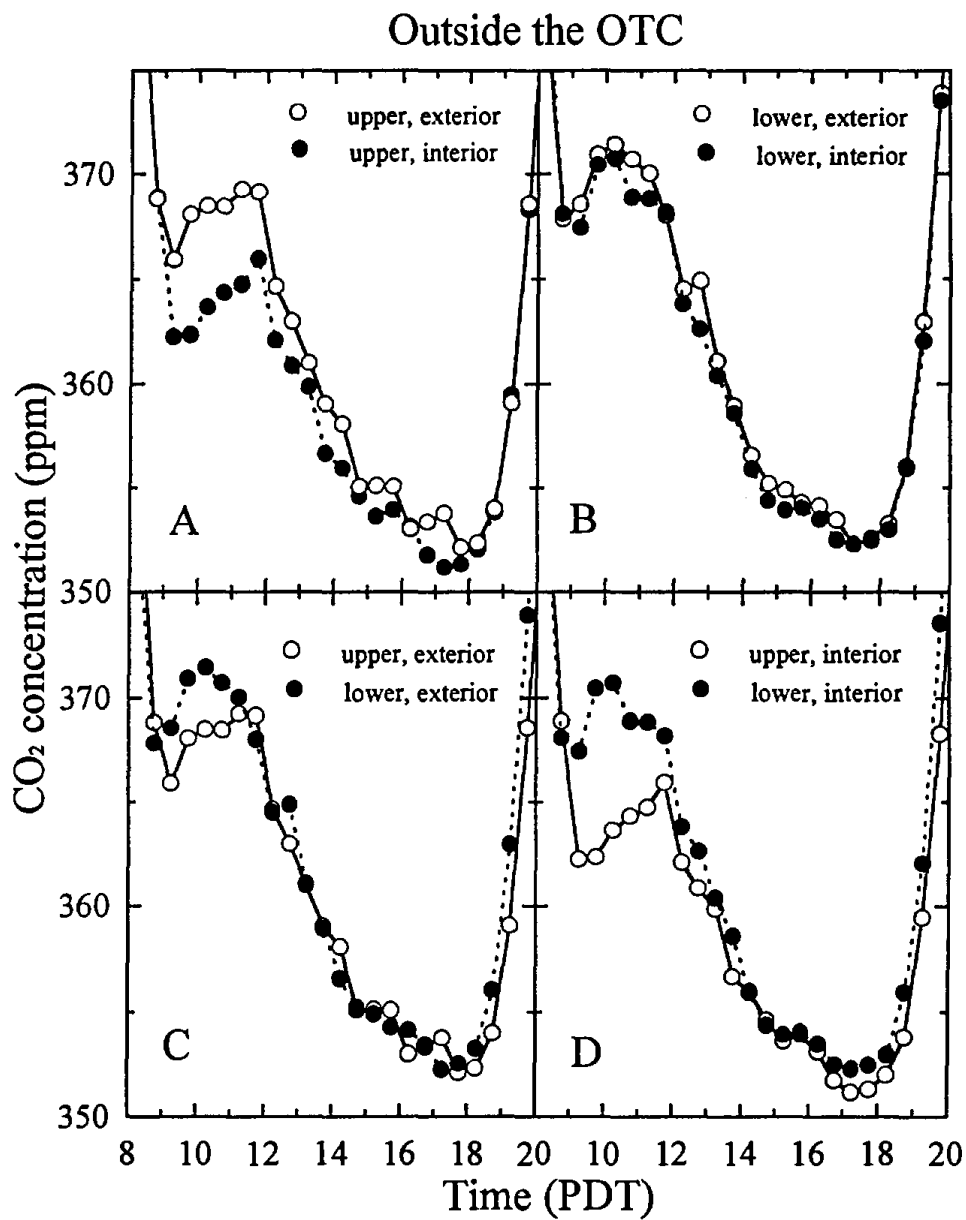


Fig. 33. Diurnal pattern of CO₂ concentration averaged over all sample dates at four pairs of contrasting locations demonstrating strictly vertical or horizontal gradients, outside the OTC.

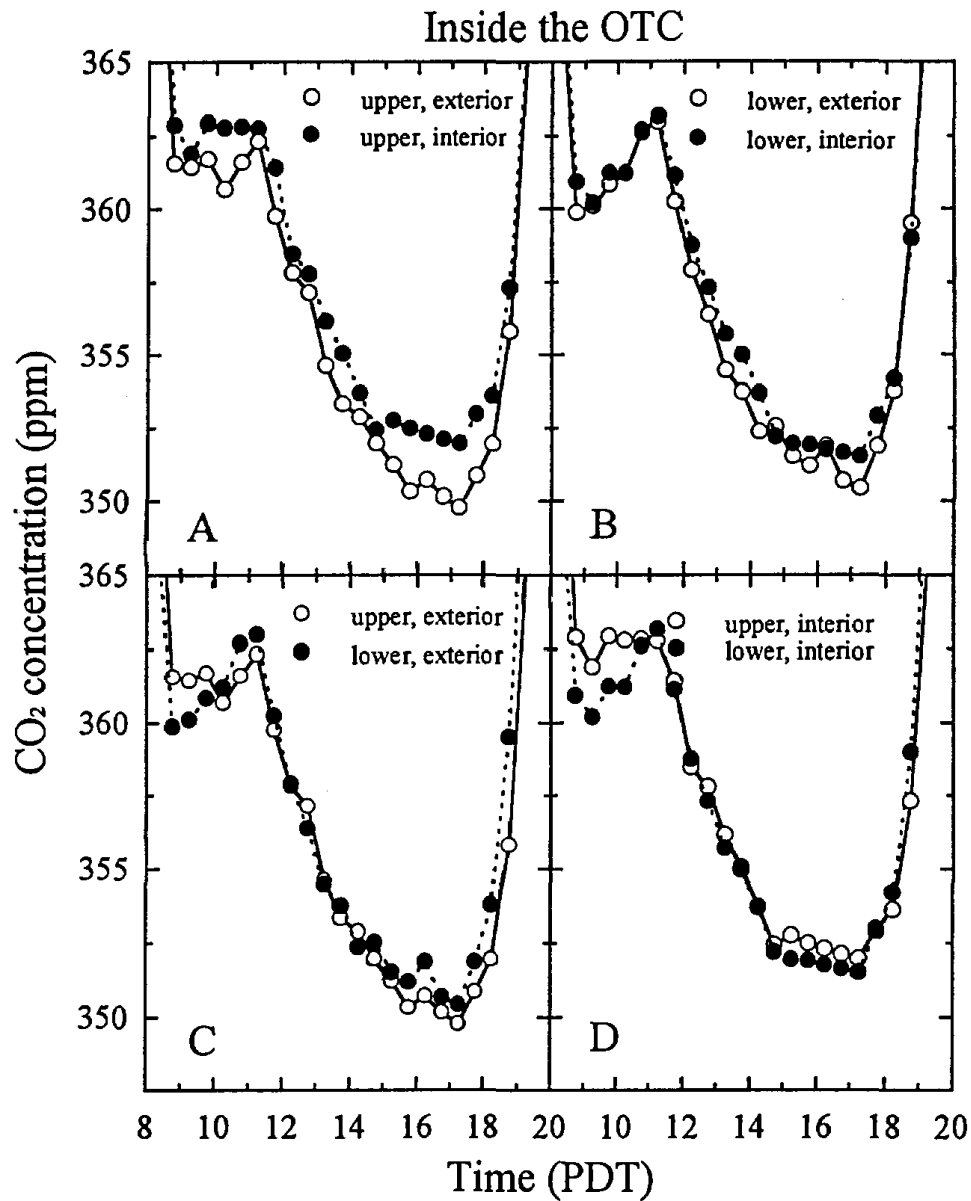


Fig. 34. Diurnal pattern of CO₂ concentration averaged over all sample dates at four pairs of contrasting locations demonstrating strictly vertical or horizontal gradients, inside the OTC.

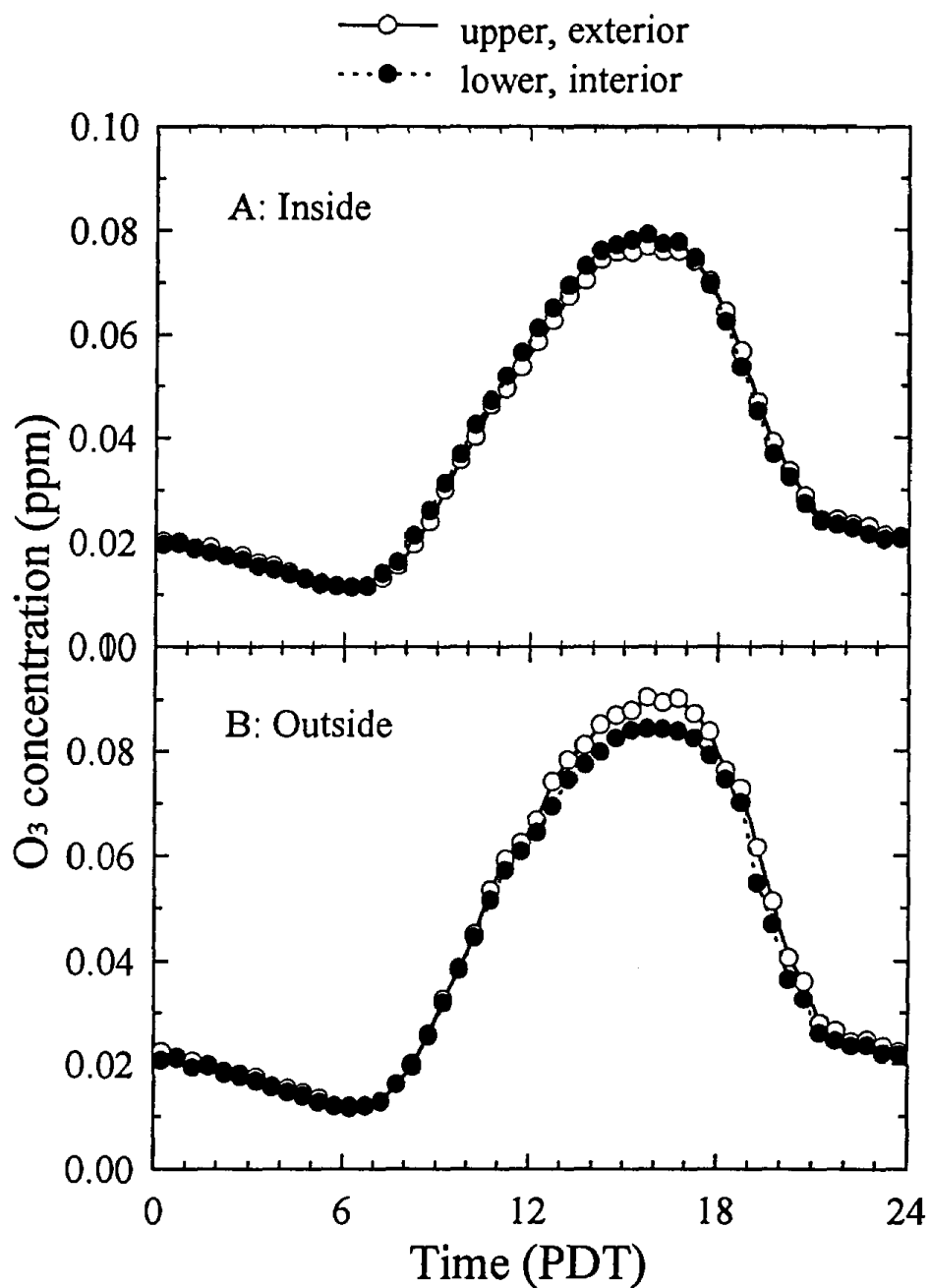


Fig. 35. Diurnal pattern of O₃ concentration averaged over all sample dates at two contrasting canopy locations (A) inside and (B) outside the OTC.

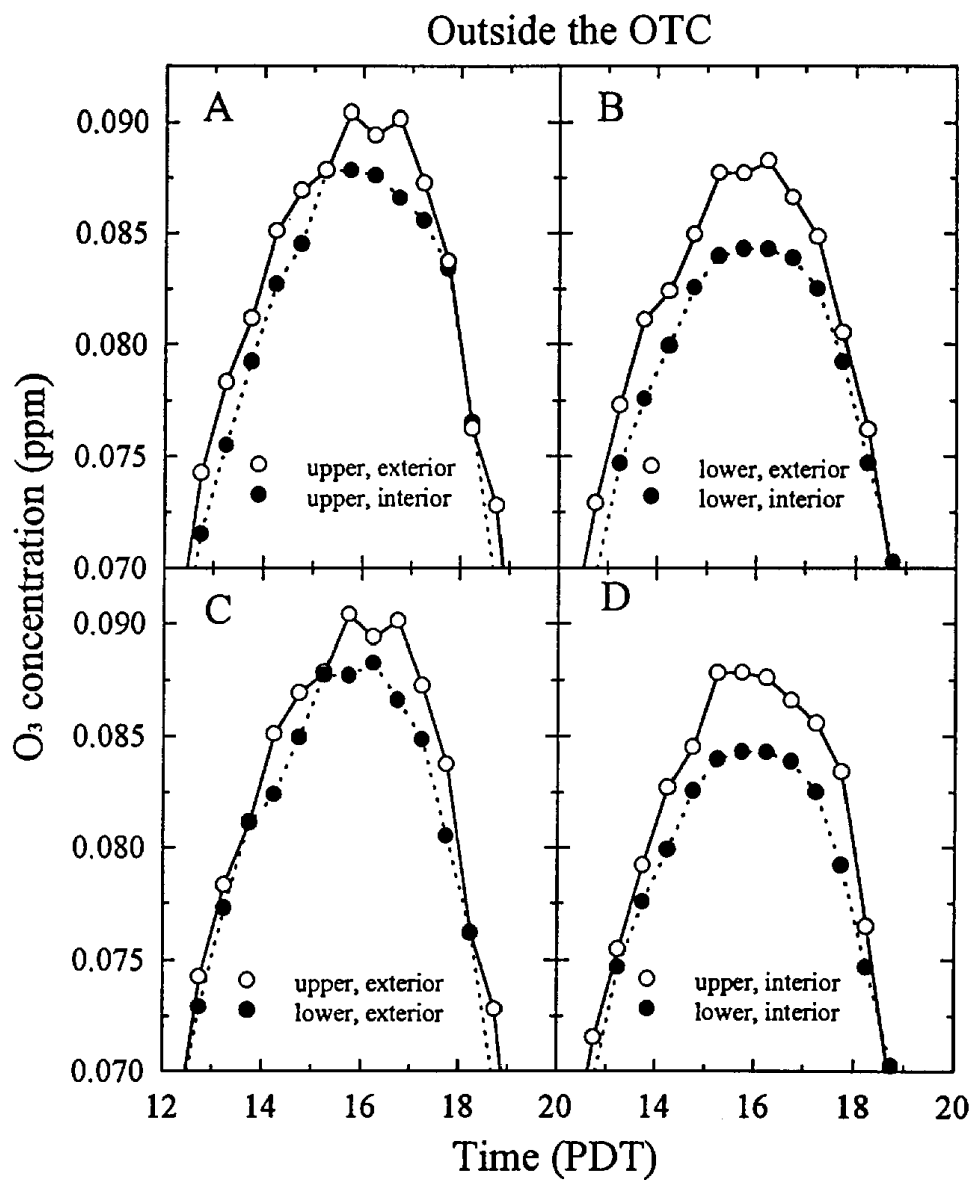


Fig. 36. Diurnal pattern of O₃ concentration averaged over all sample dates at four pairs of contrasting locations demonstrating strictly vertical or horizontal gradients, outside the OTC.

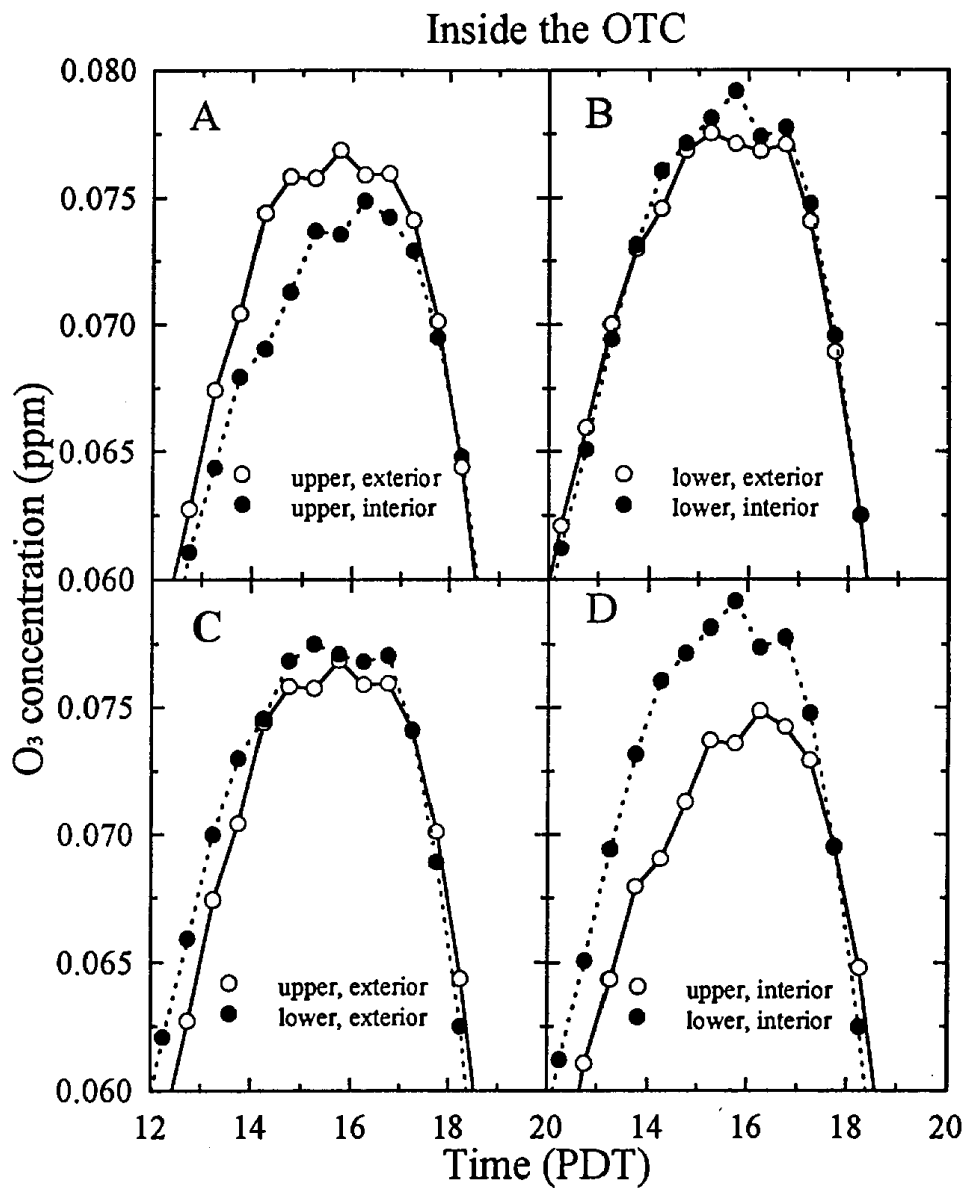


Fig. 37. Diurnal pattern of O₃ concentration averaged over all sample dates at four pairs of contrasting locations demonstrating strictly vertical or horizontal gradients, inside the OTC.

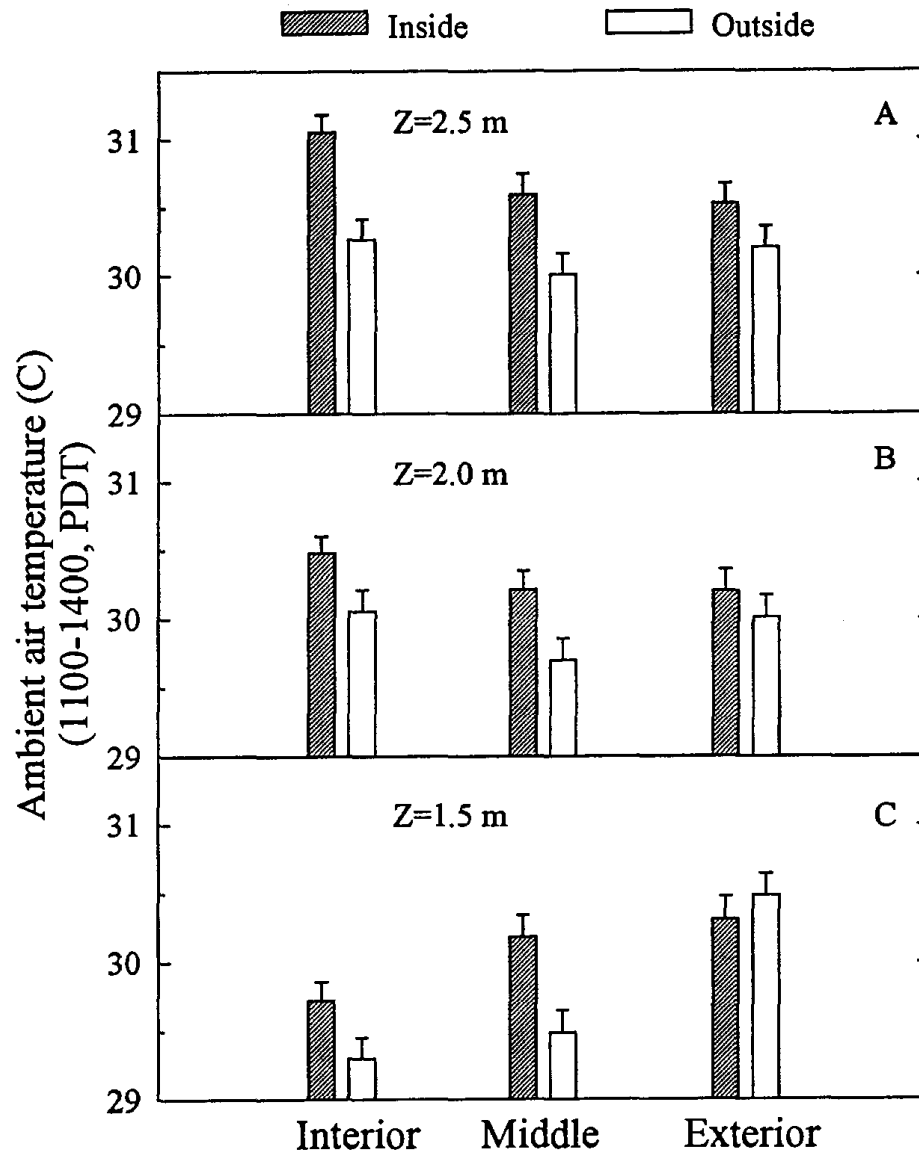


Fig. 38. Midday ambient air temperature averaged over all sample dates from 1100-1400 PDT, at each of the nine canopy locations in the upper (A), mid (B) and lower (C) canopy inside and outside the OTC.

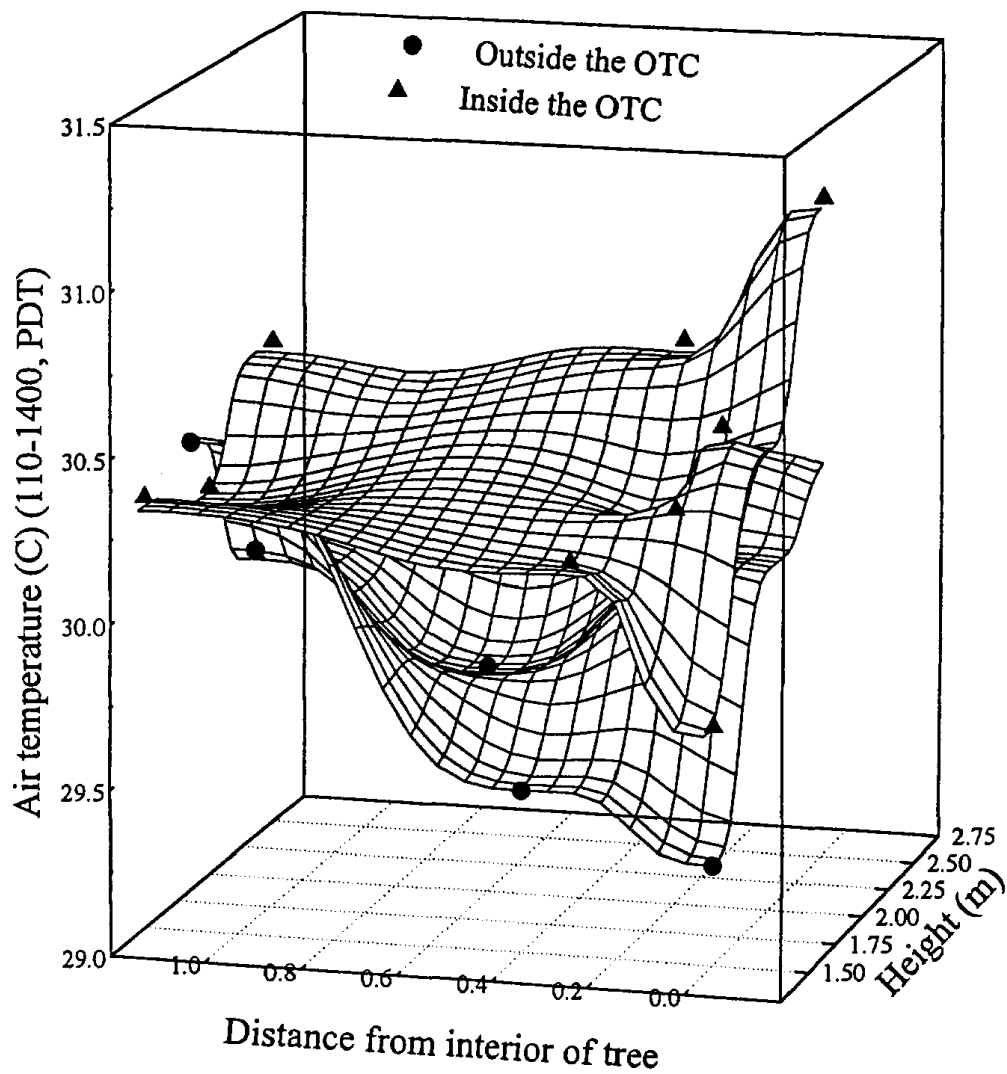


Fig. 39. Response surface of midday ambient air temperature averaged over all sample dates from 1100-1400 PDT, at each of the nine canopy locations (data points) inside and outside the OTC.

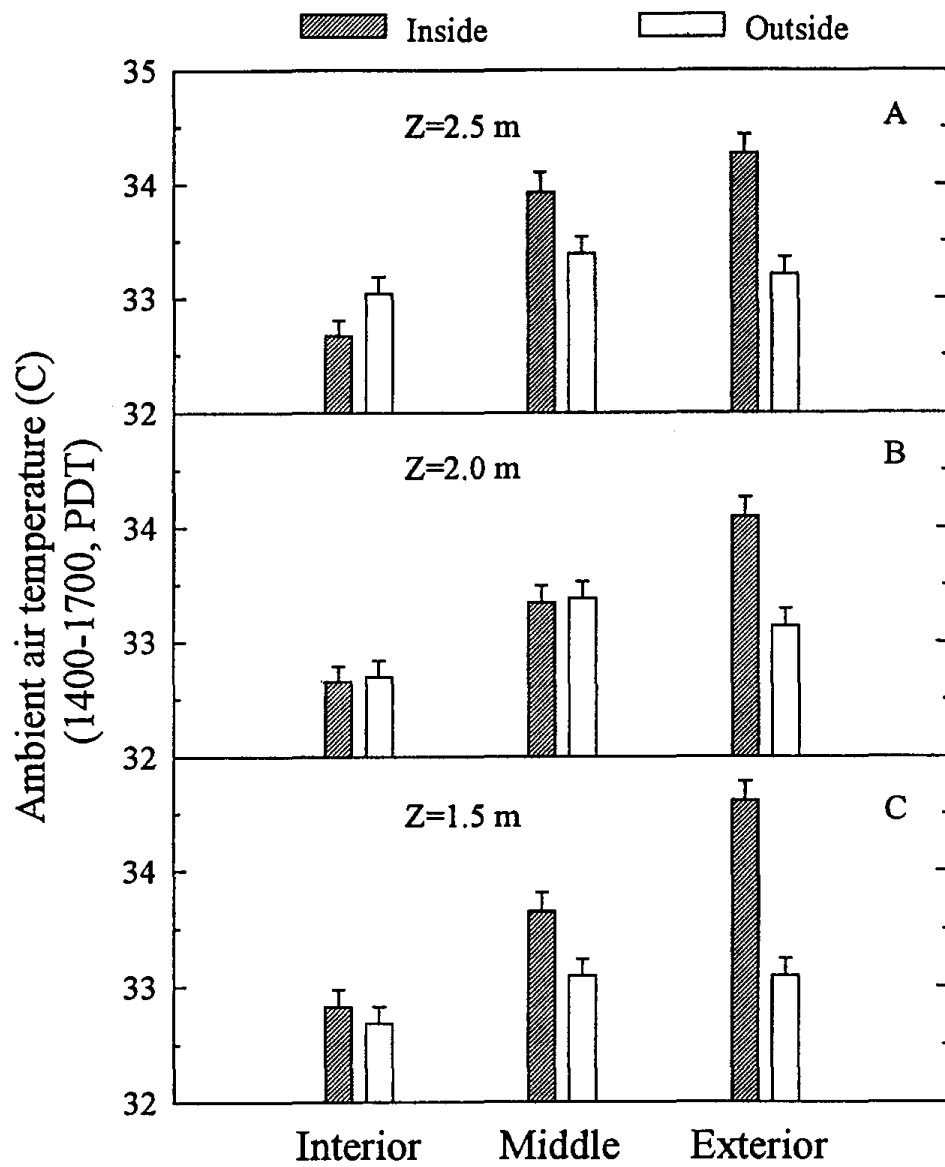


Fig. 40. Afternoon ambient air temperature averaged over all sample dates from 1400-1700 PDT, at each of the nine canopy locations in the upper (A), mid (B) and lower (C) canopy inside and outside the OTC.

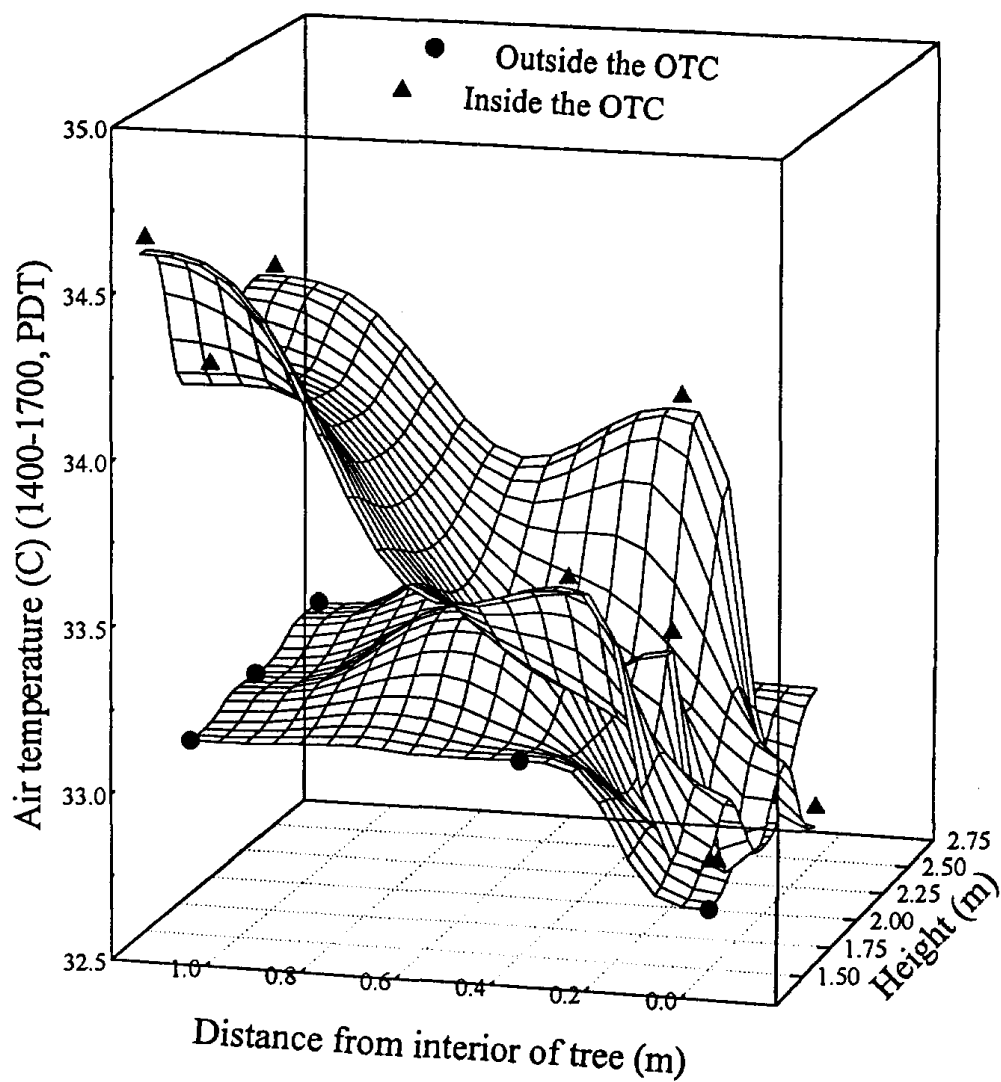


Fig. 41. Response surface of afternoon ambient air temperature averaged over all sample dates from 1400-1700 PDT, at each of the nine canopy locations (data points) inside and outside the OTC.

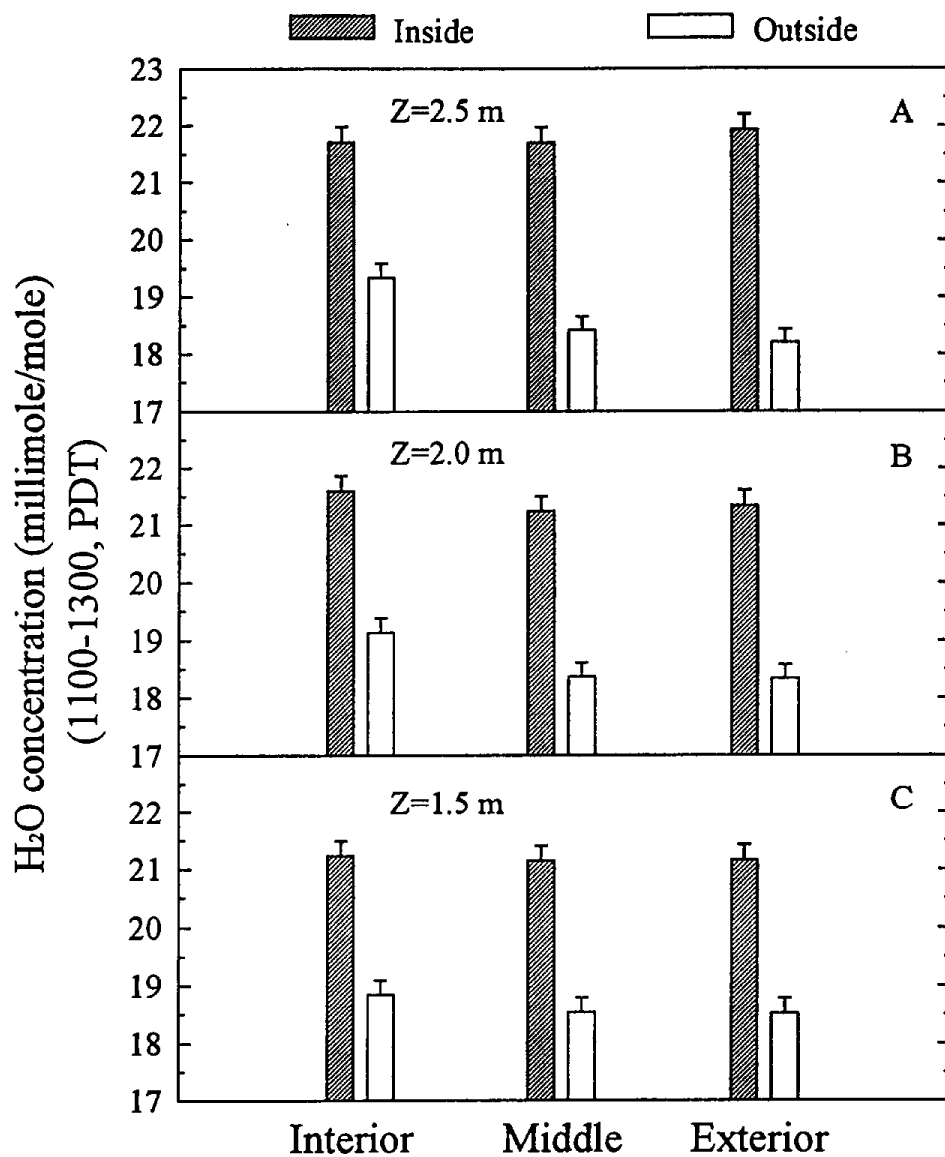


Fig. 42. Midday H₂O vapor concentration averaged over all sample dates from 1100-1300 PDT, at each of the nine canopy locations in the upper (A), mid (B) and lower (C) canopy inside and outside the OTC.

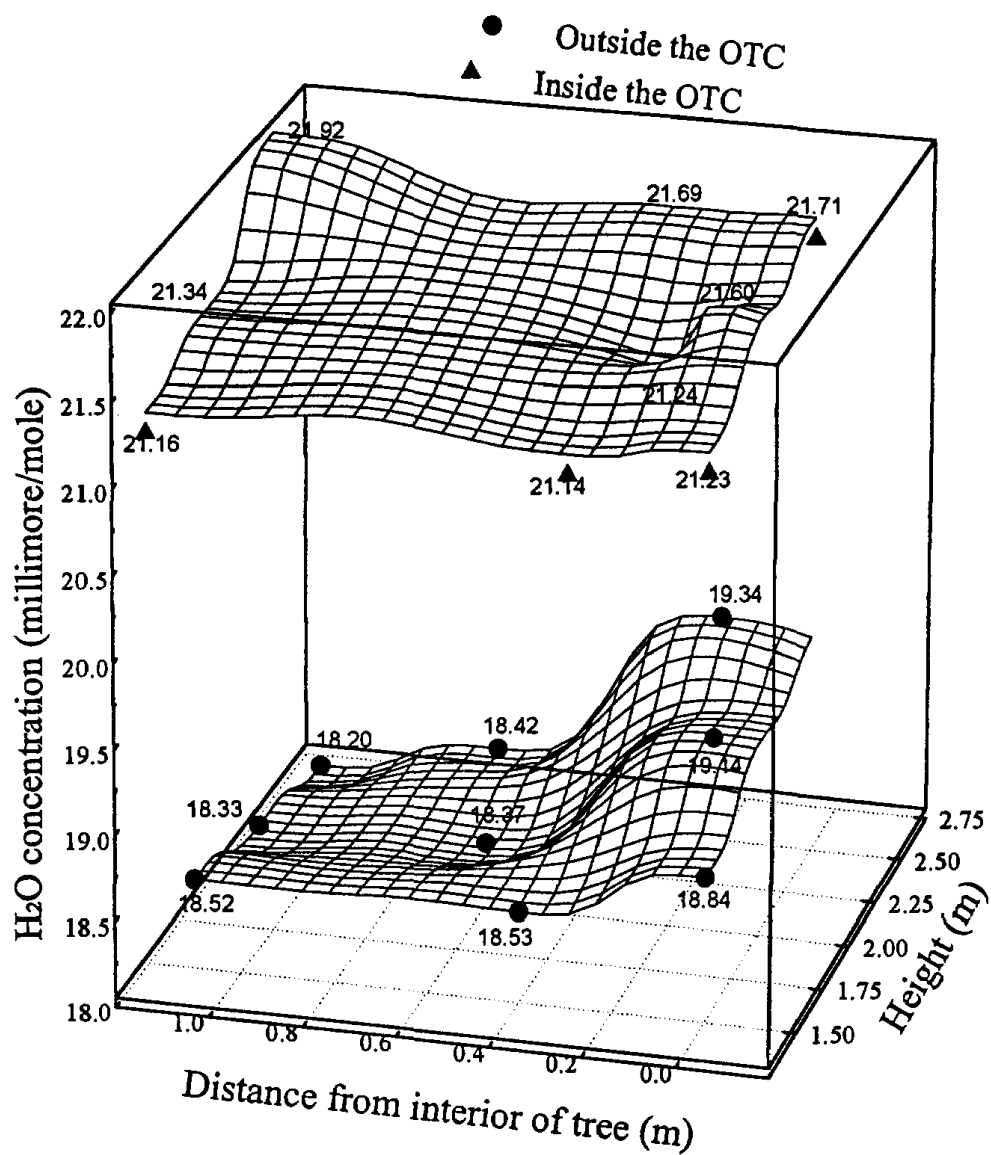


Fig. 43. Response surface of midday H₂O vapor concentration averaged over all sample dates from 1100-1300 PDT, at each of the nine canopy locations (data points) inside and outside the OTC.

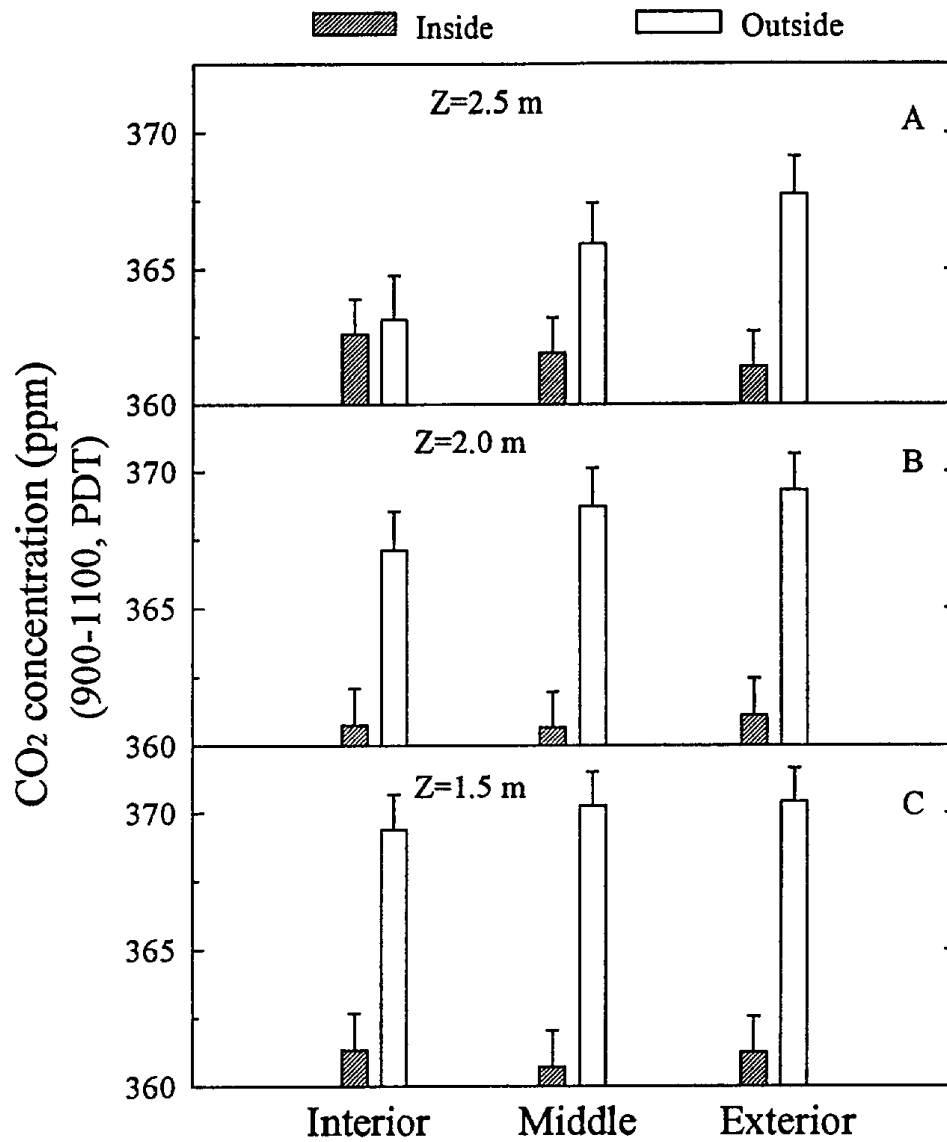


Fig. 44. Morning CO₂ concentration averaged over all sample dates from 900-1100 PDT, at each of the nine canopy locations in the upper (A), mid (B) and lower (C) canopy inside and outside the OTC.

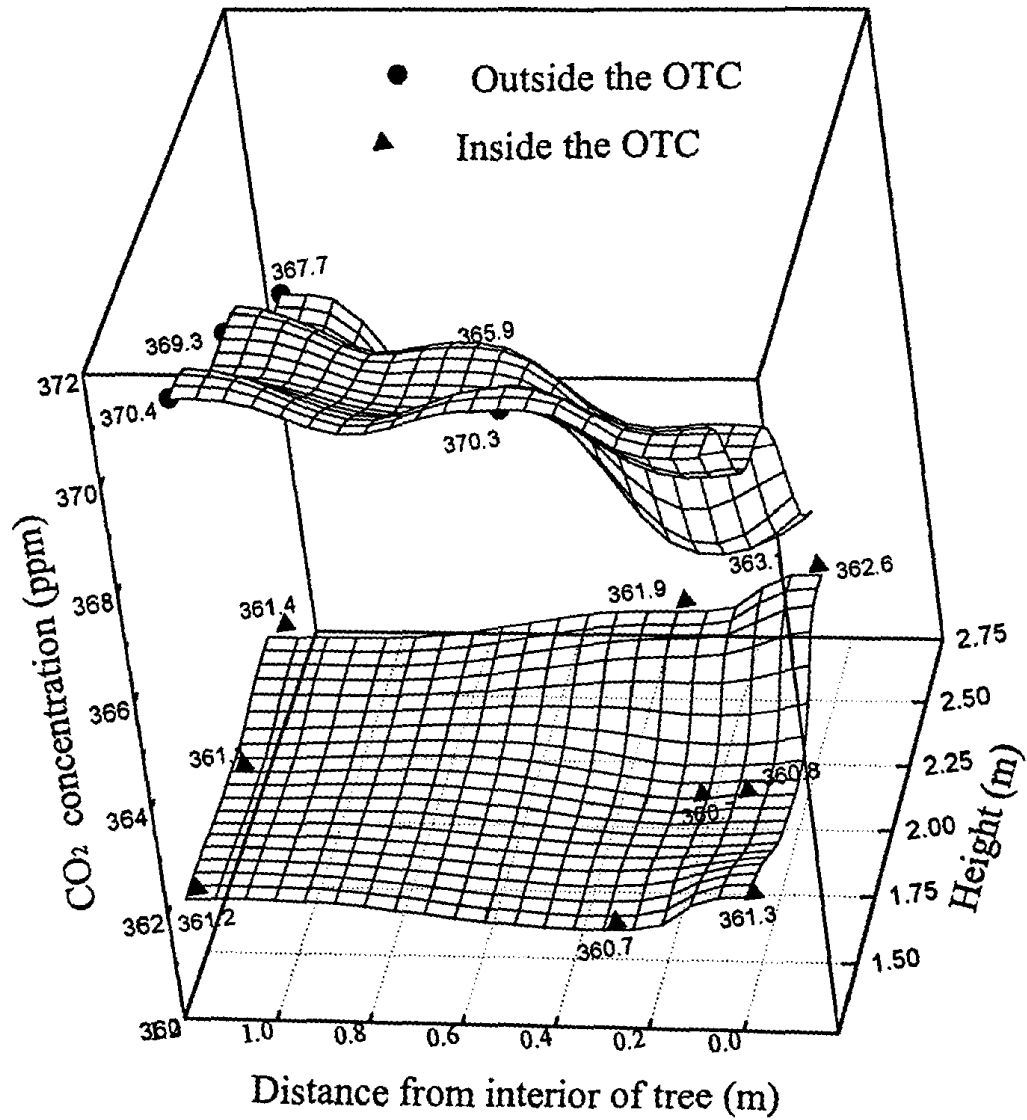


Fig. 45. Response surface of morning CO₂ concentration averaged over all sample dates from 900-1100 PDT, at each of the nine canopy locations (data points) inside and outside the OTC.

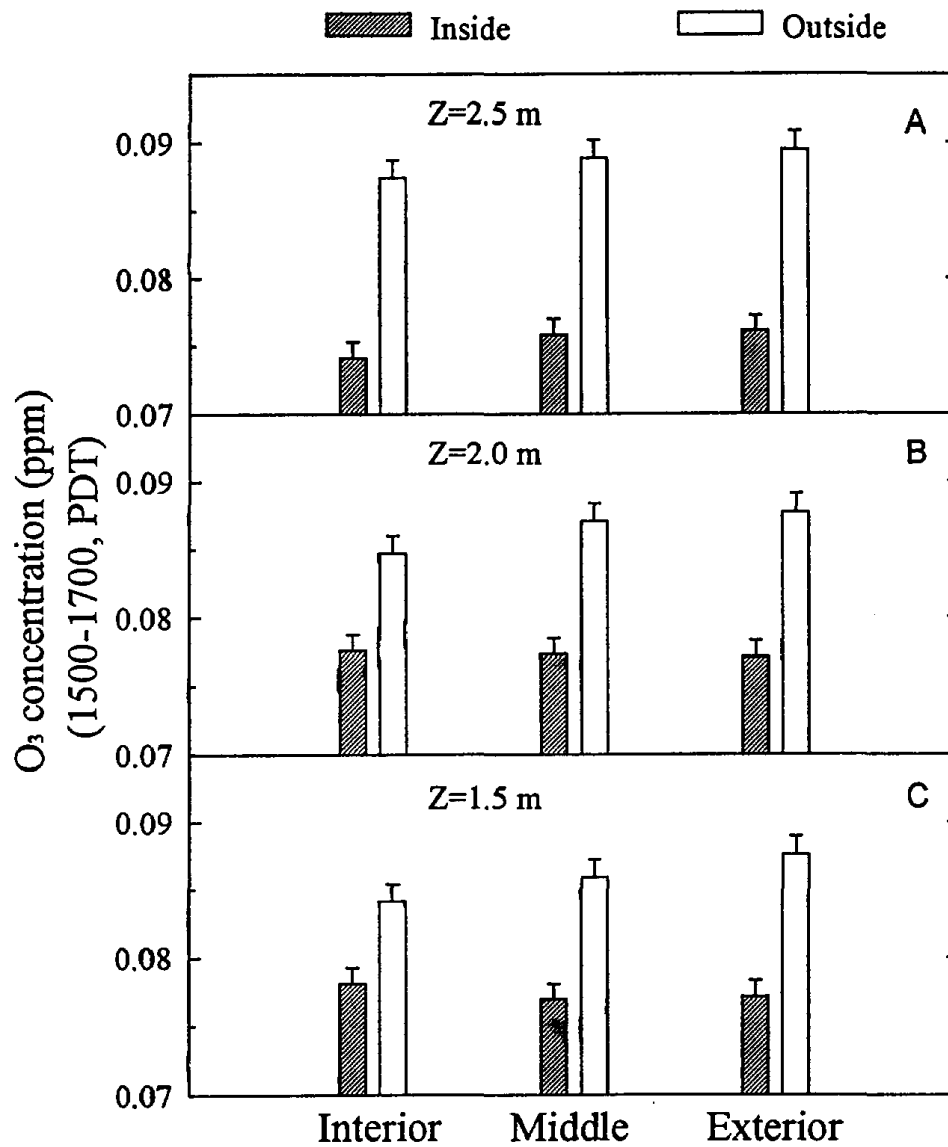


Fig. 46. Midday O₃ concentration averaged over all sample dates from 1100-1300 PDT, at each of the nine canopy locations in the upper (A), mid (B) and lower (C) canopy inside and outside the OTC.

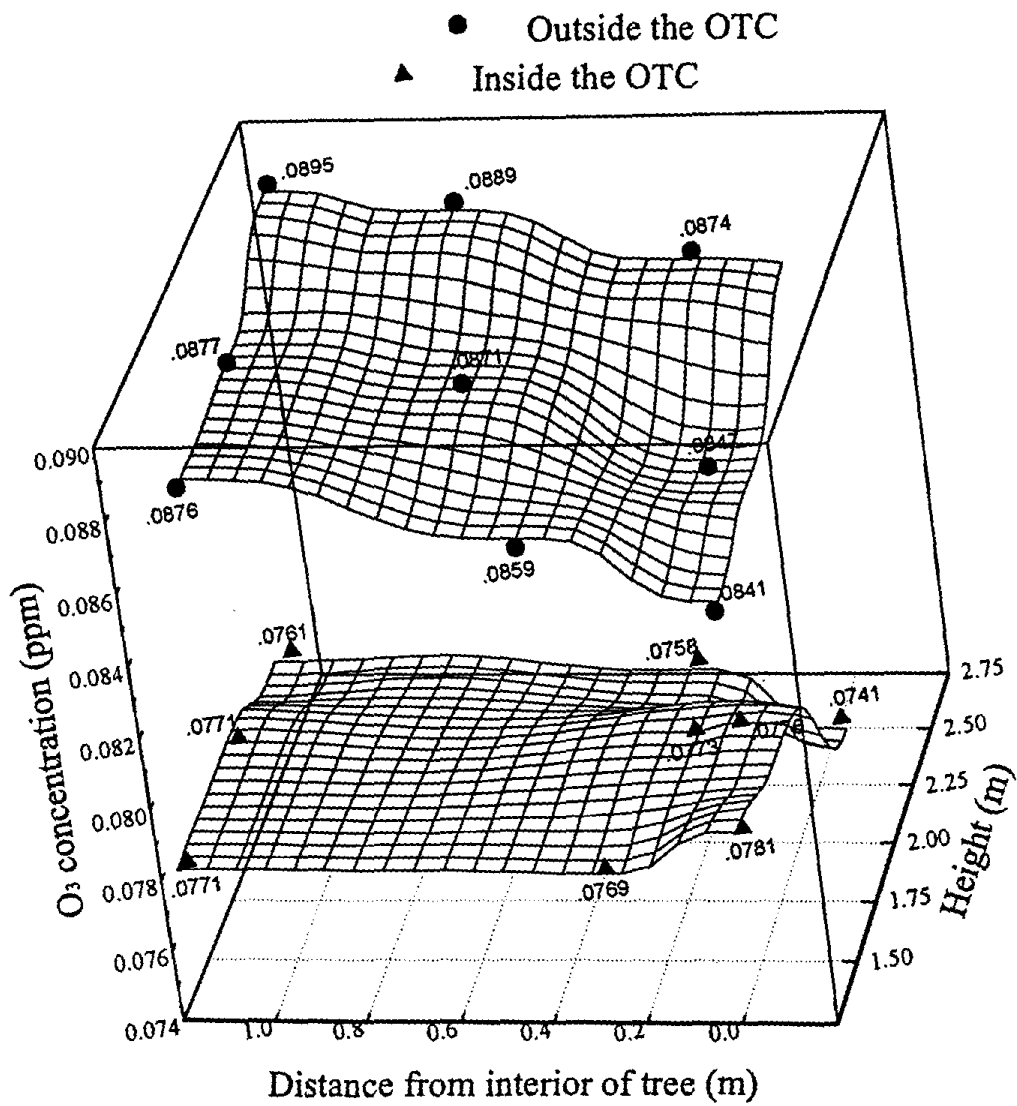


Fig. 47. Response surface of midday O₃ concentration averaged over all sample dates from 1100-1300 PDT, at each of the nine canopy locations (data points) inside and outside the OTC.

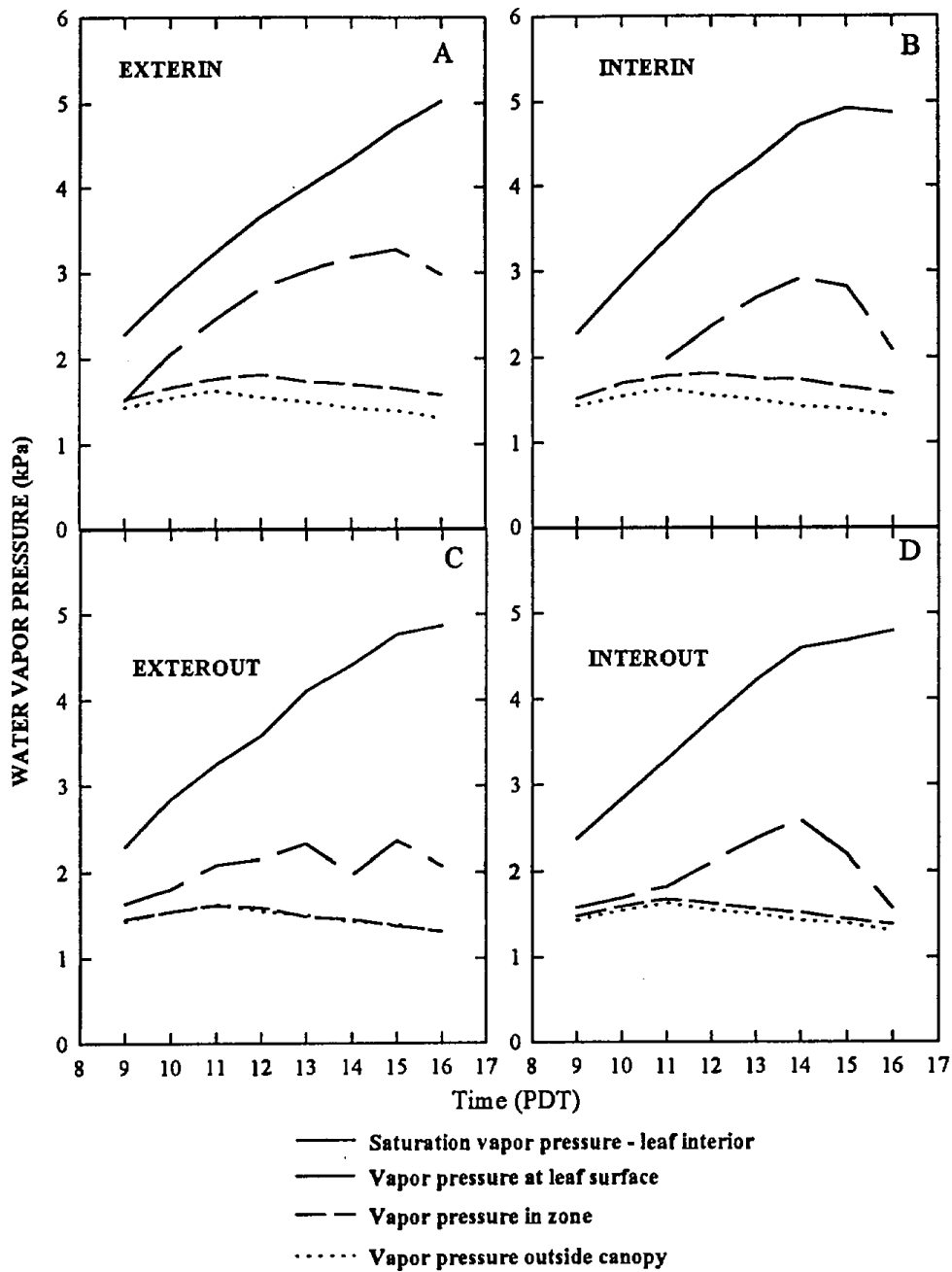


Fig. 48. Diurnal pattern of H₂O vapor pressure at the leaf interior, at the leaf surface, in the canopy air space within each zone, and in the ambient air in the canopy exterior, by zone.

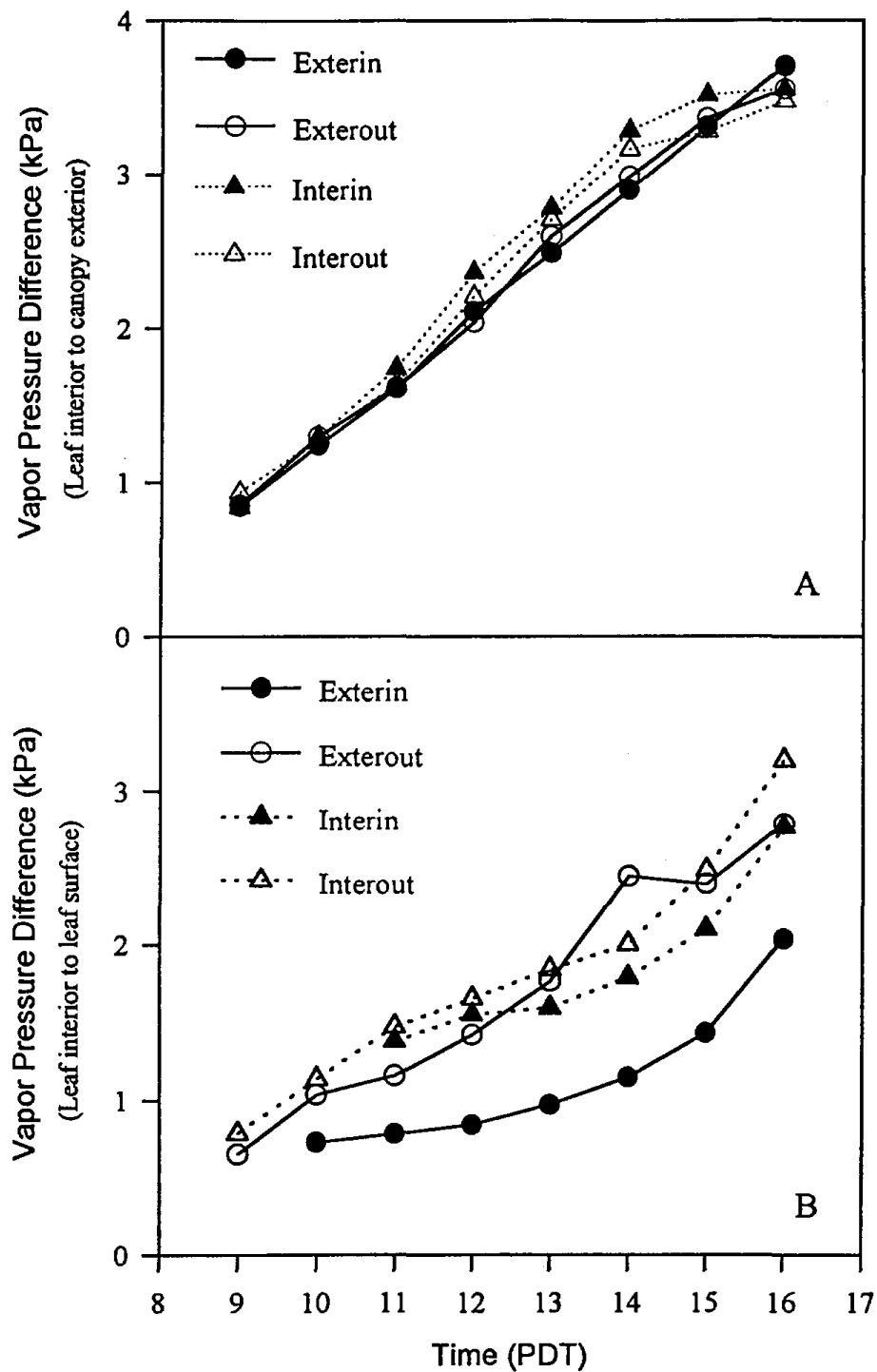


Fig. 49. Vapor pressure difference (V) from leaf interior to canopy exterior and from leaf interior to leaf surface, by zone inside and outside the OTC, averaged over the six days of intensive physiological measurements.

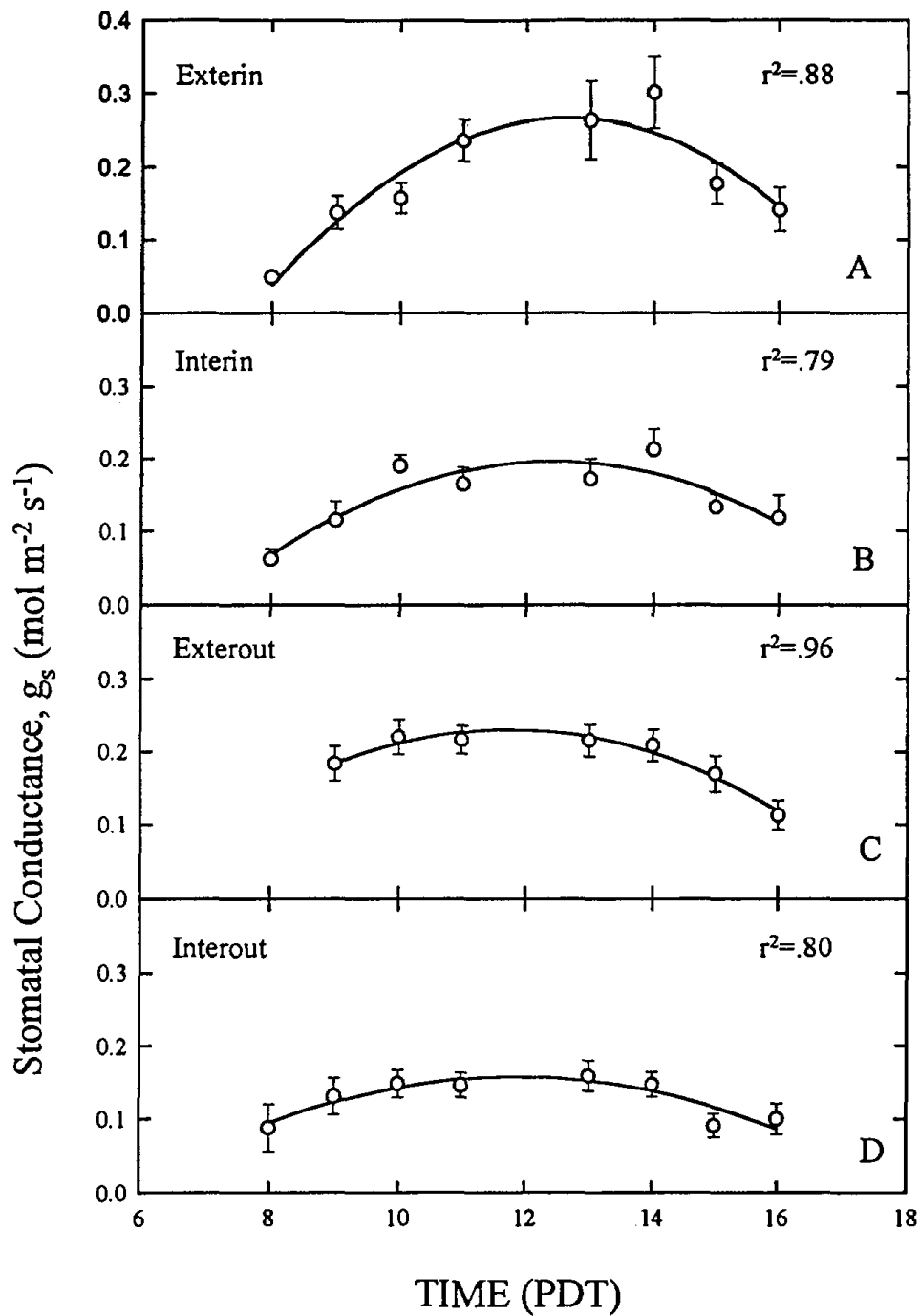


Fig. 50. Diurnal pattern of hourly means of stomatal conductance determined from single leaf gas exchange measurements by zone averaged over the six days of intensive physiological measurements. Solid lines are from polynomial regression analysis.

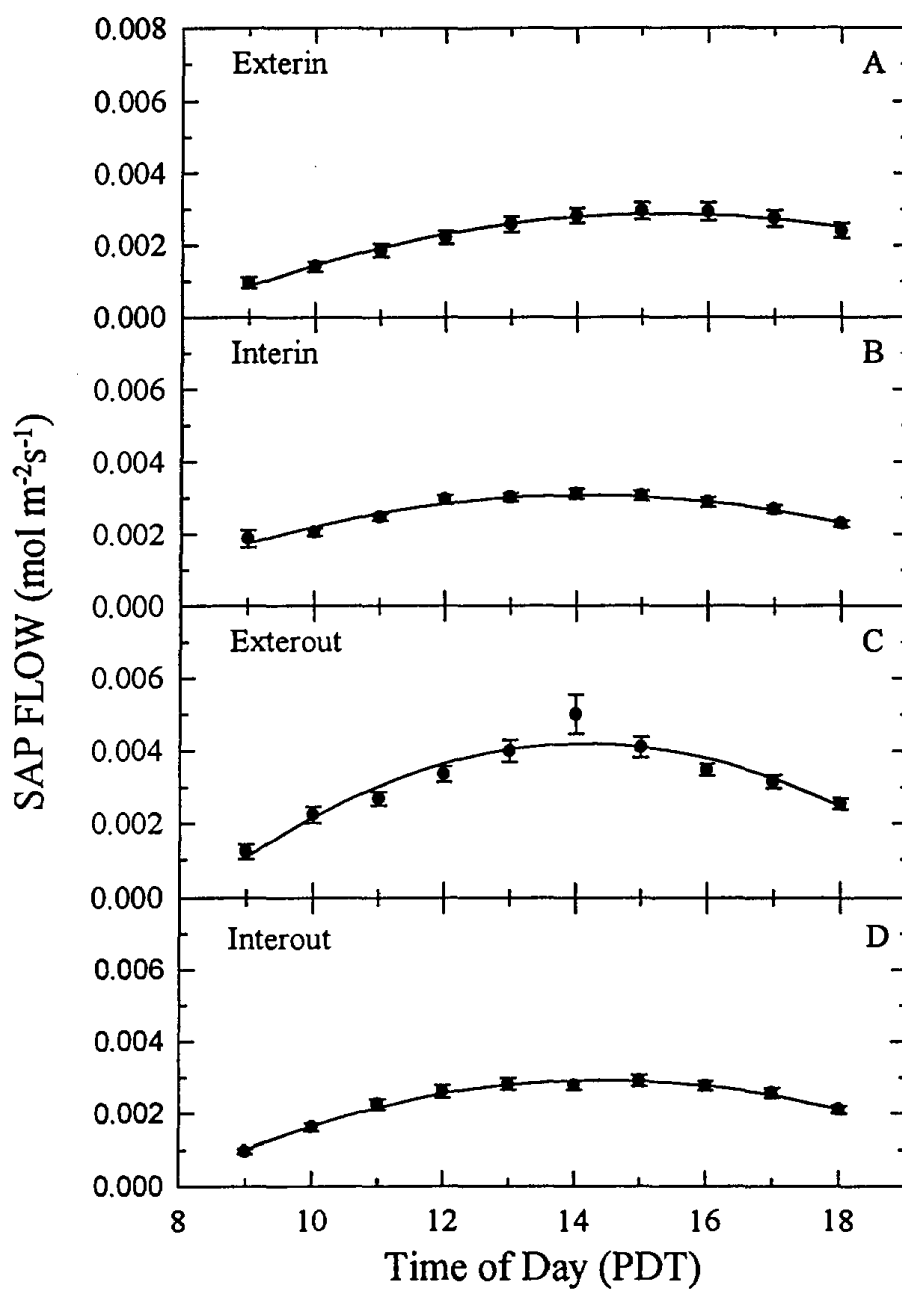


Fig. 51. Diurnal pattern of hourly means of xylem sap flow (transpiration) determined from heat balance stem flow gauges by zone averaged over the six days of intensive physiological measurements. Solid lines are from polynomial regression analysis.

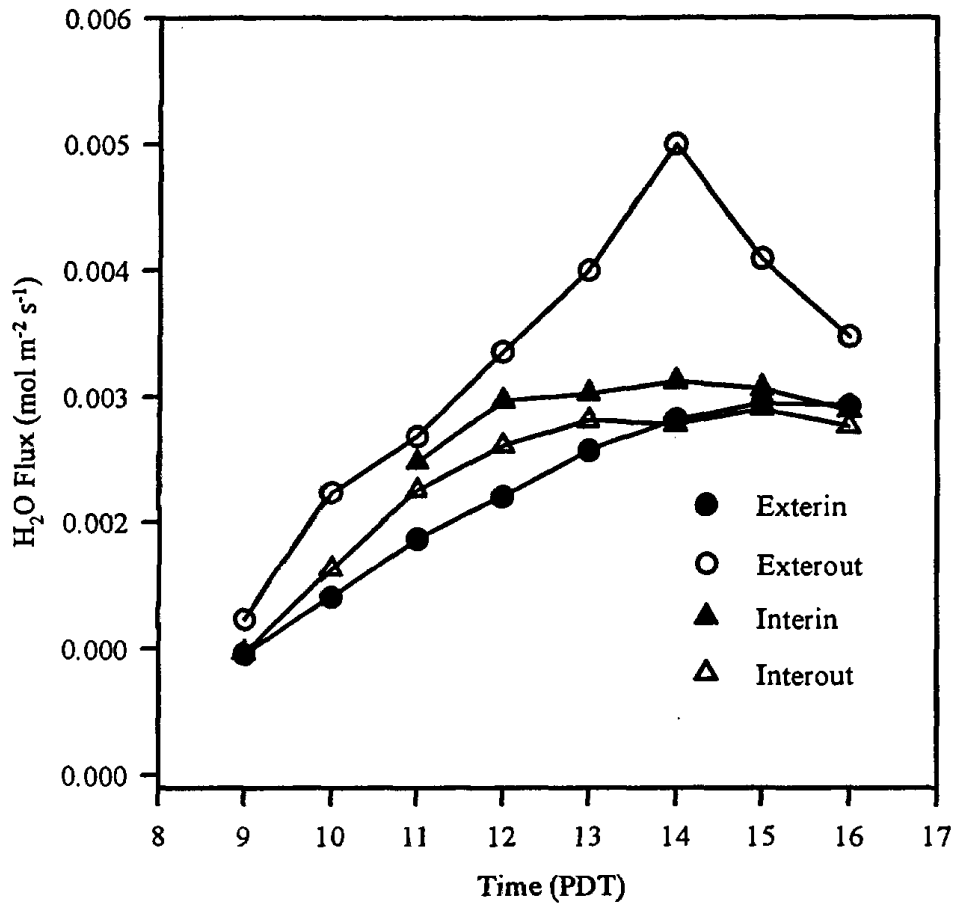


Fig. 52. Diurnal pattern of hourly means of water vapor flux (transpiration) calculated from water vapor gradients and diffusive conductances from the leaf interior to the ambient air by zone averaged over the six days of intensive physiological measurements. The similarity to Fig. 51 reflects the use of directly measured sap flow in calculating boundary layer conductances.

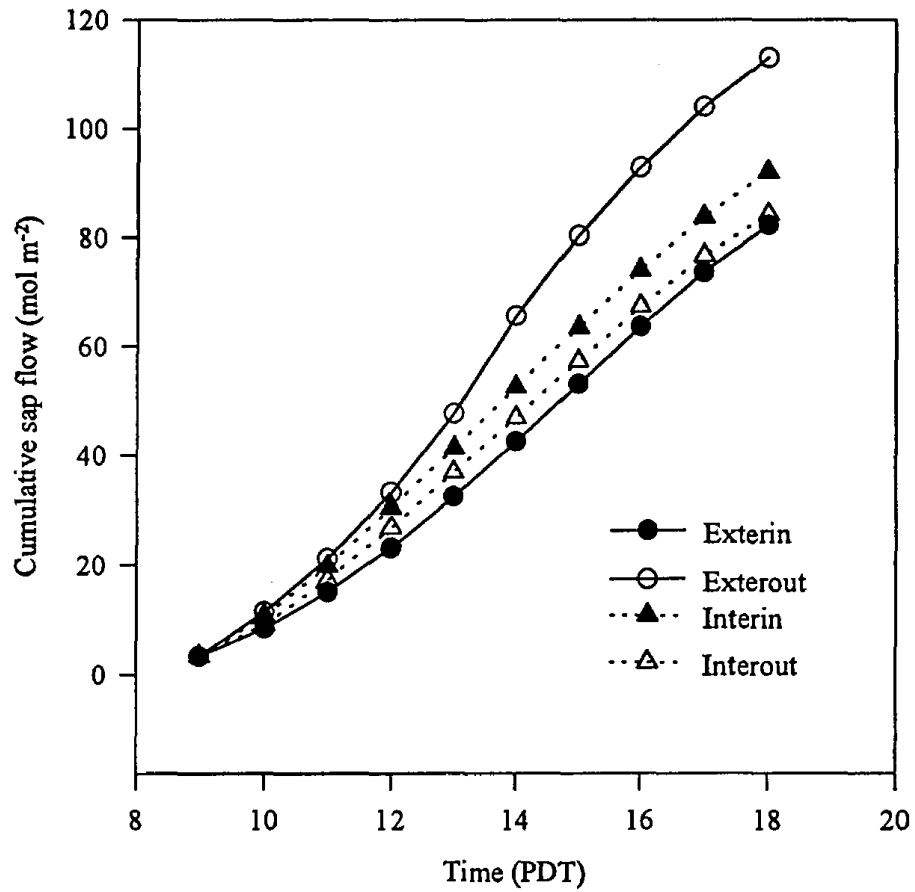


Fig. 53. Cumulative xylem sap flow by zone averaged over the six days of intensive physiological measurements.

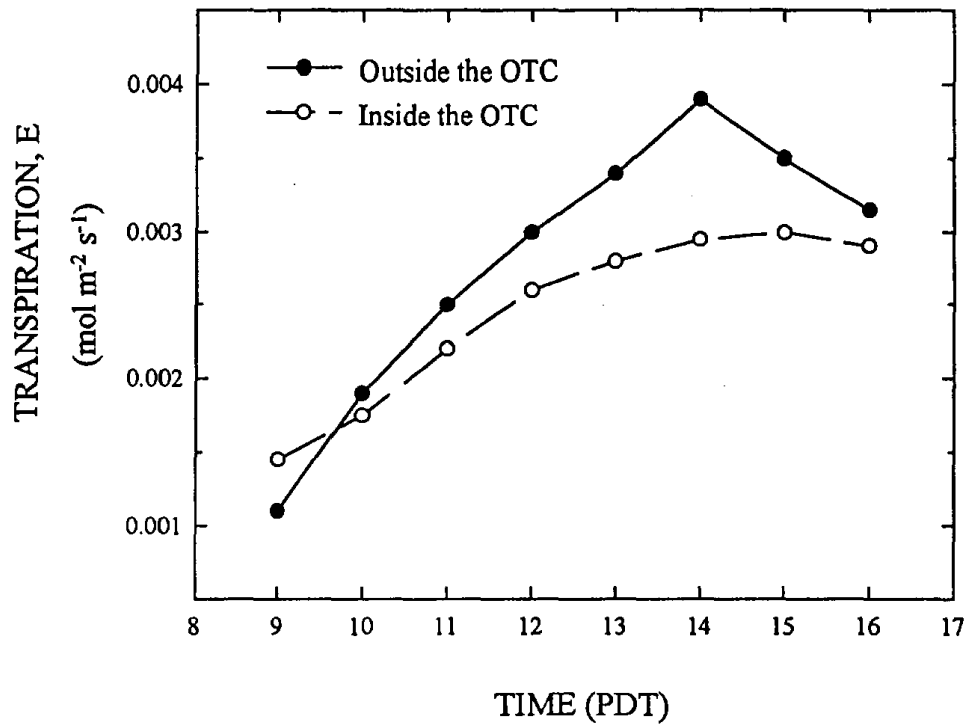


Fig. 54. Diurnal pattern of liquid water flux (sap flow; transpiration) averaged over six days of intensive physiological measurements, inside and outside the OTC, averaged over both zones.

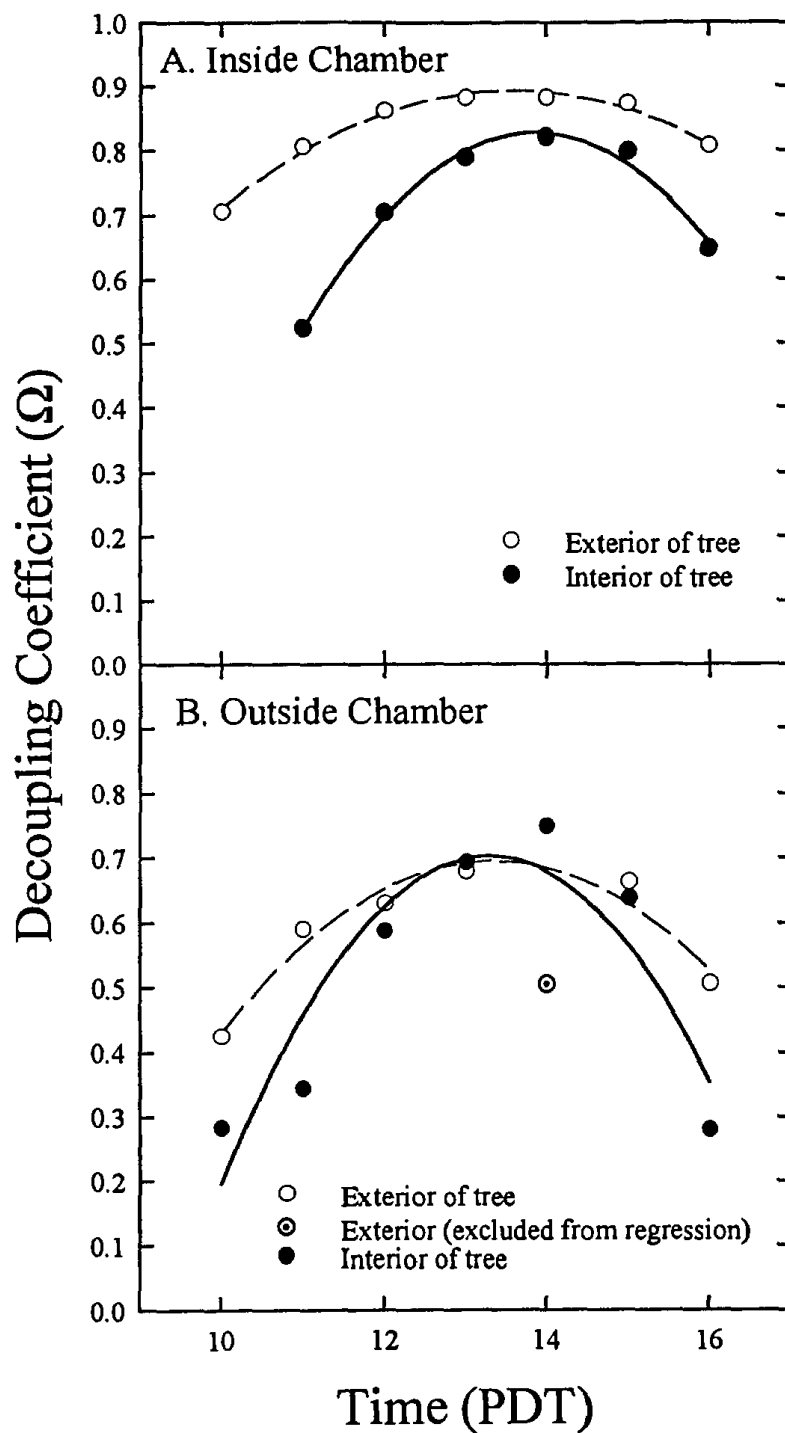


Fig. 55. Diurnal pattern of the environmental decoupling coefficient (Ω) inside (A) and outside (B) the OTC by zone averaged over the six days of intensive physiological measurements.

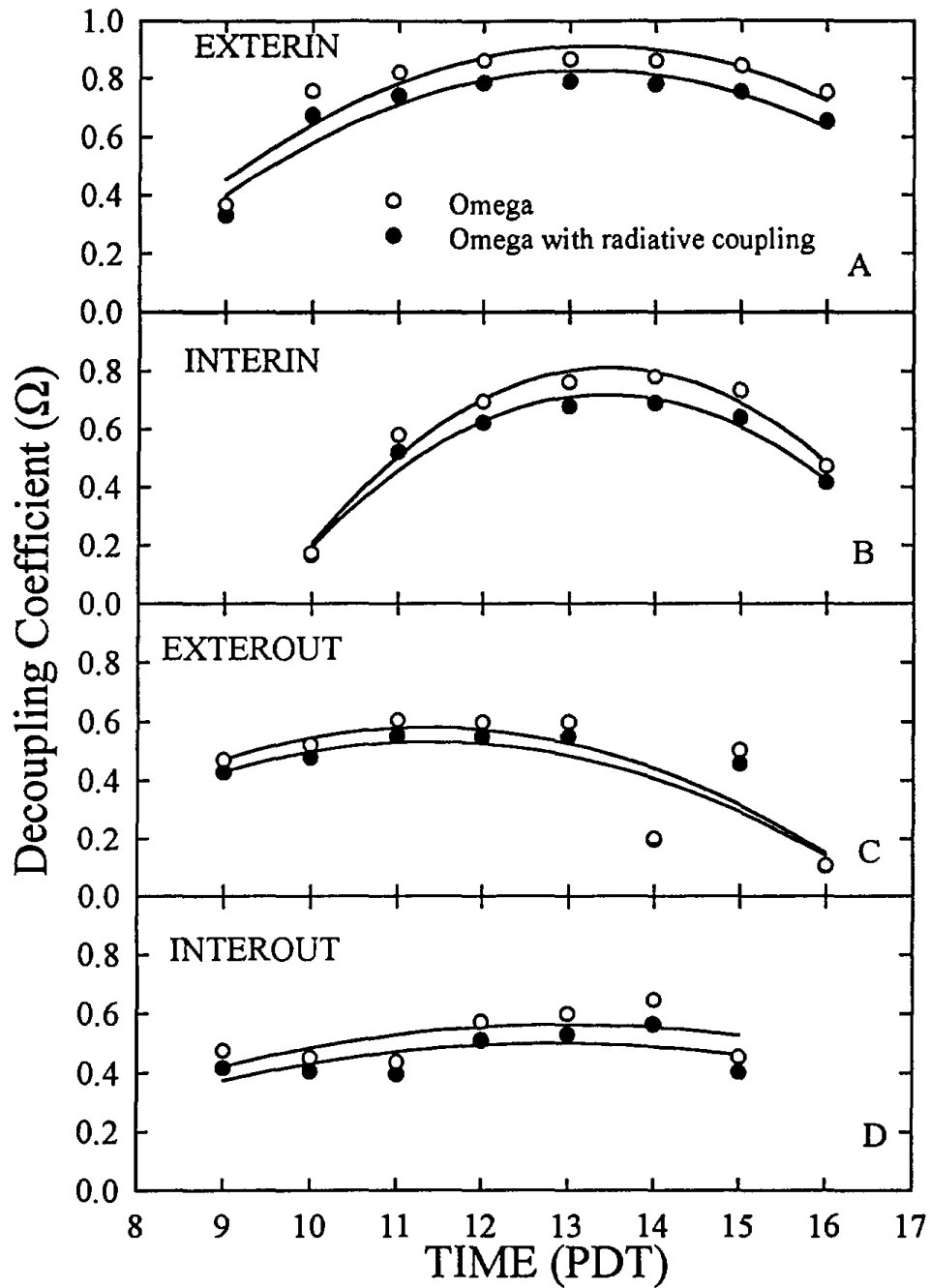


Fig. 56. Diurnal pattern of the environmental decoupling coefficient (Ω) by zone, demonstrating the impact of including (solid circle) or excluding (open circle) of radiative coupling.

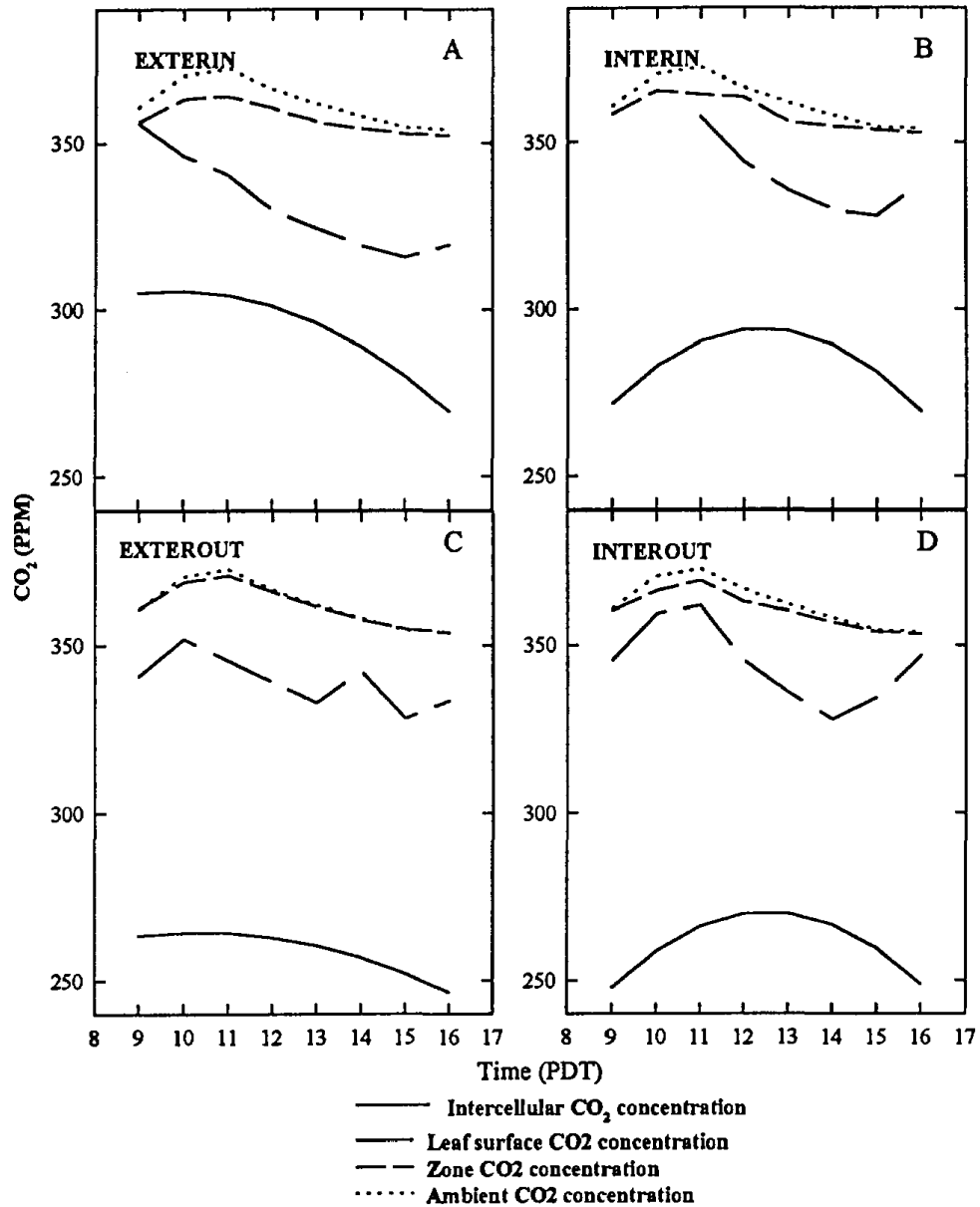


Fig. 57. Diurnal pattern of CO₂ concentrations at the leaf interior, at the leaf surface, in the canopy air space within each zone, and in the ambient air in the canopy exterior, by zone.

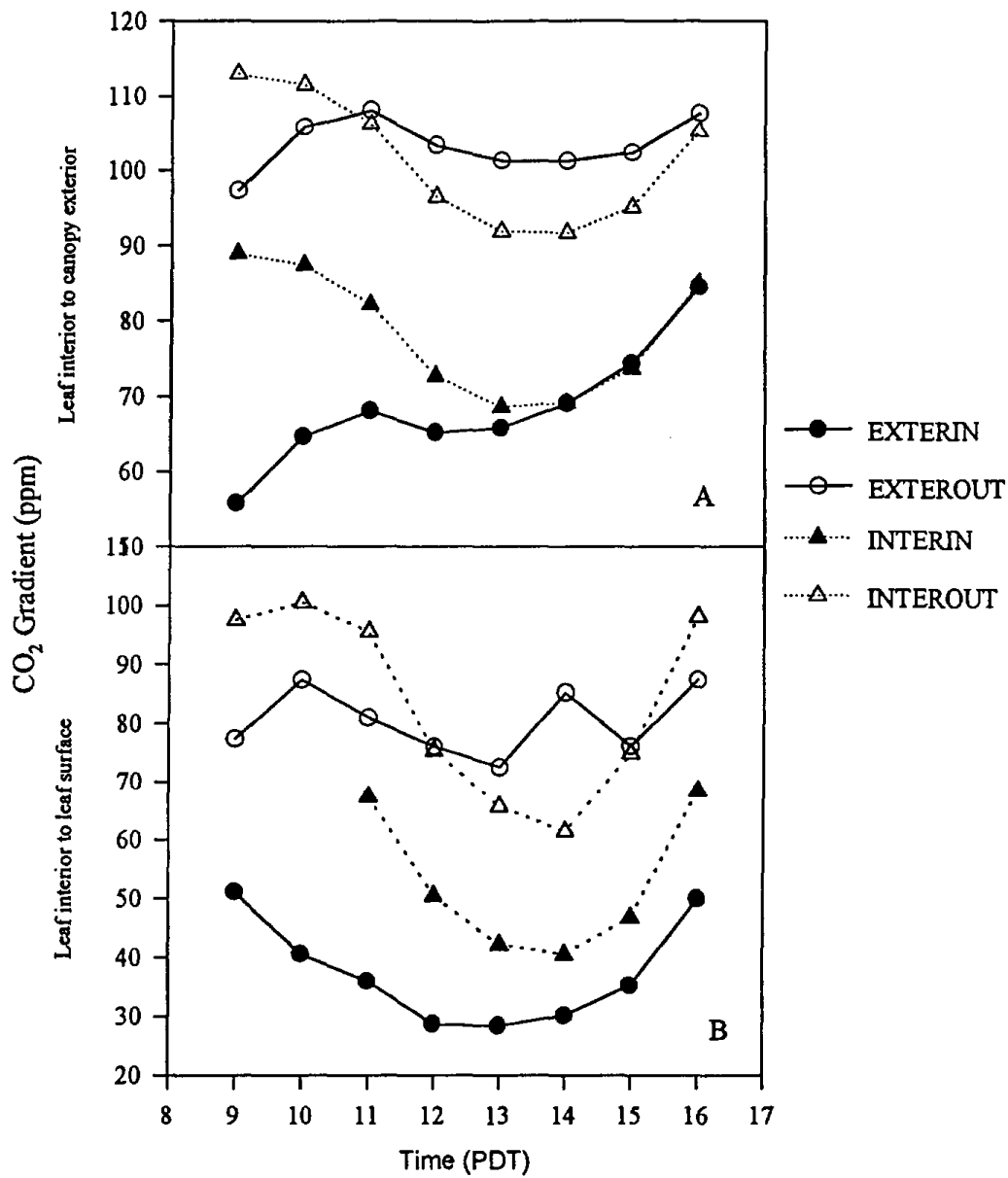


Fig. 58. Diurnal pattern of CO₂ gradients from leaf interior to canopy exterior and from leaf interior to the leaf surface by zone, inside and outside the OTC, averaged over six days of intensive physiological measurements.

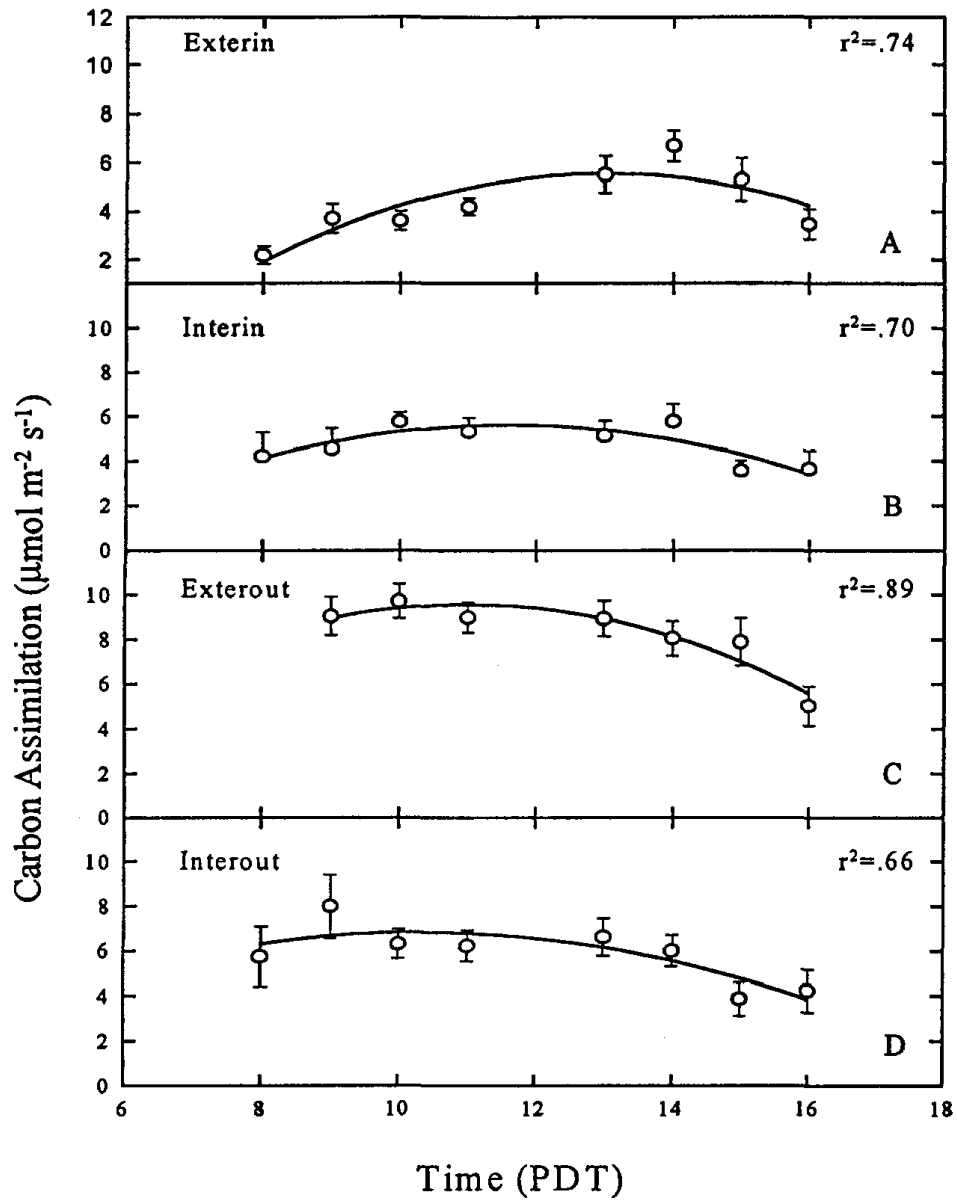


Fig. 59. Diurnal pattern of hourly means of net CO₂ assimilation (photosynthesis) determined from single leaf gas exchange measurements by zone averaged over the six days of intensive physiological measurements. Solid lines are from polynomial regression analysis.

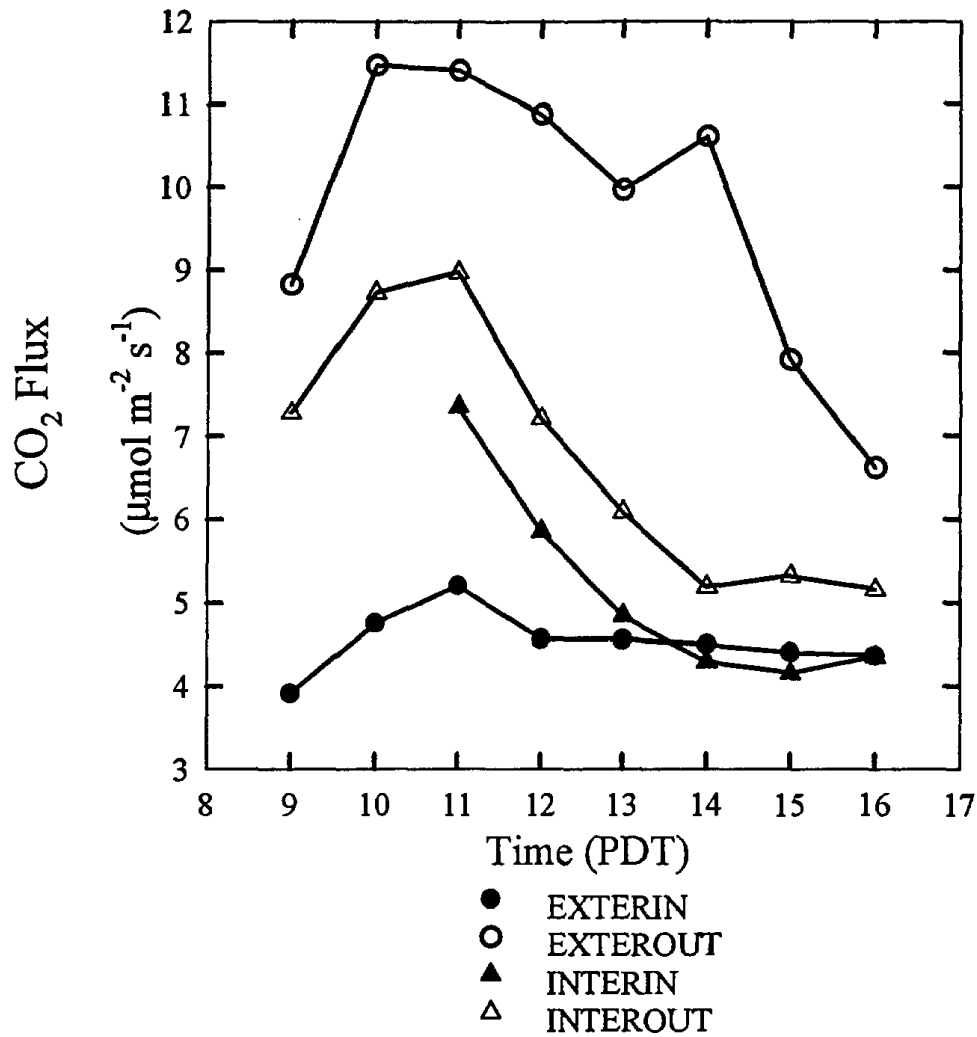


Fig. 60. Diurnal pattern of hourly means of net CO₂ assimilation (photosynthesis) determined from CO₂ gradients and diffusive conductances from the leaf interior to the ambient air, by zone averaged over the six days of intensive physiological measurements. The similarity to Fig. 59 reflects the use of single leaf measurements of CO₂ assimilation in calculating intercellular CO₂ concentration (C_i) and the resulting gradients for carbon flux.

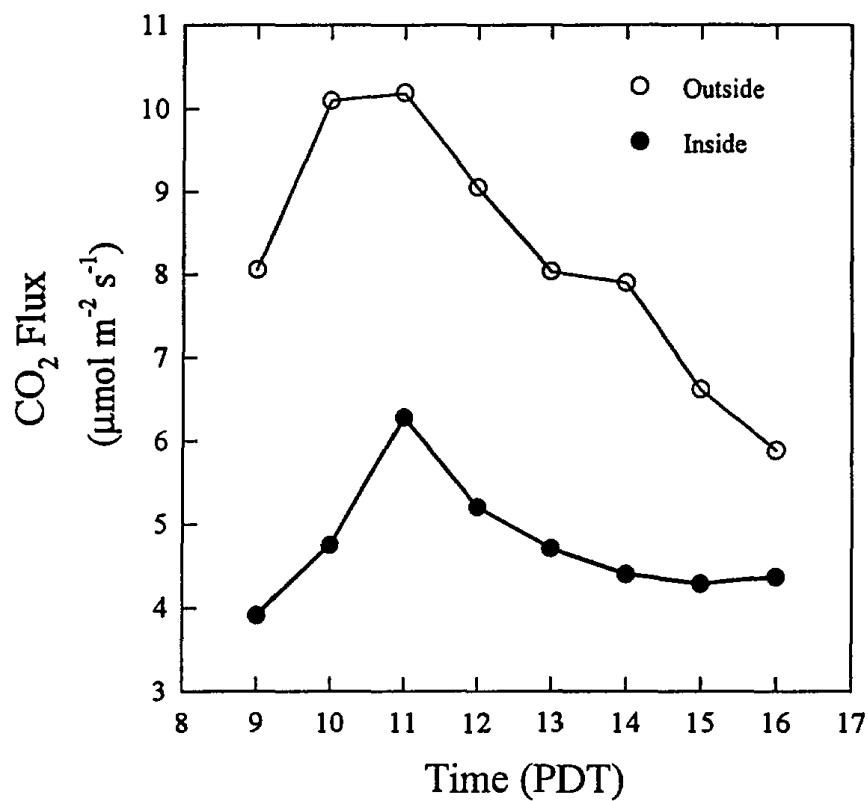


Fig. 61. Diurnal pattern of net CO₂ flux (single leaf gas exchange, photosynthesis) averaged over six days of intensive physiological measurements inside and outside the OTC, averaged over both zones.

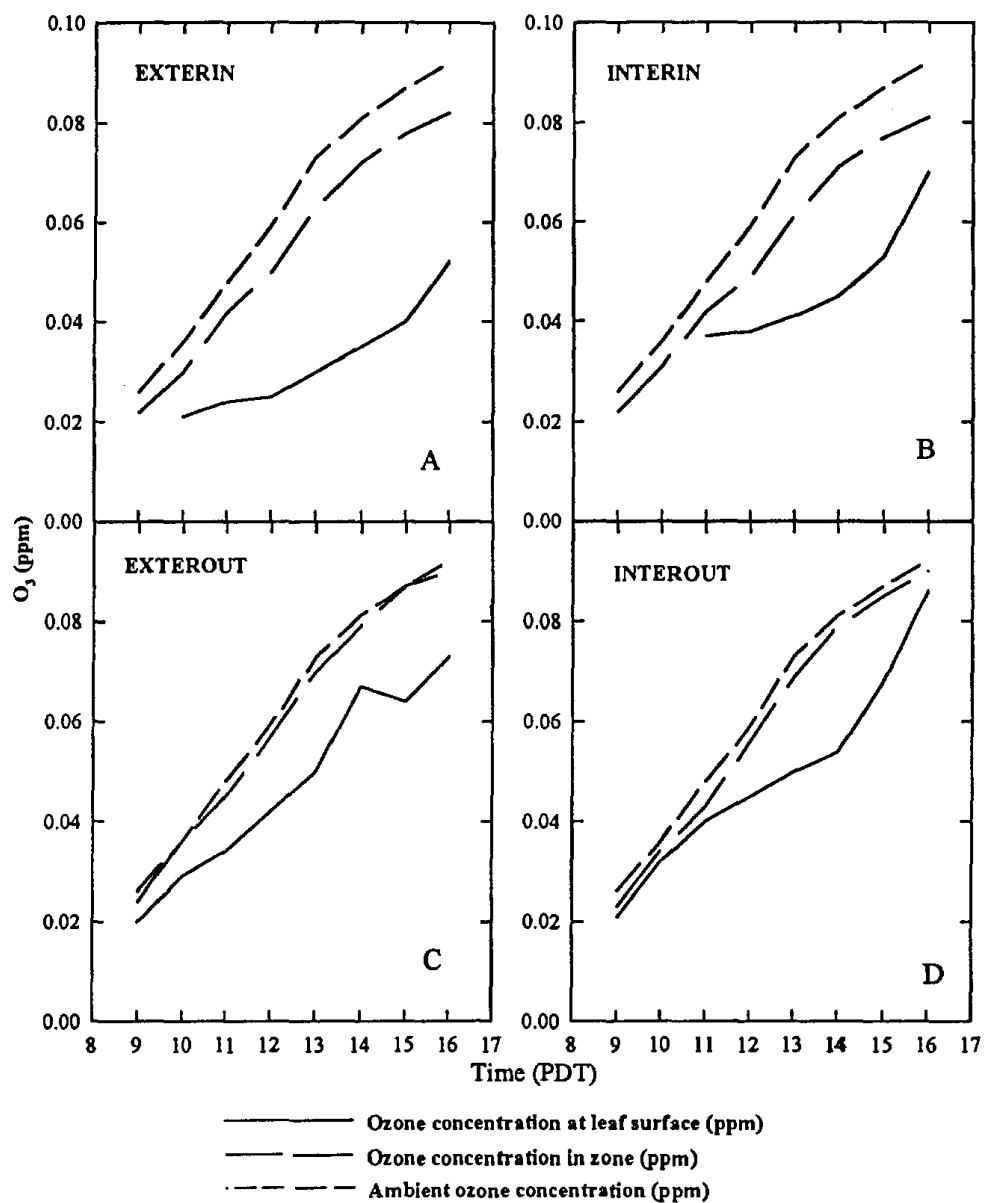


Fig. 62. Diurnal pattern of O_3 concentrations at the leaf surface, in the canopy air space within each zone, and in the ambient air in the canopy exterior, by zone. O_3 concentration at the leaf interior has been shown to be indistinguishable from 0 ppm.

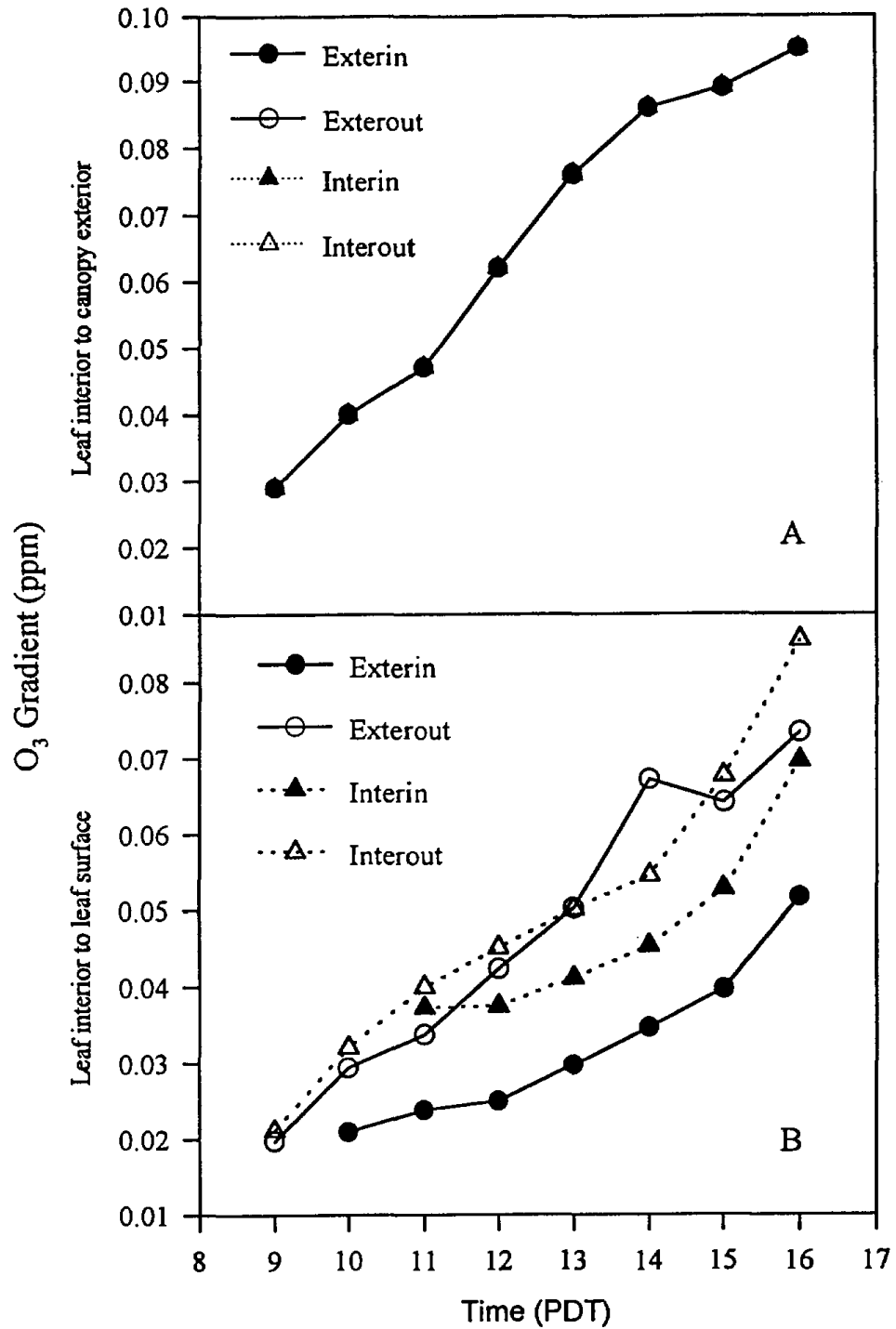


Fig. 63. Diurnal pattern of O₃ gradients from leaf interior to canopy exterior and from leaf interior to the leaf surface, by zone inside and outside the OTC, averaged over the six days of intensive physiological measurements.

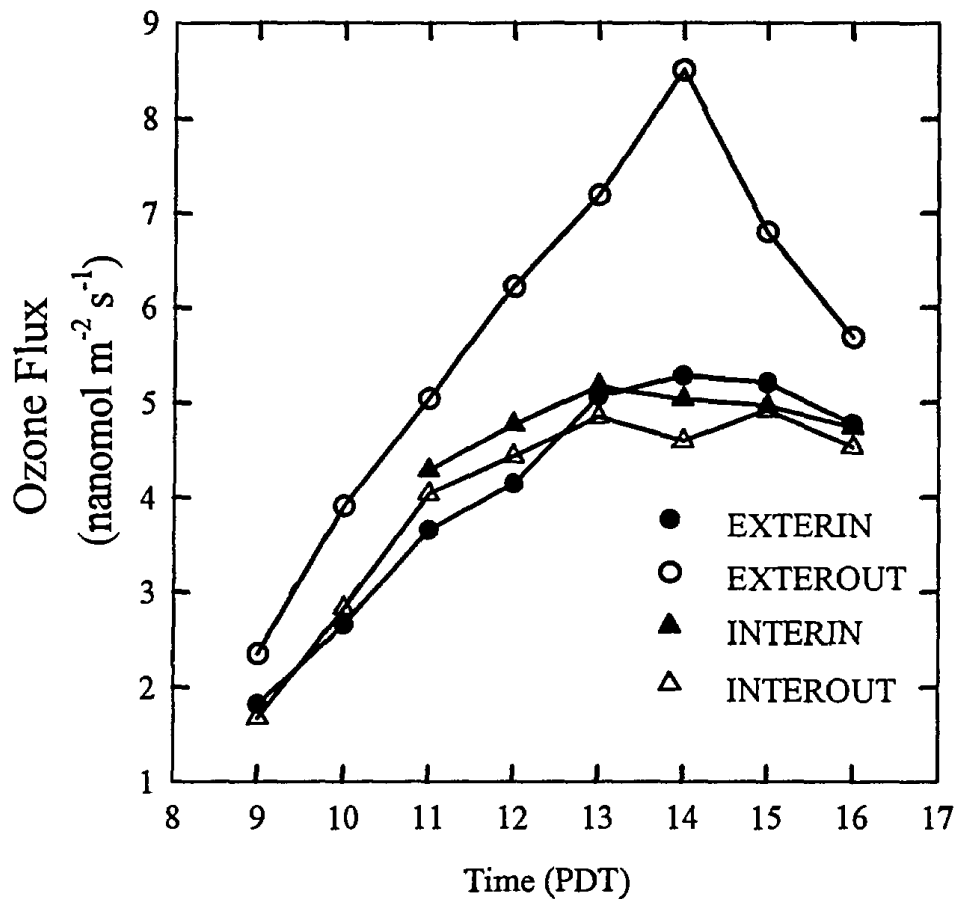


Fig. 64. Diurnal pattern of hourly means of O_3 flux (leaf uptake) determined from O_3 gradients and diffusive conductances from the leaf interior to the ambient air, by zone averaged over the six days of intensive physiological measurements. In the case of O_3 there is no alternative measurement of leaf uptake by zone, with which to compare these values.

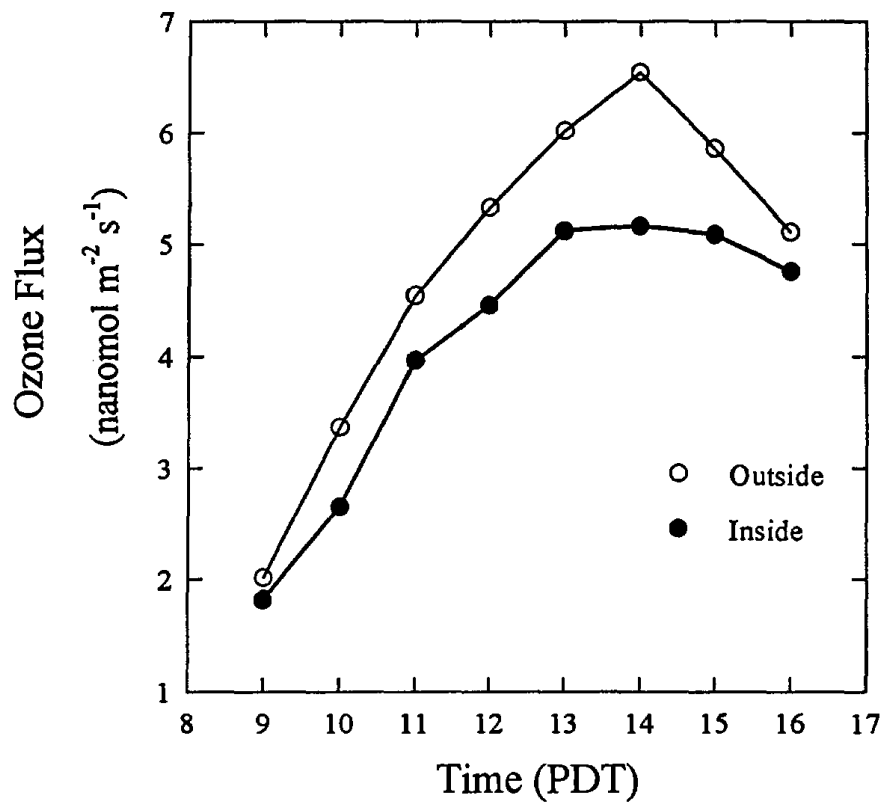


Fig. 65. Diurnal pattern of O₃ flux (uptake by leaves) averaged over six days of intensive physiological measurements inside and outside the OTC, averaged over both zones.

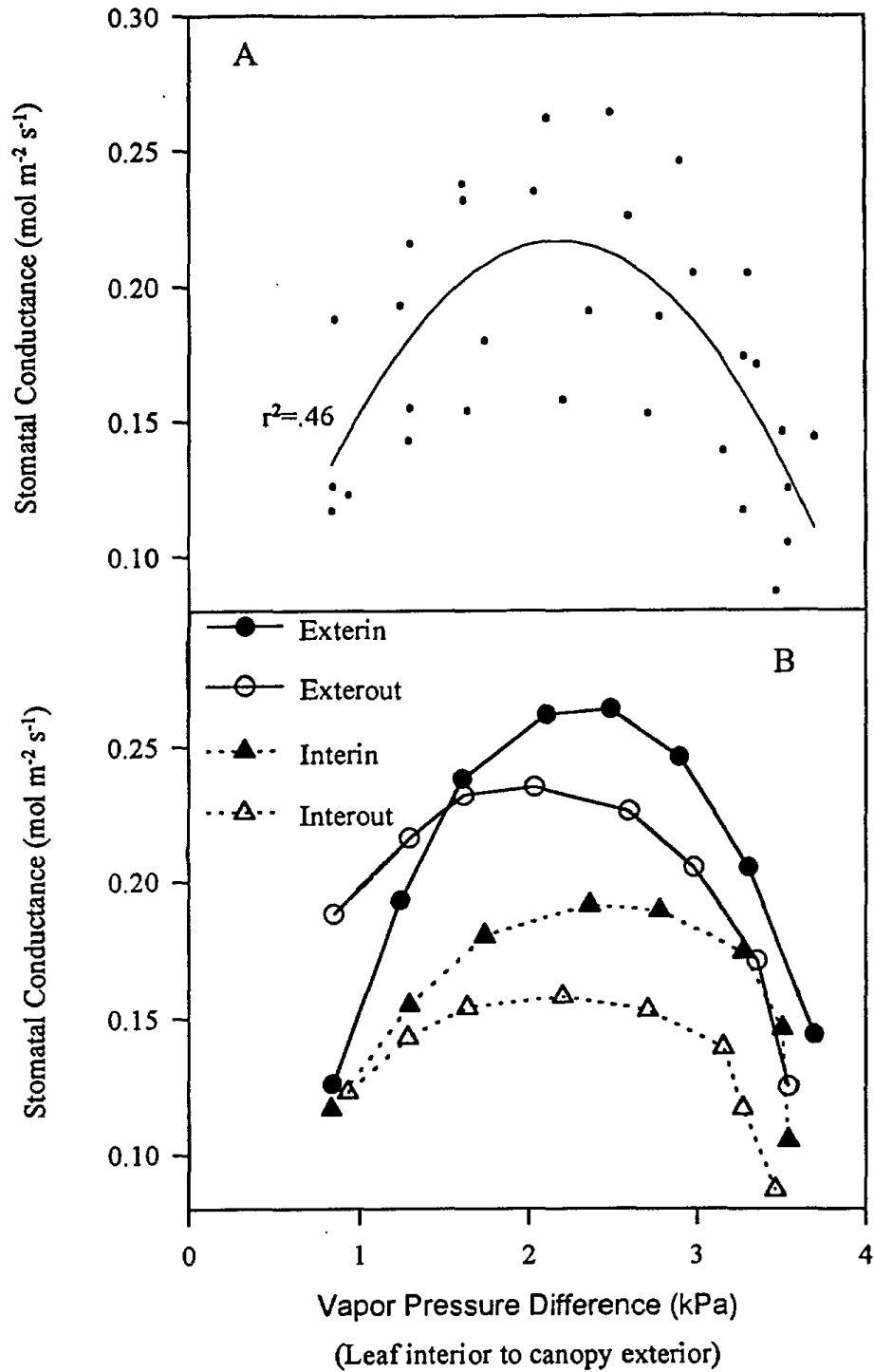


Fig. 66. Apparent response of stomatal conductance to the single environmental parameter, vapor pressure difference, calculated from the leaf interior to the canopy exterior.

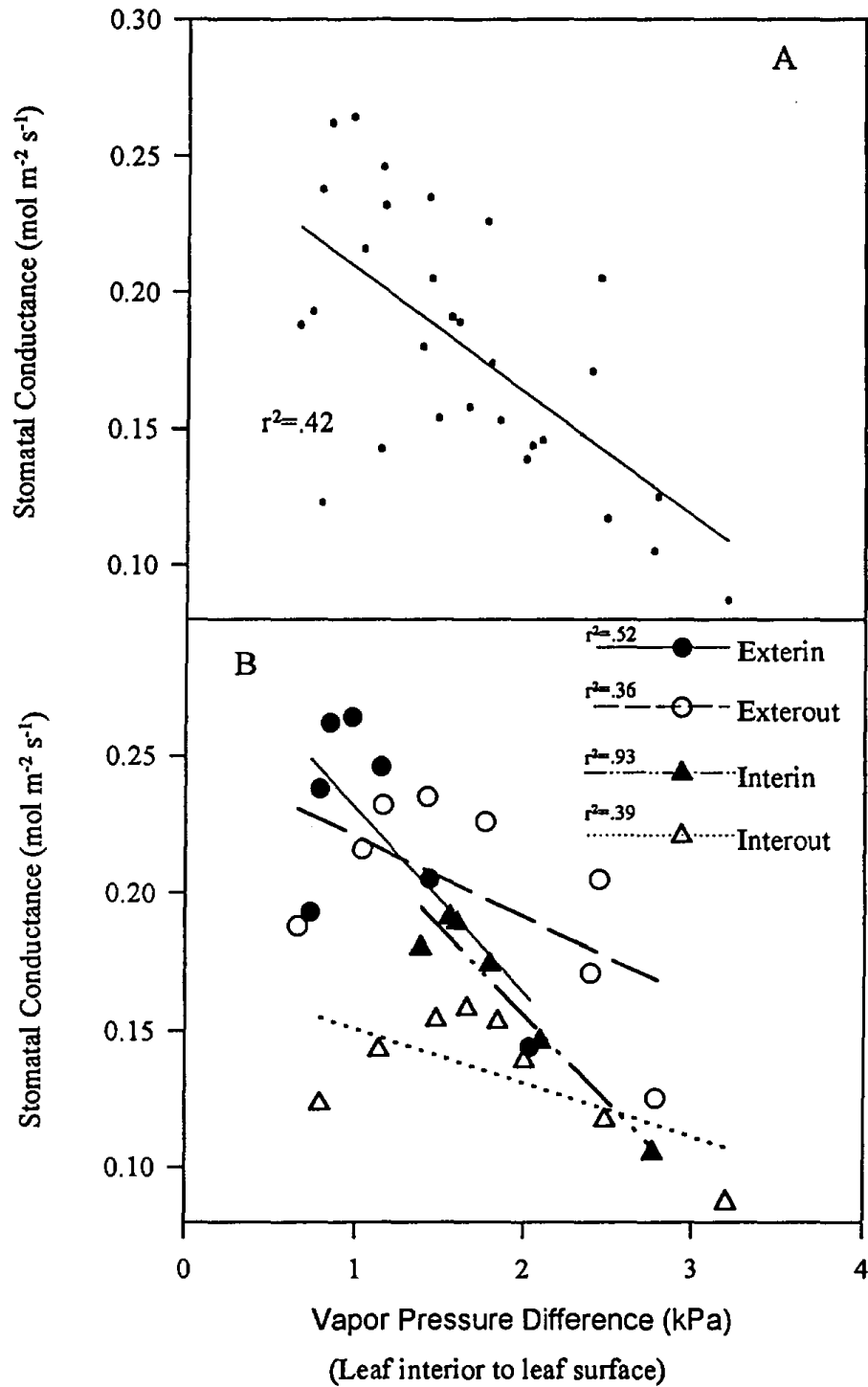


Fig. 67. Apparent response of stomatal conductance to the single environmental parameter, vapor pressure difference calculated from the leaf interior to the leaf surface.

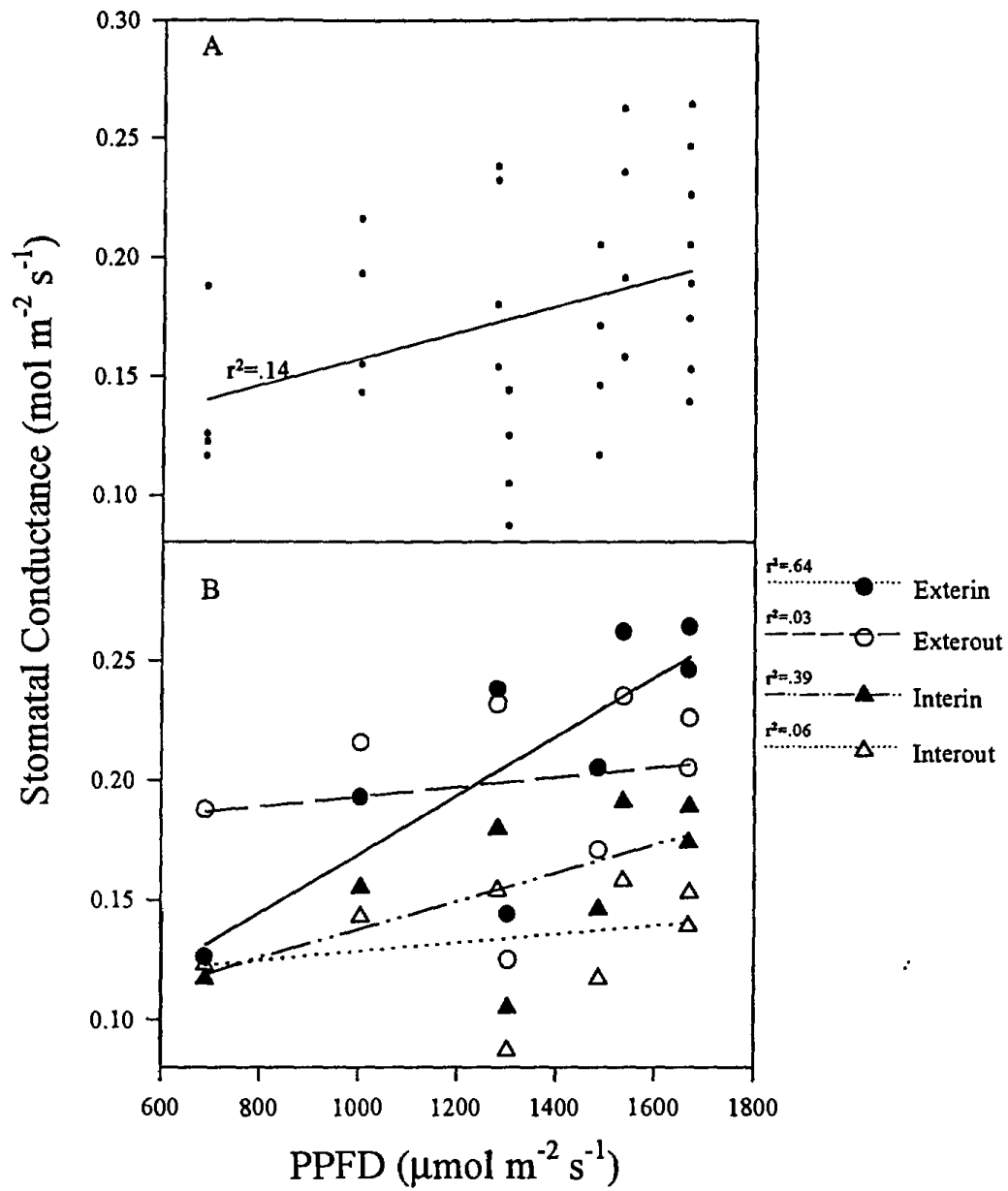


Fig. 68. Apparent response of stomatal conductance to the single environmental parameter, above-canopy photon flux density.

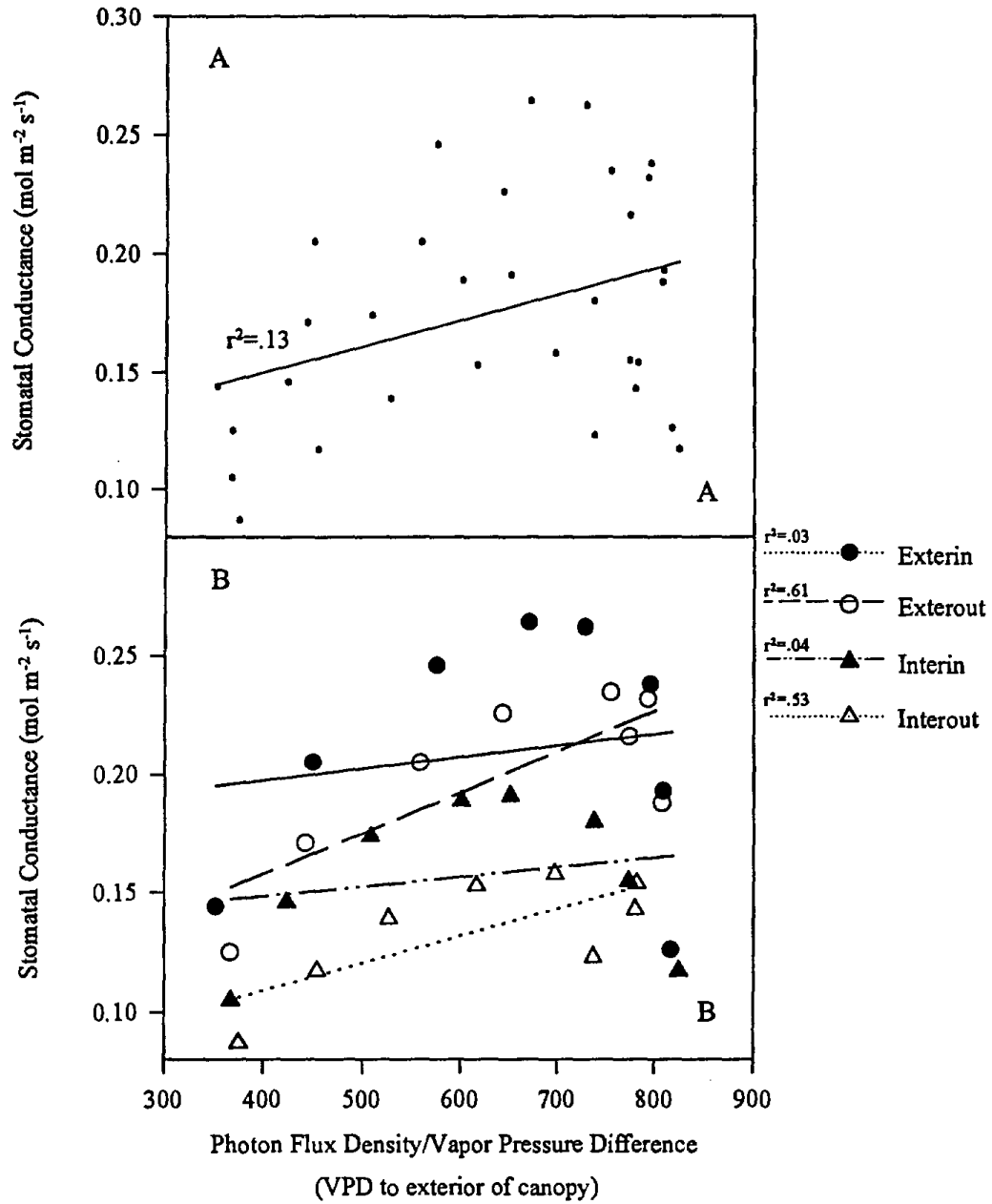


Fig. 69. Response of stomatal conductance to the composite environmental parameter, above-canopy photon flux density normalized by vapor pressure difference calculated from the leaf interior to the canopy exterior.

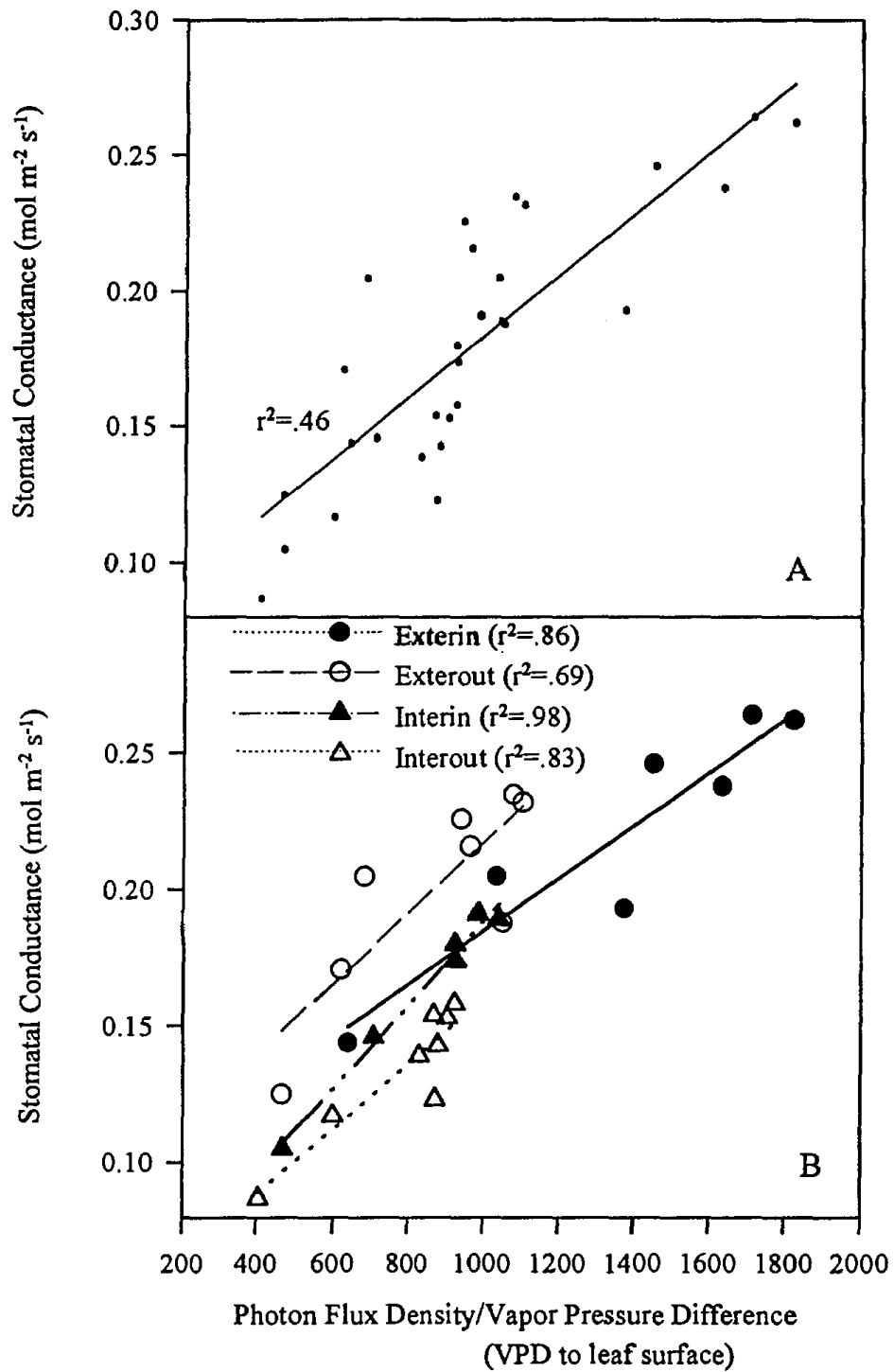


Fig. 70. Response of stomatal conductance to the composite environmental parameter, above-canopy photon flux density normalized by vapor pressure difference calculated from the leaf interior to the leaf surface.

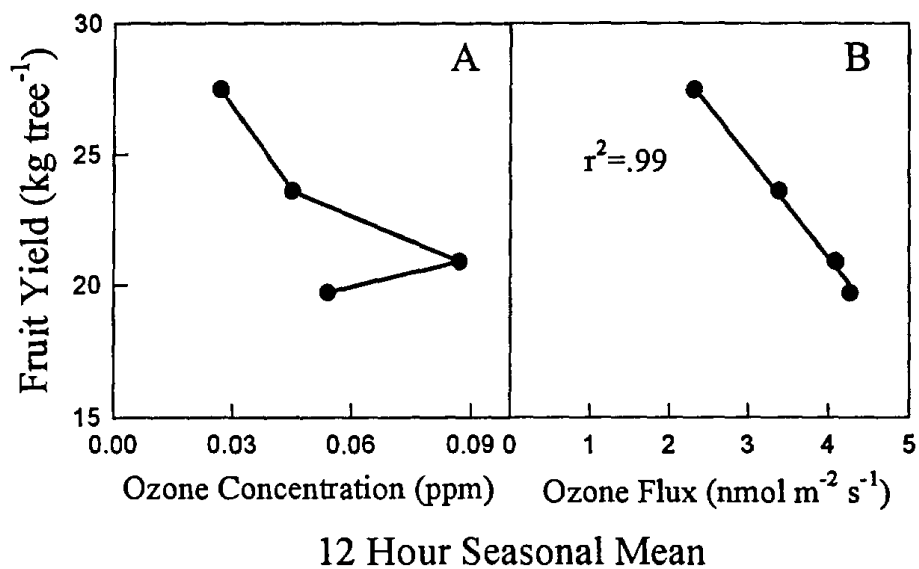


Fig. 71. Relationship between plum yield in 1992 (Williams et al., 1993) and 12 hour seasonal mean ozone concentration (A) or 12 hour seasonal mean ozone flux on a leaf area basis averaged over the entire canopy (B), calculated as in Table 16.